TAMPEREEN TEKNILLINEN YLIOPISTO
TAMPERE UNIVERSITY OF TECHNOLOGY

ESSI NIEMI

HYDROGELS FOR 3D CULTURE OF HUMAN CORNEAL CELLS AIMING FOR TISSUE ENGINEERED CORNEAL APPLICATION

Master of Science thesis

Examiners: Professor Minna Kellomäki
and PhD Alexandra Mikhailova
Examiners and topic approved by the
Faculty Council of the Faculty of
Natural Sciences
on 9th December 2015

ABSTRACT

ESSI NIEMI: Hydrogels for 3D Culture of Human Corneal Cells Aiming for Tissue Engineered Corneal Application
Tampere University of Technology
Master of Science Thesis, 74 pages, 13 Appendix pages
June 2016
Master's Degree Programme in Biotechnology
Major: Tissue Engineering
Examiners: Professor Minna Kellomäki, PhD Alexandra Mikhailova

Keywords: tissue engineering, human cornea, corneal substitute, epithelium, stroma, hydrogel

The cornea is a transparent tissue protecting the most anterior part of the eye and if it is damaged, it may result in a partial or complete loss of vision. Millions of patients are in need of donor cornea, but there is a substantial shortage of good-quality corneas and there is always a risk of tissue rejection when allogeneic tissues are transplanted. Tissue engineering offers a way to develop an artificial cornea using biomaterials together with the patients' own cells to provide an alternative for conventional tissue transplantation.

The objective of this thesis was to study and comprehend the current state of corneal tissue engineering research and investigate which biomaterials could be suitable for the purpose of creating a biomaterial-based corneal substitute. In this thesis, the experimental part concentrated on studying hydrogels with corneal cells.

In the experimental part, the behaviour of immortalised human corneal epithelial cells (HCE) and stromal keratocytes (HCK) in 2D and 3D cultures were studied. The aim of the 2D cell culture study was to test how these two cell lines behave in chosen different culture medium options, three commercially available media (CnT-20, CnT-30 and CnT-Prime-CC) and HCE and HCK maintenance media. The best suited media were then used in 3D cell culture with hydrogels. There were hydrogels A, B, C and D and one commercial hydrogel. These were tested in 3D cell culture where keratocytes were mixed with the hydrogel and epithelial cells were seeded on top. The hydrogel-cell samples were cultured in CnT media for 7 to 14 days and air-lifted for 7 days for epithelial cell stratification.

Cell proliferation in 2D culture was evaluated with PrestoBlue™ assay and cell behaviour and expression of relevant corneal proteins were analysed with immunofluorescence staining (IF). These results indicated CnT-20 to be the best option for both cell lines, but all three CnT media were tested also in 3D cell culture with hydrogels. The hydrogel experiments were also evaluated with IF staining. Interestingly, the most suitable medium for 3D cell culture was CnT-Prime-CC. The best suited hydrogel option in this study was hydrogel A and resulting cell-hydrogel samples were thin and soft but had clear, transparent and even structure.

TIIVISTELMÄ

ESSI NIEMI: Hydrogeelit ihmisen sarveiskalvon solujen 3D-kasvatukseen, tavoitteena kudosteknologinen sarveiskalvosovellus
Tampereen teknillinen yliopisto
Diplomityö, 74 sivua, 13 liitesivua
Kesäkuu 2016
Biotekniikan diplomi-insinöörin tutkinto-ohjelma
Pääaine: Kudosteknologia
Tarkastajat: Professori Minna Kellomäki, FT Alexandra Mikhailova

Avainsanat: kudosteknologia, sarveiskalvo, sarveiskalvoimplantti, epiteeli, strooma, hydrogeeli

Sarveiskalvo on silmän uloin, läpinäkyvä ja suojaava kerros, ja sen vahingoittuessa ihminen voi menettää näkökykynsä joko osittain tai kokonaan. Miljoonat ihmiset maailmalla tarvitsevat sarveiskalvosiirteen, mutta hyvälaatuisista sarveiskalvosiirteistä on valtava pula. Lisäksi kudossiirteissä on aina riskinä luovuttajan ja vastaanottajan kudosyhteensopimattomuus ja siitä johtuen siirteen hyljintä. Kudosteknologian avulla on mahdollista kehittää biomateriaalipohjainen ja potilaan omista sarveiskalvon soluista rakennettu sarveiskalvoimplantti, joka korvaisi perinteisen siirteen tarpeen.

Tämän diplomityön tavoitteena oli sisäistää tämänhetkisen kudosteknologian sarveiskalvotutkimuksen saavutukset ja selvittää, millaisia biomateriaaleja käytetään ja voitaisiin mahdollisesti käyttää sarveiskalvoimplanttitutkimuksessa. Työn kokeellinen osuus keskittyi hydrogeelien sopivuuden testaukseen sarveiskalvon solujen kanssa.

Työn kokeellisessa osuudessa käytettiin kahta immortalisoitua ihmisen sarveiskalvosolulinjaa, epiteelisoluja (HCE) sekä strooman keratosyyttejä (HCK), joita testattiin 2D-kasvatuksessa sekä hydrogeelien kanssa 3D-kasvatuksessa. 2D-testauksen tarkoituksena oli löytää näille solulinjoille soveltuvia kasvatusliuoksia, joita voitaisiin käyttää hydrogeelien 3D-solutestauksessa. Vaihtoehtoina toimivat kolme kaupallista kasvatusliuosta (CnT-20, CnT-30 ja CnT-Prime-CC) sekä verrokkeina solulinjojen omat ylläpitoliuokset. Hydrogeelitestaus sisälsi neljä eri hydrogeeliä: A, B, C ja D sekä lisäksi yhden kaupallisen hydrogeelin. Nämä valmistettiin siten, että HCK-solut sekoitettiin hydrogeeleihin ja HCE-solut kasvatettiin materiaalien päällä. 3D-kasvatuksen kesto oli 7-14 päivää, joka jatkui 7 päivän ilma-altistuksella HCE-solujen kerrostumiseksi.

Solujen jakautumiskyky arvioitiin PrestoBlue™ määrityksen avulla ja niiden käyttäytymistä sekä proteiiniekspressiota immunofluoresenssivärjäyksillä (IF) 2D-kasvatuksessa. Näiden tulosten perusteella CnT-20 olisi soveltuvin molemmille solulinjoille. 3D-hydrogeelitestaus arvioitiin myös IF-värjäyksellä, jonka mukaan soveltuvin kasvatusliuos oli 2D-kasvatuksesta poiketen CnT-Prime-CC. Soveltuvimmaksi materiaaliksi osoittautui hydrogeeli A, josta valmistetut näytteet olivat melko ohuita ja pehmeitä, mutta kuitenkin rakenteiltaan tasaisia sekä läpinäkyviä.

PREFACE

This Master of Science thesis was carried out in the Eye Group of BioMediTech, joint Institute of Biosciences and Medical Technology at the University of Tampere and Tampere University of Technology, and it is a part of the regenerative medicine project, Human Spare Parts.

First, I would like to thank Associate Professor Heli Skottman, the group leader of the Eye Group, for this terrific opportunity to conduct my thesis in the inspiring field of tissue engineering and ophthalmology. Second, I would like to thank my thesis examiner Professor Kellomäki for the important advices regarding to my thesis, as well as interesting studies in the field of tissue engineering.

Most importantly, I am very grateful for my thesis advisor PhD Alexandra Mikhailova for the wonderful guidance and support throughout this thesis project. Also, I would like to thank PhD Tanja Ilmarinen for providing help with the thesis, especially with the experimental part, Lic. Phil. Jennika Karvinen for the collaboration and help regarding the hydrogels and Docent Kati Juuti-Uusitalo for remembering your student who was looking for a challenging and interesting thesis topic. All in all, I would like to thank the whole Eye Group for the opportunity to be part of this high-spirited innovative and hard-working team.

Finally, I am deeply grateful to my family and dear friends for always supporting and encouraging me with my studies and this thesis process. Past years have not been easy, so thank you for being there and reminding me to be happy, dream big, and live my life to the fullest.

Tampere, 25.5.2016

Essi Niemi

TABLE OF CONTENTS

LIST OF ABBREVIATIONS

α-SMA	α-smooth muscle actin
ABC	ATP binding cassette transporter
ABCG2	ATP binding cassette sub-family G member 2 protein
AM	Amniotic membrane
APS	Ammonium persulphate
BSA	Bovine serum albumin
CA	Citric acid
$CaCl_2$	Calcium chloride
CK3/CK12/CK15	Cytokeratins 3, 12 and 15
CMC	*N*-cyclohexyl-*N'*-(2-morpholinoethyl) carbodiimide metho-*p*-toluenesulfonate
CnT	CELLnTEC
DAPI	4',6-diamidino-2-phenylidole
DMEM	Dulbecco's Modified Eagle Medium
ECM	Extracellular matrix
EDC	*N*-(3-dimethylaminopropyl-)-*N'*-ethylcarbodiimide
EDCM	1-[3-(Dimethylamino)propyl]-3-ethylcarbodiimide methiodide
EGF	Epidermal growth factor
EtOH	Ethyl alcohol
FBS	Foetal bovine serum
G1cA	β1-4D-glucuronic acid
G1cNAc	β1-3 N-acetyl-D-glucosamine
GAG	Glycosaminoglycan
GG	Gellan gum
H&E	Histological haematoxylin and eosin staining
HA	Hyaluronan
HCE	Human corneal epithelial cell
HCF	Human corneal fibroblasts
HCK	Human corneal keratocytes
HCSSC	Human corneal stromal stem cell
HLE	Human limbal epithelial cell
HLF	Human limbal fibroblast
HOMEC	Human oral mucosal epithelial cell
IF	Immunofluorescence staining
IgG	Immunoglobulin G
IPN	Interpenetrating polymer network
KGM-CD™	Chemically Defined Keratinocyte Growth Medium
KTN	Keratocan
KPro	Keratoprosthesis
LESC	Limbal epithelial stem cell
LSCD	Limbal stem cell defiency
MMP	Matrix metalloprotease
MSC	Mesenchymal stem cell
MPC	2-Methacryloyloxyethyl phosphorylcholine
NHS	*N*-hydroxysuccinimide
NV	Neovascularisation
O.C.T	Optimal cutting temperature
PBS	Phosphate-buffered saline

PC	Polycarbonate
PDMS	Polydimethylsiloxane
PEGDA	Poly(ethylene glycol) diacrylate
PEG-DBA	Poly(ethylene glycol) dibutyraldehyde
PET	Polyethylene terephthalate
PEUU	Poly(ester urethane) urea
PFA	Paraformaldehyde
PG	Proteoglycan
pMG	Poly(6-methacryloyl-α-D-galacto-pyranose)
PMMA	Polymethylmethacrylate
RAFT	Real Architecture For 3D Tissue
RCF	Rabbit corneal fibroblast
RFU	Relative fluorescence unit
RGD	Tripeptide arginine-glycine-aspartate ligand
RHCI	Human recombinant type I collagen
RHCIII	Human recombinant type III collagen
SJS	Stevens-Johnson syndrome
TAC	Transient amplifying cell
TEMED	N,N,N,N- tetramethyle-thylenediamine
TGFβ	Transforming growth factor beta
TUT	Tampere University of Technology
UDP	Uridine diphosphate glucose
UTA	University of Tampere
UV	Ultraviolet
WHO	World Health Organization
VIM	Vimentin
YIGSR	Laminin-derived tyrosine-isoleucine-glycine-serine-arginine polypeptide

1. INTRODUCTION

The cornea is the outermost layer of the eye and its purpose is to protect the eye from external environment. It is an avascular and transparent layer that is constructed from connective tissue and provides optical interphase to the visual system. (DelMonte & Kim 2011; Ghezzi et al. 2015) The cornea is located on top of the pupil and the iris and it has significant role in the ocular refraction, providing approximately 70 % of the refractive power of the eye (Massoudi et al. 2015; Ghezzi et al. 2015). The cornea contains three cellular layers: epithelium, stroma and endothelium, and two acellular layers which are Bowman's layer and Descemet's membrane (DelMonte & Kim 2011; Ghezzi et al. 2015; Yoon et al. 2014). The stroma is composed of rich highly organised collagen fibril network, and accounts for almost 90 % of the corneal thickness, providing the bulk of its structure (DelMonte & Kim 2011). The transparency and optical properties of the cornea are mainly dependent on the structure of the stroma as well (Drupps & Wilson 2006).

Mechanical and chemical damages as well as different diseases of the cornea can lead to partial or complete loss of vision. It is estimated that approximately 10 million people in the world suffer from cornea related vision loss due to a damage or a disease and according to World Health Organization (WHO) corneal visual impairment is the fourth leading cause of blindness globally. (Deng et al. 2010; WHO, 2016) Allogeneic corneal transplantation is currently considered to be the best solution to treat these patients (Deng et al. 2010). However, the demand for donor corneas exceeds the number of available transplantable good-quality corneas everywhere in the world (Ahn et al. 2013; Deng et al. 2010). Moreover, like with any other allogeneic tissue transplantation, there is a risk of rejection against the transplanted cornea. This acute need for transplants drives many research teams to find possible alternative solutions by means of tissue engineering. Fortunately, a lot of progress has been made already towards tissue engineered biomaterial-based corneal application but there are still numerous challenges to be faced before an artificial cornea can help patients suffering from disorders affecting the cornea.

This thesis study was conducted at the Eye Group of BioMediTech, the joint Institute of Biosciences and Medical Technology at the University of Tampere (UTA) and Tampere University of Technology (TUT). The thesis is part of the regenerative medicine project, Human Spare Parts. The corneal research of the group concentrates on developing a corneal substitute by means of tissue engineering. The objective of this thesis was to study the current state of corneal tissue engineering research and investigate which biomaterials could be the best suited options for a biomaterial-based corneal substitute. This thesis consists of a theoretical and an experimental part.

In the theoretical part, information about the structure of the cornea, wound healing processes and common diseases and injuries are explained. The theoretical part also discusses the framework to be considered, such as the physical and optical requirements for tissue engineered cornea. Important and relevant research and progress of the field are presented to give insight what kind of biomaterial options and approaches there are under development for suitable solution.

In the experimental part, hydrogels were studied with human corneal epithelial cells (HCEs) and stromal keratocytes (HCKs) in different culture media. The behaviour of the cells in different media was first studied to choose suitable culture media for 3D culture of corneal cells with the hydrogels. The hydrogels studied in this thesis were provided by the Biomaterials and Tissue Engineering Group at BioMediTech, TUT. The hydrogel samples were studied with relevant immunofluorescent staining to obtain qualitative information about the corneal cell behaviour and protein expression.

THEORETICAL PART

2. THE HUMAN CORNEA

The cornea is the most anterior layer of the eye. Its purpose is to create a protecting barrier against mechanical and infectious threats from the external environment. (DelMonte & Kim 2011) The cornea is a transparent layer of connective tissue with 80 % water content and it is located on top of the pupil and the iris of the eye, as shown in Figure 1 (Ahn et al. 2013; Ghezzi et al. 2015; Notara et al. 2010). The transparency, structure and shape of the cornea are important for the visual system as it functions as the optical interface for the eye (DelMonte & Kim 2011; Ghezzi et al. 2015). It provides approximately two thirds of the optical power of the eye and focuses incoming light to the retina, the posterior and innermost layer of the eye (West-Mays & Dwivedi 2006).

The cornea is constructed from five layers: epithelium, Bowman's layer, stroma, Descemet's membrane and endothelium. These layers contain different types of corneal cells and various extracellular matrix (ECM) components, primarily collagen type I. These layers function together by supporting each other in a well-balanced state of homeostasis. The cornea connects to the rest of the eye through the surrounding limbus, which provides essential stem cells for maintenance and regeneration of the epithelial tissue. (DelMonte & Kim 2011; Ghezzi et al. 2015; Yoon et al. 2014) The limbus is connected continuously with sclera, which is the protecting layer of the rest of the eye, shown in Figure 1 (Notara et al. 2010).

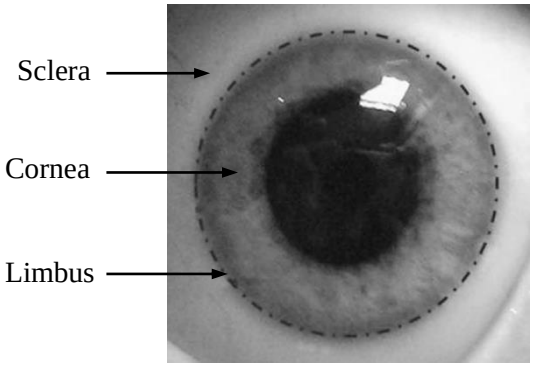

Figure 1. *The ocular surface. (Adapted from Notara et al. 2010)*

The cornea is avascular and in normal healthy state, blood and lymph vessels do not enter the corneal tissue (Dhouailly et al. 2014). However, in order to stay vital, the tissue needs nutrients, which are provided through the outermost edge of the cornea. The limbus is connected to blood vessels with end branches and ophthalmic arteries that provide those vital components via the tear film and the aqueous humour of the eye. These nutrients together with the cells and the ECM maintain the corneal structure and transparency. (DelMonte & Kim 2011; Dhouailly et al. 2004)

2.1 The structure of the cornea

The cornea can be divided to three different cellular layers which are the epithelium, stroma and endothelium. Between these layers, there are two acellular collagenous interface membranes: Bowman's layer between epithelial and stromal layers, and Descemet's membrane between stromal and endothelial layers. (DelMonte & Kim 2011; Ghezzi et al. 2015) The location of the cornea and other important structural parts of the eye are presented in Figure 2A and the layers of the cornea presented in Figure 2B.

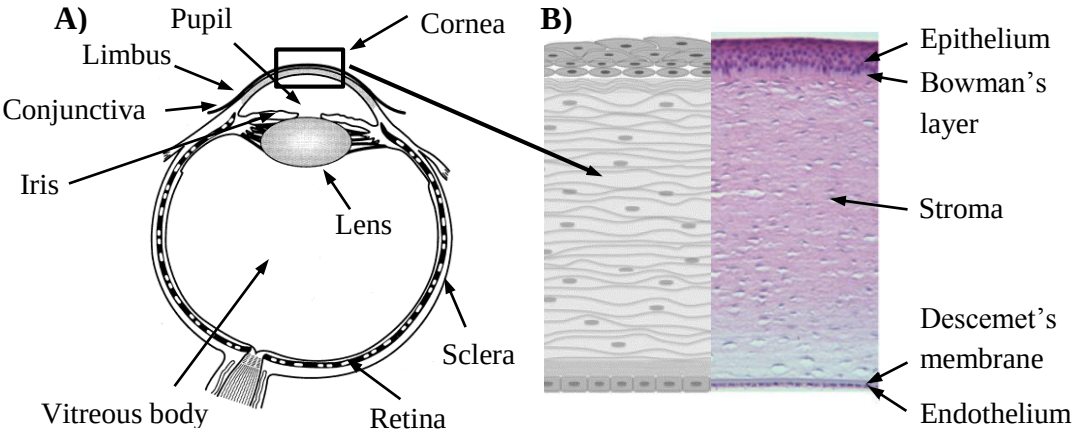

Figure 2. *A) The structure of the eye and the location of the cornea. B) The layers of the cornea. (Adapted from Germain et al. 2000 and Ghezzi et al. 2015)*

The average horizontal diameter of the cornea in an adult human is from 12.0 to 13.0 mm (Ghezzi et al. 2015) and vertical diameter is approximately 1.0 mm smaller. The cornea is 0.5 mm thick from the middle and the thickness increases towards the periphery. The shape of the cornea creates an aspherical optic system that is flatter from the periphery and steeper from the middle. (DelMonte & Kim 2011) The cornea is immediately connected to a tear film which creates the most external layer of the eye. The tear film and the cornea together create a transparent highly innervated tissue that has a significant role in the ocular refraction, creating approximately 70 % of the refractive power in the eye. (Massoudi et al. 2015; Ghezzi et al. 2015) The cornea, especially stroma and Bowman's layer are among the most densely innervated tissues (DelMonte & Kim 2011; Dhouailly et al. 2014). The terminal braches of ophthalmic trigeminal nerve enter the stroma by penetrating the Bowman's layer and the nerve ends run parallel to epithelium (Dhouailly et al. 2014).

2.1.1 Corneal epithelium

The most external cellular layer of the cornea is the epithelium. The thickness of the epithelium is approximately 40 to 60 µm, 8-10 % of the whole thickness. (Massoudi et al. 2015; Ghezzi et al. 2015) The corneal epithelium is stratified squamous tissue that has

4 to 6 cell layers. These cell layers of the epithelium can be classified into three groups, each composed of specific types of cells, shown in Figure 3. (DelMonte & Kim 2011)

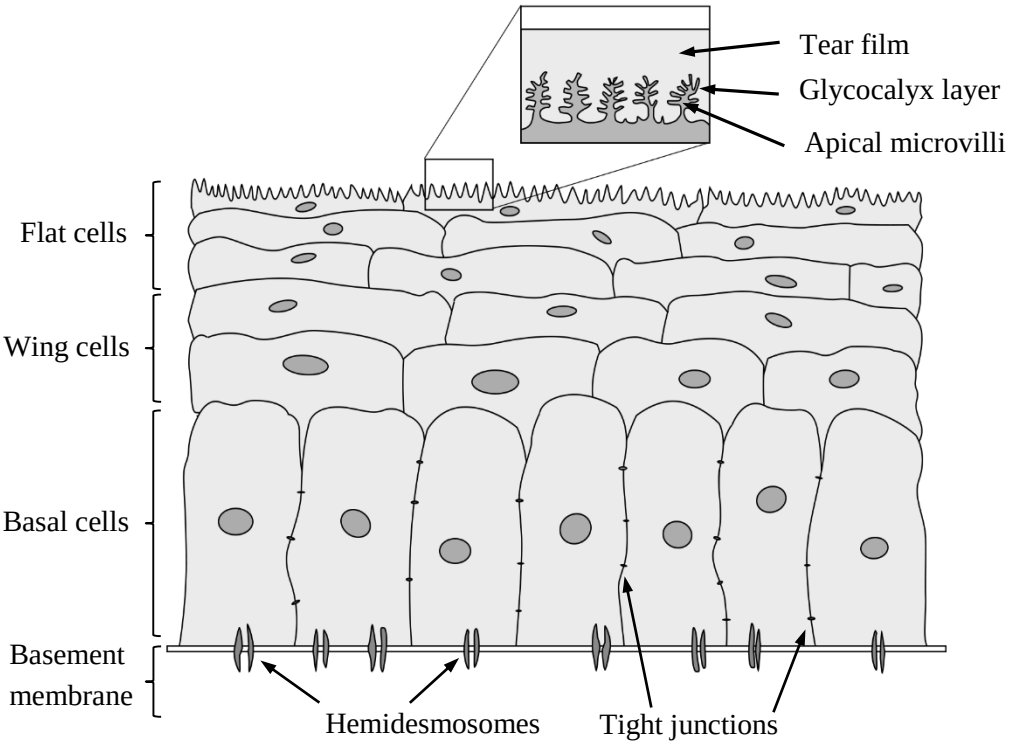

Figure 3. *The cell types of corneal epithelium: flat polygonal cells, suprabasal wing cells and basal columnar cells. (Drawn according to DelMonte & Kim 2011)*

The epithelium, in conjunction with the tear film, creates a smooth and transparent layer for the light to enter the eye with coherent refraction. Also they provide a biological barrier function that regulates the transfer of soluble components and water to the layer beneath the epithelium, the stroma. The tear film functions as a reservoir for antibacterial and growth factors. These two types of components are extremely important for maintaining the homeostasis of the cornea as well as for repairing the tissue. (Ghezzi et al. 2015) The tear film also provides protection against toxic, chemical and foreign-body damage (DelMonte & Kim 2011). The lifespan of the epithelial cells is from 7 to 10 days. In the cell cycle, the basal cells gradually rise to the surface and replace the superficial cells in apical fashion. The cells at the surface routinely undergo turnover through involution, apoptosis and desquamation. (DelMonte & Kim 2011) The limbus, which is the surrounding tissue of the cornea, is in charge of renewing the whole layer. The corneal epithelial cells are renewed by the unipotent limbal epithelial stem cells (LESCs) that proliferate and differentiate first to transient amplifying cells (TACs) and further to mature epithelial cells as they migrate from the limbus towards the central epithelium of the cornea. (Kobayashi et al. 2015; Levis et al. 2013; Kayama et al. 2007; Notara et al. 2010)

The most superficial cells of the epithelium, two to three layers, are flat polygonal cells. These flattened cells provide maximal surface area with the help of apical microvilli and

microplicae that are covered with fine charged glycocalyceal layer. (DelMonte & Kim 2011) This layer attaches the tear film to the cell membrane every time the eye blinks (Cholkar et al.2013). These flat cells are in close proximity with each other creating tight junctional complexes. This type of tight structure prevents the tear fluid from entering the intercellular space and prevents toxins and microbes from entering the deeper layers of the cornea. (DelMonte & Kim 2011) Beneath the superficial layer is a layer of wing cells, also called the suprabasal layer, consisting of two to three layers of cells. These cells are not as flat as the polygonal cells on the surface but they possess a similar tight structure. (DelMonte & Kim 2011) The deepest layer of the epithelium is the basal layer which consists of a single layer of approximately 20 µm tall columnar epithelial cells. These columnar cells are the only cells in the epithelium capable of mitosis, which means that they are responsible for renewing the epithelium by creating wing and flat superficial cells. The columnar cells have lateral intercellular junctions, more specifically gap junctions and zonulae adherens. (DelMonte & Kim 2011)

The basal cells are tightly attached to the underlying epithelial basement membrane through hemidesmosomal system. The hemidesmosomes, anchoring fibril and filament, create an anchoring complex which function as a link between intracellular cytoskeleton of the epithelial basal cells and the stroma. (Hejtmancik & Nickerson 2015) The epithelial basement membrane is approximately 0.05 µm thick and it consists mainly of type IV collagen and also slight amounts of type VII collagen (anchoring fibrils) and laminin 322 (anchoring filaments) that are all secreted by the basal cells (DelMonte & Kim 2011; Massoudi et al. 2015; Torricelli et al. 2013). The basement membrane includes also other important structural components such as glycoprotein laminins, heparin sulphate proteoglycans (PG) and nidogens (Torricelli et al. 2013). The health of this membrane is crucial since if damaged, the healing will take fairly long time, and during this time the epithelial bond to the deeper layers of the cornea is weak and unstable. (DelMonte & Kim 2011)

2.1.2 Corneal stroma

The stroma is a unique transparent collagenous structure that comprises roughly 90 % of the whole corneal thickness (Ghezzi et al. 2015; Hassell & Birk 2010). The stroma provides the bulk structure of the cornea, and is composed of dense and highly organised collagen fibril structure, ECM and stromal cells, keratocytes (DelMonte & Kim 2011; Hassell & Birk 2010). This kind of ordered structure is the key to maintaining the mechanical stability for corneal shape and curvature (Chen et al. 2015).

The collagen mainly found in the stroma is heterodimeric complex consisting of type I and type V collagen fibres, arranged to parallel bundles called fibrils, which are arranged to layers or lamellae (DelMonte & Kim 2011; Hassell & Birk 2010; West-Mays & Dwivedi 2006). The small fibrils, with a diameter of 25 to 30 nm, are homogeneously distributed within the lamella structure and their spacing is regulated by rich and hydrated

PG matrix (Deng et al. 2010; Meek & Knupp 2015). This sort of spacing created by the PGs is essential for corneal transparency (Carlson et al. 2005). A healthy stroma contains four leucine-rich PGs: keratocan, lumican, decorin and mimecan (Meek & Knupp 2015). The PGs are macromolecules that are constructed from a core protein and one or more negatively charged linear repeating saccharides, glycosaminoglycans (GAGs), such as keratan and chondroitin sulphates, which are covalently bound to this core protein (Deng et al. 2010; Hassell & Birk 2010; Hatami-Marbini & Etebu 2013).

The stroma contains approximately 200 to 300 lamellae which are organised in a way that each layer is arranged at right angles relative to fibres in adjacent lamellae, shown in Figure 4 (DelMonte & Kim 2011; Gil et al. 2010; Meek & Boote 2004). The packing density of these lamellae is higher in the middle of the stroma and lower closer to the limbus (Meek & Krupp 2015). This highly organised and homogeneous nature of the fibrils allows only minimal scattering of light contributing to corneal transparency (Hassell & Birk 2010) and has a huge impact on the mechanical strength of the cornea (DelMonte & Kim 2011; Gil et al. 2010; Meek & Knupp 2015). The collagen fibrils continue to the limbus and sclera, and gradually fuse with the thicker fibrils found in the sclera (Meek & Boote 2004).

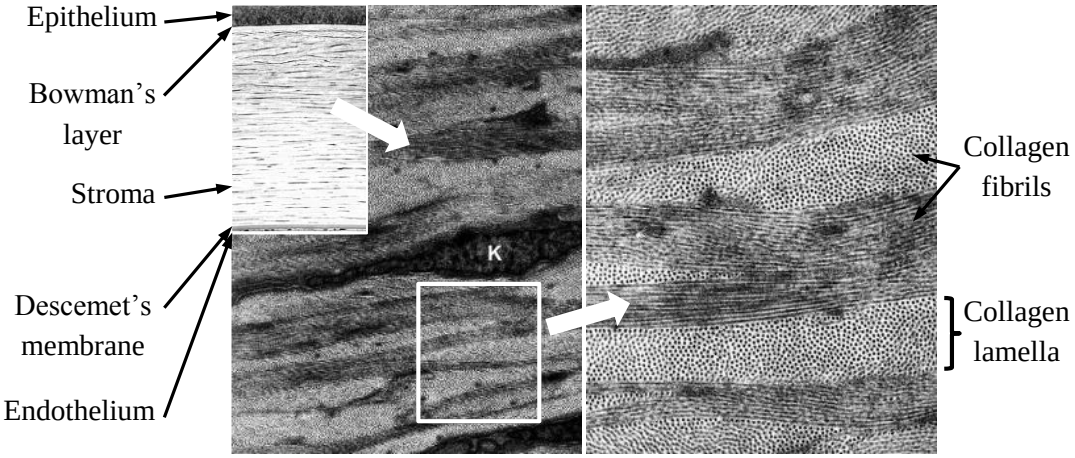

Figure 4. *The structure of the stroma. The lamellae or layers are constructed from regularly packed collagen fibrils and the lamellae are at right angles to one another. K represent stromal keratocyte. (Adapted from Hassell & Birk 2010 and Ruberti & Zieske 2008)*

The cells in the stroma, keratocytes, are mesenchymal cells of neural crest origin, and are normally quiescent in a healthy stroma (Dhouailly et al. 2014; West-Mays & Dwivedi 2006). The cells have compact cell body but are attached to the organised ECM with numerous plasmic lamellipodia. This sort of structure gives keratocytes a dendritic morphology and advantageous shape to reduce light scattering. Also the cells contain crystalline proteins in their cytoplasm which further reduce light scattering. (Hassell & Birk 2010) Keratocytes reside between the lamellae but mainly in the anterior stroma (DelMonte & Kim 2011). Keratocytes maintain the ECM structure of the stroma and are

responsible for developing the tissue by synthesising important structural components such as collagen molecules, GAGs and matrix metalloproteinases (MMPs) (DelMonte & Kim 2011; Petroll & Miron-Mendoza 2015). All of these synthesised components are essential for maintaining the stromal homeostasis (DelMonte & Kim 2011).

2.1.3 Corneal endothelium

The most posterior layer of the cornea is the endothelium. A healthy human corneal endothelium is a monolayer and the endothelial cells resemble a honeycomb-like mosaic structure, shown in Figure 5. During foetal development the endothelium is orderly arranged and the cells obtain a cuboidal morphology creating approximately 10 µm thick layer. Over time, the cells become more adherent to each other and flatten creating a thin but tight monolayer that is approximately 4 µm thick. As an adult, an individual has approximately 3 000 to 5 000 endothelial cells/mm^2. (Bartakova et al. 2014; Espana et al. 2015) The cells have extensive lateral interdigitations as well as gap and tight junctions. Numerous hemidesmosomes in the basal endothelium provide adhesion to the Descemet's membrane. (DelMonte & Kim 2011)

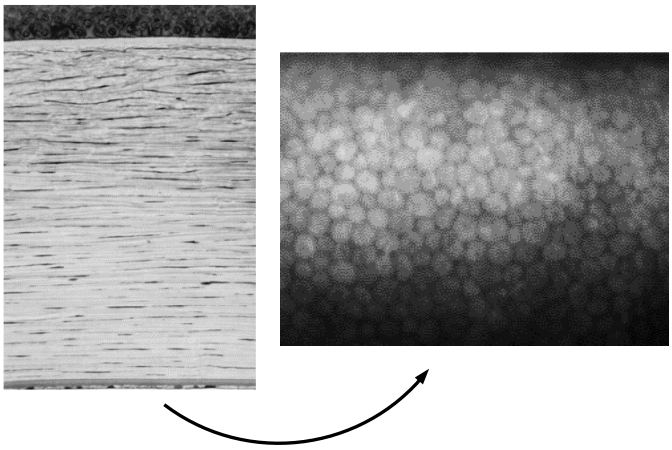

Figure 5. *A healthy corneal endothelium is a monolayer of hexagon shaped endothelial cells. (Adapted from Rio-Cristobal & Martin 2014 and Ruberti & Zieske 2008)*

The main purpose of the endothelium is to function as a metabolic pump that removes excess water but keeps the stroma well hydrated. The constant level of stromal hydration at around 78 % is essential for keeping the whole cornea transparent. (DelMonte & Kim 2011; Ghezzi et al. 2015) The regulation of nutrient balance and removal of excess water are mediated by diffusion through tight junctions and with active pump-leak process. The active pumps remove water from stroma towards the aqueous humour of the eye. (Bartakova et al. 2014; DelMonte & Kim 2011)

The morphology of the endothelial cells has a distinctive impact on the pump function. Variation in the shape and size of the cells correlate negatively with ability to maintain stromal deturgescence. The morphology of corneal endothelial cells can change with aging, due to a trauma or other disease that may cause a decrease in cell number, because the cells have virtually no mitotic activity *in vivo.* To cope with the loss, the cells have a capacity to stretch to take over the gaps left behind by the degenerated cells. In this process, the cells get thinner and may lose their hexagonal shape. An average decrease of cell density in healthy endothelium proceeds with the rate of 0.6 % per year. (DelMonte & Kim 2011)

2.1.4 Bowman's layer and Descemet's membrane

Bowman's layer (also known as Bowman's membrane or anterior limiting lamina) is a layer of acellular amorphous condensed collagen fibrils located immediately below the epithelial basement membrane (Ghezzi et al. 2015; Wilson & Hong 2000). The layer contains mainly types I, III and V collagens and also type VII collagen has been found from the anchoring fibrils within the Bowman's layer to the epithelium (Wilson & Hong 2000). This interwoven collagenous structure is a smooth layer approximately 15 µm thick, and helps the cornea to maintain its shape. If the layer is damaged or otherwise disrupted, it will not regenerate and the damaged part will form scar tissue. (DelMonte & Kim 2011)

Descemet's membrane is located between the corneal stroma and the corneal endothelium. The membrane thickens with age from about 3 µm at birth, up to 8-10 µm in adults and is rich in collagen types IV and VIII. (Massoudi et al. 2015) This type of membrane gives an anchoring structure for the endothelial layer (DelMonte & Kim 2011; Ghezzi et al. 2015). The development of the membrane begins early during foetal development and in this process corneal endothelial cells begin to secrete highly organised collagen. This highly organised part of the membrane is called the banded region. The rest of the membrane is secreted as the individual ages, and it has less organised amorphous texture. This region that is created after birth is called the amorphous region and it is located between the banded region and the endothelium. (DelMonte & Kim 2011)

2.2 Mechanical and optical properties of the cornea

From the perspective of material science, the cornea is a complicated anisotropic composite with viscoelastic and non-linear elastic properties due to its heterogeneous structural components of different corneal layers. The overall structure of these components is not directionally uniform since the dimensions of the cornea vary from central to peripheral and anterior to posterior. (Drupps & Wilson 2006)

Material stiffness and the optical properties of the cornea are dependent mainly on the microstructure of the stroma due to its highly organised PG rich collagen fibril matrix (Drupps & Wilson 2006; Lewis et al. 2016). If this highly ordered structure of the corneal tissue is diseased or damaged, there is a direct causal connection of degradation between mechanical and optical properties (Drupps & Wilson 2006; Whitford et al. 2015). The topography and thickness have a strong effect on mechanical stiffness of the cornea which means how well the cornea resists deformation of the shape and curvature. It is important for cornea to keep its distinct shape intact since it accounts for more than two thirds of the optical power of the eye. After the shape, the most important features of the cornea for optical properties are regularity, clarity and refractive index. (Whitford et al. 2015)

The mechanical properties for healthy human cornea are presented in literature with the following values. The corneal tensile strength is 3.81 ± 0.40 MPa according to measurements performed by Zeng et al. (2001) and elastic modulus varies from 3 to 16 MPa, depending on the measurement method (Ahn et al. 2013; Rafat et al. 2008). The main optical properties of the cornea are its refractive index of 1.375 to 1.380 and light backscatter of approximately 3 % (Deng et al. 2013). The cornea transmits over 90 % of white light and its structure causes most of the light to scatter at angles larger than 30° (Hatami-Marbini 2015).

2.3 Healing mechanisms of the cornea

The healing mechanism of the cornea is a complex process which involves cellular changes and interlayer molecular cell signalling, especially between the epithelium, epithelial basement membrane and stroma (Qazi et al. 2010; Kobayashi et al. 2015). It is regulated by growth factors, soluble cytokines and ECM components which have been shown to act as autocrine and paracrine factors (Lim et al. 2003; Ljubimov & Saghizadeh 2015; Kobayashi et al. 2015). The healing mechanism of the cornea depends on the type of injury and how deep the injury reaches into the corneal layers. Injuries vary from touching the epithelium to full-thickness penetrating injuries. Most common injuries of the cornea are mechanical, but also chemical and thermal injuries are possible. (DelMonte & Kim 2011) During the wound healing process, the overlaying tear film lubricates the cornea and provides nutrition, protection and growth factors (Lim et al. 2003).

In case of mechanical epithelial injury, if any part of an individual cell is disrupted, the whole cell will be lost. This leaves a defect or a break in the layer which causes anatomical and biochemical cellular function alterations so the cells around the defect could try to cover the area by cell migration and spreading. Changes in the cells include creating membrane extensions for the spreading and disappearance of the hemidesmosome adhesions allowing basal cell migration. This kind of non-mitotic wound coverage can progress at a rate of 0.75 to 1 µm per minute. (DelMonte & Kim 2011; Lim et al. 2003) The first migrating cells are thought to pull the epithelial sheet behind them over the defect for coverage as the cells migrate and attach to the underlying substrate. The ECM

proteins fibronectin and vitronectin have been found to be essential elements for this cell-substrate binding and cell migration. (Chow & Di Girolamo 2014; DelMonte & Kim 2011) Approximately 24 to 30 hours after the injury, cells begin to proliferate through mitosis to restore the epithelial cell population. As mentioned in Chapter 2.1.1, the only cells capable of mitosis are the basal epithelial cells and LESCs. (DelMonte & Kim 2011)

If the damage reaches the deeper layers, breaching the Bowman's layer and the stroma, the homeostasis of the whole cornea is endangered (DelMonte & Kim 2011). The acellular Bowman's layer is not able to regenerate after injury (Massoudi et al. 2015). Stromal wound healing is similar to the skin wound healing and it has three distinct phases: repair, regeneration and remodelling (DelMonte & Kim 2011). In normal state, keratocytes are quiescent which means that the cells have dendritic morphology and they do not express stress fibres or generate contractile forces (West-Mays & Dwivedi 2006). If the stroma undergoes a trauma, the damaged cells undergo apoptosis (DelMonte & Kim 2011). The first reaction to this situation is the activation of the quiescent keratocytes which is thought to be the primary wound healing process. The cells are activated by cytokines present in the wound area (Lim et al. 2003) and they enter into the cell cycle and start to transform into fibroblasts (Kobayashi et al. 2015; West-Mays & Dwivedi 2006). These corneal fibroblasts proliferate and develop stress fibres. The cells migrate to the wound site and begin reorganisation of the stromal ECM by using mechanical forces. (Lakshman et al. 2010; Petroll & Miron-Mendoza 2015) The activation and migration of the keratocytes can occur within hours after the injury has happened (DelMonte & Kim 2011).

The remodelling of the stromal tissue begins within one to two weeks from injury. Part of the keratocytes transform to myofibroblasts as a response to transforming growth factor beta (TGFβ) secretion by the epithelial cells in stress situations. (West-Mays & Dwivedi 2006) It has been hypothesised that basement membrane functions as a barrier between the epithelium and the stroma by modulating the amount of growth factors released to the stroma by the epithelial cells (Torricelli et al. 2013). As the cells transform to myofibroblasts, these cells can be distinguished from fibroblasts due to their larger size and expression of α-smooth muscle actin (α-SMA). These cells are found at the injury site, where they are thought to be responsible for strong mechanical wound contraction (Petroll & Miron-Mendoza 2015) as well as ECM deposition and organisation. (West-Mays & Dwivedi 2006) The cells secrete MMPs, collagenase and cytokines, all found to be important factors in remodelling of the stromal tissue. The remodelling process may take from months to years and still the resulting tissue may retain decreased corneal clarity. (DelMonte & Kim 2011)

Usually, if endothelium is injured, it is caused by full-thickness penetrating injury or due to rapid focal distortion of this cellular layer. It has been long believed that human endothelial cells are not able to undergo mitosis *in vivo* which means that the layer cannot be repaired through proliferation of the cells. (DelMonte & Kim 2011) Although recent

studies have given some indication that possibly some endothelial cells might be able to replicate in appropriate environment, since it was discovered that transplanted cornea contained both, recipient and donor endothelial cells. Also some clinical studies have shown that human endothelial cells might replicate in periphery of the cornea and migrate to restore Descemet's membrane and the endothelial layer and this way restore corneal transparency. (Espana et al. 2015)

In case of smaller defects, the damaged areas are repaired by irregular cell enlargement of the neighbouring cells and their centripetal migration to the injured region. In this repair mechanism, the cells try to repair the incomplete barrier, compensate for the reduced pump functions and restore tight junctions. These actions aim to return the homeostasis and transparency of the cornea. Lastly is the remodelling of the enlarged endothelial cells to regular hexagons which may take several months. In case of more severe trauma, this type of repair mechanism is not enough to restore the layer. It is very possible that in more severe cases also the underlying Descemet's membrane is damaged and needs to be repaired. If the cells undergo greater stress, the state may cause cell loss and irreversible alterations to the cytoskeleton of the endothelial cells. (DelMonte & Kim 2011) One probable alteration is the loss of optical clarity and the only way to treat endothelium related vision loss is transplantation (Ozcelik et al. 2013).

As a conclusion, the healing mechanisms of different corneal layers are complex and the processes may take from months to years. The cells of each layer are in key role regenerating and repairing the damaged areas, and small-scale repairs with good results are possible. All of the corneal layers must heal for the corneal transparency to be retained but if the damage is too large for the cells to handle, usually the injured cornea does not return to its original transparency or tensile strength. This means that the patient's vision is compromised, either partially or completely. (Qazi et al. 2010)

2.4 Damages and diseases

Mainly corneal damages are mechanical, since the cornea is the outermost layer of the eye which is exposed to the environment and most likely to get damaged due to various mechanical insults (Ljubimov & Saghizadeh 2015). However, thermal burns and chemical injuries are also common, especially in developing countries (DelMonte & Kim 2011). Chemical injuries can vary from mild irritation to complete destruction of the corneal tissue. Depending on the invading reagent, the chemical injuries are divided to traumatic acidic and more severe alkaline damages. Acidic damages cause corneal tissue to become denaturised and precipitated to prevent further penetration of the chemicals to cause more damage. Due to this preventive reaction, damages usually affect only the superficial layers. In alkali burns, strong alkalis cause cellular disruption due to saponification of cell membrane fatty acids, which causes the chemicals to penetrate to corneal stroma. In stroma, alkalis destroy GAGs around the collagen fibres which collapses the ECM structure of the stroma. Both of these chemical injury types can cause

severe tissue necrosis and inflammation with poor healing capacity, usually causing scarring and blood vessel growth, neovascularisation (NV). (Tsai et al. 2015)

Furthermore, there are also numerous diseases endangering corneal health, some of these diseases affect the whole cornea and some particular layers of it, some alter physical appearance and some cellular properties. The diseases may be hereditary, congenital, age-related or caused by infections and unhealthy lifestyle choices or prolonged contact lens wear. (Meek & Knupp 2015; DelMonte & Kim 2011; Tsai et al. 2015) Infectious diseases can be caused by pathogens such as bacteria, fungi and viruses, and even when properly treated may cause scarring and corneal thinning (Tsai et al. 2015).

One of the most common corneal diseases, mainly affecting the corneal stroma, is keratoconus which develops progressively due to elevated internal pressure of the eye and causes abnormalities in the structure, composition and changes in optical and mechanical properties (Ambekar et al. 2011). It is characterised as non-inflammatory irreversible deterioration of the corneal structure, leading to localised loss of corneal tissue even up to 75 % from full thickness (Gefen et al. 2009). The shape of the cornea turns to more conical which leads to distorted vision, thinning and scarring of the cornea. The compositional changes include changes in the amounts of GAGs, collagens and keratocytes which lead to structural changes in the highly organised collagen ECM. (Ambekar et al. 2011; Gefen et al. 2009) The main causes involved in development of keratoconus are believed to be genetics, sunlight overexposure, chronic eye irritation and continuous use of ill-fitting contact lenses (Gefen et al. 2009).

As one very concerning condition, limbal stem cell deficiency (LSCD) is a disease that leads to decreased renewal of corneal epithelium, recurrent erosion, epithelial ingrowth and destruction of basement membrane. LSCD is caused either by destruction of LESCs due to a damage, or disruption of the LESC niche. As the renewal of the corneal epithelium is limited, conjunctival tissue proliferates to replace the damaged corneal tissue. This leads to opacification and vascularisation of corneal tissue, causing vision loss, photophobia and pain. (Haagdorens et al. 2016; Notara et al. 2010; Wright et al. 2013)

One example of epithelial diseases resulting in LSCD is aggressive Stevens-Johnson syndrome (SJS). It is a severe acute inflammatory disease which is associated with infections agents that cause mucocutaneous blistering of mucosal tissue. On the ocular surface it causes strong inflammatory reaction followed by difficult epithelial defects such as epithelial breakdown with ulceration, blinding infections, keratopathy, dry eye, perforation and LESC failure. (Ueta et al. 2008; Williams et al. 2013; Notara et al. 2010) Other damages and diseases affecting corneal layers are for example chronic inflammatory conditions such as sicca disease, cicatricial diseases, ocular mucous membrane pemphigold, and herpetic infections, corneal opacities and bullous keratopathy (Avadhanam et al. 2015; Notara et al. 2010). There are also some genetic disorders that

affect corneal health such as different types of corneal dystrophies and aniridia, which both cause structural abnormalities (Hingorani et al. 2012; Klintworth 2009).

All of the diseases affecting corneal health endanger the homeostasis and transparency of the layered corneal tissue and usually partial or complete loss of vision is a possible outcome. Some diseases may be treated, but mostly the diseases are slowly progressing and conditions that are difficult to treat and require novel and effective approaches that tissue engineering possibly can provide.

3. PROSPECTIVE BIOMATERIALS, ONGOING RESEARCH AND APPLICATIONS

Tissue engineering is a fast developing field that combines biomaterials and cells to create artificial substitute tissues to replace damaged and diseased parts of the human body. This field gives patients with difficult conditions a new chance in life with innovative discoveries. In the field of corneal tissue engineering, the aim of these artificial substitutes is to bring new treatment options for corneal patients alongside conventional donor transplants.

At the moment there are numerous different approaches for creating an artificial biomaterial-based cornea as the substitutes may be developed to replace the whole cornea or just parts of it (Ghezzi et al. 2015). The properties of the substitutes can be refined to resemble the functionalities of native tissues, promote healing and regeneration of damaged sites and in the end possibly be replaced by patient's own tissue. The ideal situation is a biocompatible biomaterial-based substitute tissue which would contain patient's own cells. The use of patient's own cells would eliminate the risk of tissue rejection which is a highly possible and harmful outcome of allogeneic tissue transplants.

This chapter first discusses the current state of corneal tissue engineering, and problems associated with the use donor tissues. The chapter continues to requirements of a corneal substitute and potential biomaterials for an artificial tissue engineered corneal application. After this, focus turns to corneal research, approaches and recent advances. Relevant biomaterials and especially the use of polymeric hydrogels are presented and how these materials support and interact with human corneal cells, especially with epithelial and stromal cells, since these layers are the main focus in this thesis. Most of the examples about the research and the biomaterials presented here are naturally occurring in the cornea, such as collagen, but some synthetic approaches are introduced as well. The main focus of this chapter is to understand the options that tissue engineering can provide for this specific field of research and what are the requirements for a tissue engineered cornea substitute.

3.1 Current state of corneal tissue engineering

The use of allogeneic corneas is still necessary and the best solution to treat patients suffering from corneal diseases, since there is no superior tissue engineered solution yet (Deng et al. 2010). Fortunately, corneal transplantations have high success rate, but the patients need immunosuppressive medication to avoid tissue rejection and it can take years for the transplants to retain their clarity after transplantation. Usually the transplanted corneas suffer from NV, which impairs the transparency of the cornea. (Qazi

et al. 2010; Tsai et al. 2015) NV can also occur during normal wound healing after injury which was explained in Chapter 2.3. This may be induced during the healing process due to several inflammatory, infectious and traumatic corneal disorders. Angiogenic cytokines induce NV which causes ECM degradation and endothelial cell invasion with inflammatory cells to the stroma. The endothelial cells begin to form blood vessels to the cornea impairing its transparency. (Qazi et al. 2010)

In corneal tissue engineering, the clinical standard for regenerative approach is the use of human amniotic membrane (AM). This was first reported by de Roth in 1940 as a treatment to corneal chemical burns. The AM is the inner avascular layer of the foetal sac which is composed of amniotic epithelial cells, a thick basement membrane and an avascular stroma. This foetal membrane has anti-scarring and anti-inflammatory properties and also contains numerous growth factors that promote epithelial cell growth and the healing process of a damaged cornea. (Bray et al. 2011; Nakamura et al. 2016; Rahman et al. 2009) The AM can function as a biological dressing to help the epithelium to heal, or it can be applied in corneal tissue engineering as a cell culture platform or a scaffold due to its advantageous properties. (Rahman et al. 2009) Nevertheless, the AM and donor corneas have some concerning disadvantages since these are tissue grafts from another person, who is genetically different from the tissue recipient. These disadvantages include disease transmission possibility, as well as physiological and biological variations depending on the donor, low availability and high cost of the tissues. (Bray et al. 2011; Rahman et al. 2009)

From medical point of view, one treatment option for damaged and diseased corneas is use of keratoprostheses (KPro) if donor transplants have failed or otherwise patient is not a suitable donor recipient. KPros are implantable corneal devices made from different materials such as polymethylmethacrylate (PMMA) and titanium but these are used only in end-stage corneal blindness when no other options are available. KPros can be categorised to three groups depending on the fixation method: collar-stud devices where cornea is between two skirt plates such as Boston KPro, intracorneal skirt inside stromal layers such as AlphaCor and epicorneal device in the surface of cornea and sclera such as osteo-odonto-KPro. However, the survival rate of these implantable devices is quite poor, and the risk of severe complications is very high, hence these should be considered only as a final option. (Avadhanam et al. 2015)

Due to concerns related to use of donor tissues and implantable corneal devices, these cannot be considered as viable and long-term solutions. The problems associated with these treatment methods have further encouraged the development of alternative synthetic membrane matrices from biomaterials such as collagen and other polymers for corneal reconstruction. (Nakamura et al. 2016; Rahman et al. 2009)

3.2 Ideal properties of a tissue engineered cornea

The most important factors to be considered for a functioning corneal application were summarised well by Ghezzi et al. (2015): the replacement should provide protection, the finished application should be transparent and also, it should function as an optical interface with substantial refractive power. Additionally, the application should withstand the intraocular pressure and maintain the structural integrity of the eye (Grinstaff 2007). Ideally, the materials used in a tissue engineered scaffold with suitable mechanical and chemical properties would be biodegradable and match the properties of the target tissue. Optimal biomaterial scaffold would contain important cytokines, growth factors and other molecules that promote tissue regeneration postoperatively. (Chen & Liu 2016; Deng et al. 2010; Malafaya et al. 2007)

In research and applications, which will be introduced shortly, different biomaterials are used as scaffolds. If cells are used in the application, the vitality of the cells is examined carefully since biomaterials affect cell behaviour. It is important to comprehend how the studied biomaterials and their chemical and biophysical properties such as stiffness, topography and biodegradation by-products may affect the cell behaviour properties such as cell adhesion, morphology and differentiation. (Tocce et al. 2010) In a successful approach, the chosen biomaterial-based scaffold would function as a surface for cells to proliferate, secrete, and organise collagen-based ECM (Gil et al. 2010). Also the scaffold would mimic corneal structure to direct growth and regeneration of the tissue until it is replaced by the native tissue (Drury & Mooney 2003).

3.3 Biomaterials

Usually the studied biomaterials for corneal applications are in the form of hydrogels or films prepared from biodegradable polymers. Polymers may be natural or synthetic, and either polysaccharide or protein-based, such as collagen, chitosan and HA (Diao et al. 2015; Gil et al. 2010; Malafaya et al. 2007). Protein-based polymers mimic ECM and direct cell migration, growth, and organisation during wound healing and tissue repair. Polysaccharide-based polymers are natural non-toxic, low-cost, biocompatible biomaterials. (Malafaya et al. 2007)

Natural polymers are very attractive biomaterials in tissue engineering, due to their biocompatible, biodegradable and bioactive properties. As a disadvantage, natural polymers have some limitations in material performance: they may lack proper mechanical strength, suitable degradation profile and durability as a long-term solution. Usually, natural polymers need further modifications to obtain better suited material properties. (Jiang et al. 2014; Malafaya et al. 2007) Natural polymers are usually derived from animal (protein polymers) or bacterial (polysaccharide polymers) sources and these materials suffer from weaknesses such as chemical heterogeneity, variations in mechanical properties and may even evoke immune response due to contamination risk

of foreign proteins, viruses and bacterial endotoxins (Chen & Liu 2016; Boeriu et al. 2013; Stoppel et al. 2014).

Meanwhile, synthetic polymers can be produced with well-defined tailored properties such as architecture, mechanical modulus, tensile strength and degradation speed depending on the target use (Chen & Liu 2016). Mostly synthetic polymers are safe since there is no risk of immune response due to foreign biological components but also due to this fact, lack the aspect of biocompatibility. Also as a downside, degradation products of the materials may be acidic and cause change of pH in the surrounding environment in the body and this way alter cell behaviour and even cause inflammatory symptoms. (Chen & Liu 2016; Stoppel et al. 2014) To improve biocompatibility, synthetic polymers may be modified by incorporating biologically active domains to enhance cell-material interactions such as adding a collagen coating to improve cell attachment and viability. The modifications enable the synthetic polymers to mimic cellular ECM materials and influence cell behaviour. (Chen & Liu 2016)

Hydrogels are hydrophilic polymeric networks that are able to absorb and retain up to thousands times their dry weight in water (Hoffman 2002; Kopěcek 2007). Hydrogels can be prepared from either natural or synthetic polymers, or composites of both and can be homopolymers and copolymers (Zhu & Marchant 2011). Dry hydrogel first binds water to its polar and hydrophobic sites and continues to bind additional *free water* due to osmotic driving force until it reaches swelling level equilibrium, which is material dependent. The distinct 3D matrix network structure is crosslinked together either chemically of physically. In chemical crosslinking, covalent bonds form stable hydrogels whereas physical crosslinking includes hydrogen bonding, hydrophobic interaction and entangled chains which prevent polymer chain dissociation. (Annabi et al. 2012; Zhu & Marchant 2011) Physically crosslinked hydrogels are formed due to environmental changes such as pH and temperature (Annabi et al. 2014). Basic macromolecular structure varies since there can be crosslinked or entangled networks, linear, block and graft copolymers, interpenetrating networks and blends (Hoffman 2002).

Hydrogels are very attractive for tissue engineering since they provide soft tissue-like environment and allow diffusion of nutrients and cellular waste through the polymeric network (Annabi et al. 2014; Zhu & Marchant 2011). Hydrogel networks may include varying sized pores and interconnected pore structures which can be utilised in tissue engineering to accommodate cells, growth factors, and drugs (Hoffman 2002). Also, hydrogels have many advantageous properties over other polymeric scaffolds in tissue engineering since almost all properties of hydrogels are tuneable depending on the material or its composition, properties such as biodegradability, mechanical strength, shape, pore size and water content. Especially for tissue engineering purposes, hydrogel matrices provide biocompatible aqueous and protecting environment for the cells and can be easily modified with cell adhesion ligands. (Annabi et al. 2014; Hoffman 2002; Zhu & Marchant 2011) The highly hydrated and soft structure of hydrogels makes them a very

attractive option especially for scaffolds in ophthalmic research (Zhu & Marchant 2011). However, other forms of polymers besides hydrogels are also used. The following chapters present the most widely researched and promising natural polymers of corneal research at the moment.

3.3.1 Protein-origin polymers

Collagens are a major structural element of connective tissues and the most abundant proteins found in ECM, which contribute to the stability and integrity of tissues (Gelse et al. 2003). Collagen is a generic term for proteins that are formed from triple helix of polypeptide α-chains, and 27 genetically distinct types of collagen have been described (Gelse et al. 2003; Malafaya et al. 2007). The different types of collagens are present in different tissues of the body, but overall the most abundant collagen is type I, fibril forming collagen, found in almost all tissues. Type I-VI, VIII, IX, XII-XIV, XX and XXIV collagens have been found from different structures of the eye. (Gelse et al. 2003; Hayes et al. 2015)

Collagens are known to bind growth factors and cytokines, and therefore to influence cellular microenvironments, wound healing and tissue repair. In tissue engineering, different types of collagens are widely used due to excellent biocompatibility and properties such as biodegradability and low immunogenicity. (Gelse et al. 2003) As drawback, crosslinking of collagens is often necessary to obtain suitable mechanical and water-uptake properties, as well as degradation profiles appropriate for different tissue engineering applications. (Malafaya et al. 2007) Collagens are mainly isolated from animal tissues that may cause immune response, but recombinant collagens can be produced by transfected mammalian cells, mice, silk worms, *Escherichia coli*, yeast and insect cells. Recombinant collagens are found to have more consistent properties and also the risk of immune response is lower compared to animal-derived collagens. (Malafaya et al. 2007; Liu et al. 2008)

Collagen-derived **gelatin** is a biocompatible and biodegradable natural polymer that contains glycine, proline and 4-hydroxyproline residues. It is a denatured protein which can be obtained by acid or alkaline processing of collagen, but in the process it loses the antigenicity of collagen. Gelatin-based hydrogels can be prepared by chemical crosslinking of acidic or basic gelatin and the degradation profile can be tailored by altering the water content of the resulting hydrogels. As a biomaterial, it is widely used as a carrier for various biomolecules, such as growth factors or drugs, and the release happens as the hydrogel degrades enzymatically in the body with time. (Malafaya et al. 2007)

Silk is produced by *Bombyx mori* silkworm and depending on the extracting methods, its biological and physical properties vary. Silk has been used for a long time as a surgical suture material, and more recently also for tissue engineering due to its material stability,

mechanical robustness, biocompatibility and slow degradation rate (Malafaya et al. 2007). The main useable components for tissue engineering purposes are fibroin, a fibrous core protein of silks, and sericin, a glue-like protein that surrounds fibroin. Fibroin is composed of three components: fibroin H-chain, fibroin L-chain and fibrohexamerin. (Chen et al. 2013; Malafaya et al. 2007) It is the strongest and toughest natural fibre and it can be fabricated to films or membranes, 2D or 3D, with varying thicknesses, that have excellent optical transparency (Perry et al. 2008). These kinds of silk-based films have been found to support cell adhesion and proliferation, and to direct cell and ECM alignment with the help of surface patterning (Gil et al. 2010).

3.3.2 Polysaccharide-origin polymers

Hyaluronic acid, *in vivo* as polyanion **HA**, is a naturally occurring highly hydrophilic and biocompatible polysaccharide found mainly from extra and pericellular matrices of soft connective tissues such as vitreous body, skin, umbilical cord and synovial fluid (Malafaya et al. 2007; Necas et al. 2008; Rah 2011). Hyaluronic acid is a high molecular weight, linear and unbranched polymer, structured from repeating disaccharide units: β1-4D-glucuronic acid (G1cA) and β1-3 N-acetyl-D-glucosamine (G1cNAc). It is a member of a group including similar polysaccharides, GAGs and mucopolysaccharides, which are known as connective tissue polysaccharides. HA has unique viscoelastic properties and excellent water-retaining properties and influences the distribution of water in connective tissues, such as corneal stroma, epithelium, tears and the vitreous body of the eye. (Malafaya et al. 2007; Rah 2011) It is believed also that HA has anti-inflammatory properties that promote wound healing and regeneration (Laurent & Fraser 1992; Necas et al. 2008).

Despite its excellent biocompatibility and biodegradability, HA needs to be modified to be suited for tissue engineering applications due to its softness and short half-life *in vivo.* HA is usually chemically modified to adjust the degradation profile and mechanical properties better suited for tissue engineering applications. (Dicker et al. 2014; Jia et al. 2006) High molecular weight HA is mainly produced with two methods, extraction from animal tissues and microbial fermentation using bacterial strains such as streptococcus bacteria. As a disadvantage, these methods carry the risks of contamination with foreign proteins, viruses and bacterial endotoxins. To avoid these risk factors, more recently a small-scale method has been developed, enzymatic HA synthesis, in which contamination-free HA is produced with polymerisation of uridine diphosphate (UDP) glucose monomers. (Boeriu et al. 2013)

Biopolymer **chitosan** is a biocompatible and biodegradable linear polysaccharide. It is deacetylated form of chitin, which is obtained from the shells of shrimp and other crustaceans. Chitosan is a cationic polymer containing copolymers β(1→4)-glucosamine and N-acetyl-D-glucosamine, that has biofunctional, non-antigenic and non-toxic properties that support cell adhesion, proliferation and differentiation. (Grolik et al. 2012;

Malafaya et al. 2007) The amino and hydroxyl groups of chitosan can be chemically modified to bring versatility to the material and also crosslink chitosan-based hydrogels to obtain better mechanical properties and prevent enzymatic degradation. As chitosan is used in tissue engineering, it is important to note the pH dependent solubility of the material: chitosan dissolves easily in low pH, but is nearly insoluble in high pH. (Malafaya et al. 2007)

Gellan gum (GG) is a high-molecular weight linear anionic exopolysaccharide secreted by *Sphingomonas elodea* bacterium and it is constructed from repeating tetrasaccharide units: β-D-glucose, β-D-glucuronate, β-D-Glucose and α-L-rhamnose with carboxylic groups (Malafaya et al. 2007; Osmałek et al. 2014). GG was originally used as a food additive, but more recently it was discovered to be biocompatible and useable as an injectable hydrogel, forming transparent heat-resistant gels and promoting cell viability and functionality. (Gong et al. 2009; Malafaya et al. 2007; Osmałek et al. 2014) GG has been utilised in many tissue engineering applications and in ophthalmology, it has been mainly used as thickening ophthalmic tear fluid due to its suitable physical and gelling properties (Osmałek et al. 2014). It is a thermosensitive gel and its gelation temperature of +42 °C is quite high for the human body. It means that the gelling point of GG needs to be reduced, which can be done for example by decreasing molecular weight, usually with chemical scissoring. (Gong et al. 2009)

3.4 Ongoing research and applications

This chapter presents the relevant and more recent approaches to corneal tissue engineering. Mainly the research concentrates on natural polymers such as collagen, chitosan, HA and silk, and some approaches research the possibility of using composites and blends of these and other materials. Different cell lines are used to test biocompatibility of these different biomaterials *in vitro*. Suitable cell lines are especially HCEs and HCKs, but also other cell lines are used such as endothelial cells and different types of human limbal cells: epithelial cells (HLEs) and fibroblasts (HLFs), as well as stem cells such as LESCs and mesenchymal stem cells (MSCs).

As it can be seen from Table 1, there are quite many approaches that concentrate on animal-derived collagens such as bovine, porcine and rat, but also human recombinant type I and III collagens (RHCI, RHCIII) are tested. Collagens are usually crosslinked with water-soluble *N*-(3-dimethylaminopropyl)-*N'*-ethylcarbodiimide (EDC), due to its low toxicity and the crosslinking efficiency is improved with *N*-hydroxysuccinimide (NHS), also crosslinkers such as poly(ethylene glycol) diacrylate (PEGDA) and *N*-cyclohexyl-*N'*-(2-morpholinoethyl) carbodiimide metho-*p*-toluenesulfonate (CMC) can be used. (Ahn et al. 2013) Additionally, physical crosslinking methods such as ultraviolet-radiation (UV) with riboflavin and plastic compression can be used as well (Levis et al. 2010; Petsch et al. 2014; Xiao et al. 2014).

Table 1. *Collagen-based approaches to corneal tissue engineering.*

Material	Cells	Reference
RAFT optimisation	HLEs	Massie et al. 2015
• RAFT, rat-tail type I collagen constructs	HLEs, LESCs, HCEs & HLFs	Levis et al. 2013; Levis et al. 2015
• Plastic compressed rat-tail collagen I	LESCs & HLFs	Levis et al. 2010;
EDC/NHS crosslinked RHCIII	Cell-free	Fagerholm et al. 2014
• EDC & CMC crosslinked recombinant human collagen III (RHCIII) & porcine atelo-collagen I	HCEs & endothelial cells	Ahn et al. 2013
• EDC/NHS crosslinked RHCI and RHCIII	HCEs	Merrett et al. 2008
EDC/NHS crosslinked RHCIII with incorporated MPC phospholipid network	Cell-free	Hayes et al. 2015
• EDC/NHS RHCIII-MPC hydrogels		Islam et al. 2015
• EDC/NHS crosslinked RHCIII		Islam et al. 2013
NHS crosslinked pMG - porcine atelo-collagen I IPN hydrogels	HCEs	Deng et al. 2010
EDCM/NHS and PEGDA/APS/TEMED/MPC crosslinked therapeutic core-skirt porcine atelo-collagen I implants	HCEs	Rafat et al. 2016
• EDCM/NHS crosslinked porcine atelo-collagen I	HCEs & MSCs	Koulikovska et al. 2015
Micro-rough surface freeze-dried bovine collagen I films	HCEs	Liu et al. 2014a
Rat-tail collagen I fibrillated matrices	HCEs & 3T3 murine feeders	Tidu et al. 2015
UV/riboflavin and non-crosslinked equine collagen I membranes	HOMECs	Petsch et al. 2014
Plastic compressed rat-tail collagen I scaffolds with AM	Cell-free	Xiao et al. 2014

Abbreviations: APS, ammonium persulphate; EDCM, 1-[3-(dimethylamino)propyl]-3-ethylcarbodiimide methiodide; HOMECs, human oral mucosal epithelial cells; IPN, interpenetrating polymer network; MPC, 2-methacryloyloxyethyl phosphorylcholine; pMG, poly(6-methacryloyl-α-D-galacto-pyranose); RAFT, Real Architecture For 3D Tissue and TEMED, N,N,N,N-tetramethylethylenediamine.

The first presented application in Table 1 is a commercially available RAFT rapid one-step protocol for creating cellular type I collagen tissue equivalents and these can be used according to Levis et al. (2013) to model LESC niche to function as bioengineered limbal crypts. Other interesting corneal tissue engineering approach with collagen is by Fagerholm et al. (2014), cell-free RHCIII bio-interactive implants and their testing has continued already to clinical studies. These implants did not cause rejection and also repopulation of corneal cells has occurred. Histopathological tests after four year study showed normal corneal architecture. Promising results are also received from Rafat et al. (2016) study which combines two merged type I collagen hydrogel constructs, central

core and peripheral skirt, with different mechanical properties. Faster degrading skirt provides support for the slowly degrading long-term core scaffold and mainly functions as a reservoir for therapeutic substances which are released through degradation to interact with the surrounding environment to stimulate corneal regeneration.

Table 2 presents some approaches that combine collagen with different materials and components such as HA, chitosan, elastin, tobramycin and citric acid (CA). The purpose of adding these components to collagen is to improve and promote cell adhesion and proliferation. For example Duan et al. (2007) used multifunctional dendrimers to improve mechanical strength of collagen and addition of laminin-derived tyrosine-isoleucine-glycine-serine-arginine polypeptide (YIGSR) was to improve biological functionality of the material. Other interesting approach is by Liu et al. (2014b) where collagen films were coated with tobramycin to obtain anti-bacterial properties which would help resist inflammatory reactions after implantation.

Table 2. *Collagen-based approaches with other biomaterials and components.*

Material	Cells	Reference
Carbodiimide crosslinked dendrimer modified bovine collagens I & III with incorporated laminin peptide YIGSR with EDC/NHS	HCEs	Duan et al. 2007
PEG-DBA EDC/NHS crosslinked porcine atelo-collagen I and chitosan scaffolds	HCEs	Rafat et al. 2008
EDC/NHS crosslinked collagen I-gelatin-HA films	HCEs	Liu et al. 2013
EDC/NHS crosslinked antibacterial bovine collagen I - tobramycin films (Col-Tob)	HCEs	Liu et al. 2014b
EDC/NHS crosslinked collagen I - CA membranes	HCEs	Zhao et al. 2015
EDC/NHS crosslinked collagen - silk fibroin blend membranes	HCEs	Long et al. 2014

Abbreviation: PEG-DBA, poly(ethylene glycol) dibutyraldehyde.

Table 3 presents research approaches with other biomaterials besides collagen, such as synthetic polymers polydimethylsiloxane (PDMS) and poly(ester urethane) urea (PEUU). The first applications are chitosan-based membranes that are crosslinked with natural genipin due to its low toxicity and suitability with many natural polymers. Use of genipin as crosslinker increases ultimate tensile strength but slows down biodegradability. (Li et al. 2015) PDMS approach by Koo et al. (2011) is also important to understand in corneal research, since the mitotic activity of keratocytes is highly dependent on the environment. For the stroma to stay transparent, HCKs need highly ordered structure to function normally and by using grating patterned chitosan-PDMS, the effect of topography to HCK behaviour can be studied.

Lastly, there are some approaches to corneal tissue engineering that use silk fibroin as scaffold material since silk films demonstrate very good transparency but also the

material itself can be patterned to function as ECM to affects cell behaviour (Gil et al. 2010). Wu et al. (2014b) created silk substrate with tripeptide ligand arginine-glycine-aspartate (RGD) that induces HCK specific behaviour. Gil et al. (2010) uses as well RGD patterning on their silk protein lamellar system, where seven porous silk films are stacked to 3D constructs and cultured with HCKs between the films to mimic stromal tissue architecture.

Table 3. *Other biomaterial approaches to corneal tissue engineering.*

Material	Cells	Reference
Genipin crosslinked chitosan membranes	HCEs	Li et al. 2015
Genipin crosslinked chitosan membranes with, rat collagen I, elastin and hydroxypropyl cellulose	HCEs	Grolik et al. 2012
Grating patterned PDMS and chitosan membranes	HCKs	Koo et al. 2011
Laminin and fibronectin mimetic peptide - amphiphile nanofibre scaffolds	HCKs	Uzunalli et al. 2014
RGD patterned and porous 3D stacked 2 µm silk films	HCKs	Gil et al. 2010
• Surface patterned silk 2 µm films stacked to biomimetic lamellar corneal constructs	HCKs & RCFs	Lawrence et al. 2009
Patterned silk substrate with RGD surface coupling	HCSSCs & HCFs	Wu et al. 2014b
Highly-aligned fibrous PEUU substrates	HCSSCs & HCFs	Wu et al. 2014a

Abbreviations: HCSSCs, human corneal stromal stem cells; HCFs, human corneal fibroblasts and RCFs, rabbit corneal fibroblasts.

Several material characteristics need to be taken into account to create a successful biomaterial-based tissue engineered substitute. All of these studies present various important methods for measuring mechanical and optical properties, as well as the biocompatibility and degradation rates of resulting scaffolds such as implants and membranes.

For corneal approaches, the main optical properties to be measured are light transmission and scatter (Deng et al. 2010; Rafat et al. 2016) and refractive index (Hayes et al. 2015) to evaluate the suitability of the scaffold to mimic transparent outer layer of the eye. The mechanical properties of studied material should be as well measured to evaluate the suitability to be implanted to corneal tissue and how the scaffold would withstand mechanical challenges associated with cornea and also, the scaffold should survive the implantation process as mainly this can be done by suturing (Deng et al. 2010). Main mechanical characteristics to be measured are tensile strength, the maximum stress that the material can withstand, and elongation at break, the amount of strain at fracture (Fagerholm et al. 2014; Grolik et al. 2012). Other important parameters to be measured are the swelling equilibration and hydration. The swelling characteristics of the material needs to be determined since there cannot be too much changes in the size of scaffold

when it is implanted into the eye. As the cornea is a highly hydrated tissue, also the replacing material should function similarly supporting the hydrated state of the eye. (Deng et al. 2010; Ghezzi et al. 2015; Grolik et al. 2012; Li et al. 2015)

Biocompatibility is evaluated with cell culturing to study if a biomaterial provides suitable environment for the cells to stay viable and proliferate, but also cell specific behaviour needs to be studied as well. This can be done with immunofluorescence staining (IF) by using specific corneal protein markers such as CK3, CK12, p63 and Ki67 (Grolik et al. 2012; Li et al. 2015), giving vital information about the cell behaviour and protein expression, and how well it resembles corneal cells *in vivo*. Histology and structure of the scaffold with cells can be observed with histopathological haematoxylin and eosin (H&E) staining (Liu et al. 2014b; Grolik et al. 2012). The degradation rate of scaffold needs to be studied as well to see if it can match the regeneration rate of the receiving native tissue. For example, in collagen approaches this can be measured *in vitro* enzymatically with collagenase and in chitosan studies, this is performed with lysozyme. (Ahn et al. 2013; Deng et al. 2010; Li et al. 2015; Rafat et al. 2016)

Also the preparation and processing of the scaffolds are very important factors to be considered in cornea tissue engineering. These presented research approaches introduce and explain different ways to prepare hydrogels and films that mimic corneal shape. Some of the groups concentrating on collagen use 10 to 12 mm diameter and 500 µm thick curved polypropylene moulds, shown in Figure 6A (Fagerholm et al. 2014; Hayes et al. 2015). Also some approaches prepare collagen films by casting or compressing collagen-based solution between two glass plates with resulting thickness varying from 150 µm to 500 µm, shown in Figures 6B and 6C (Ahn et al. 2013; Deng et al. 2010; Merrett et al. 2008; Rafat et al. 2016). In RAFT, the collagen-based hydrogels, shown in Figure 6E, are simply prepared on a well plate (Levis et al. 2013). In chitosan-based approaches the films are mainly prepared by casting the solutions on planar surfaces such as glass plate or Petri dish (Grolik et al. 2012; Li et al. 2015). Finally, the approaches utilising silk, the silk solutions are casted on top of patterned PDMS substrates, forming films with thickness of 2 to 3 µm, such as aforementioned stacked construct of seven silk films shown in Figure 6D (Gil et al. 2010; Wu et al. 2014b).

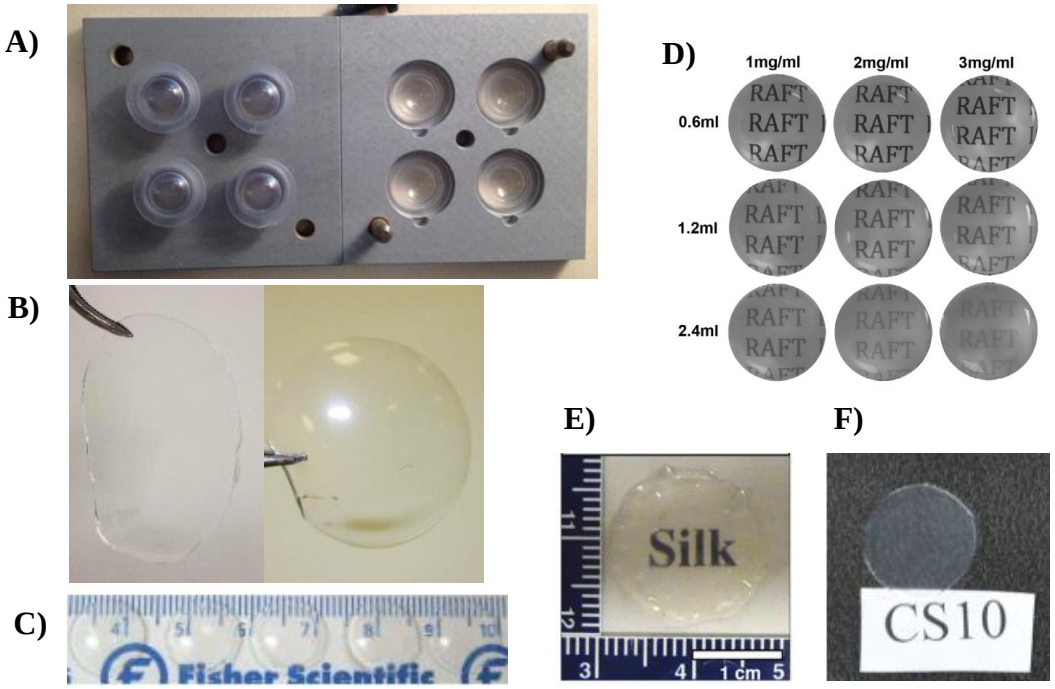

Figure 6. *A) Curved polypropylene mould with stainless steel frame, B) glass mould prepared flat collagen sheet and curved cornea-shaped implant prepared with curved polypropylene mould, C) collagen-pMG IPN hydrogels, D) RAFT with different collagen volumes and concentrations, E) stacked silk construct of seven films and F) silk fibroin reinforced collagen-based film. (In order, adapted from Islam et al. 2013; Hayes et al. 2015; Deng et al. 2010; Massie et al. 2015, Gil et al. 2010 and Long et al. 2014).*

All of the presented approaches are very innovative and it could be concluded that the research conducted so far gives strong guidelines for the future of corneal tissue engineering. Overall, it is very possible that in the near future there will be more efficient ways to treat patients suffering from corneal disorders.

4. AIM OF THE THESIS

The primary aim of this thesis was to test the suitability of different hydrogels with corneal cells. The aim was also to learn to utilise the methods such as immunostaining, cryoblock preparation, microscopy imaging and cell culturing, and possibly further optimise the protocols for future studies using hydrogels.

The experiments were conducted with two human corneal cell lines: epithelial cells, HCEs, and stromal keratocytes, HCKs. First, the proliferation and behaviour of these cell lines were tested in 2D cell culture with 5 different culture media. This medium test was performed to find suitable medium options to co-culture the cell lines in 3D cell culture with hydrogels.

The 3D cell culture with hydrogels contained five different hydrogels. The suitability of these hydrogels was studied to define how these performed with cells, influenced the cell behaviour and supported cell proliferation.

EXPERIMENTAL PART

5. MATERIALS AND METHODS

This chapter describes the experiments conducted for this thesis. The work flow and order of the experiments and analysis methods are presented in Figure 7.

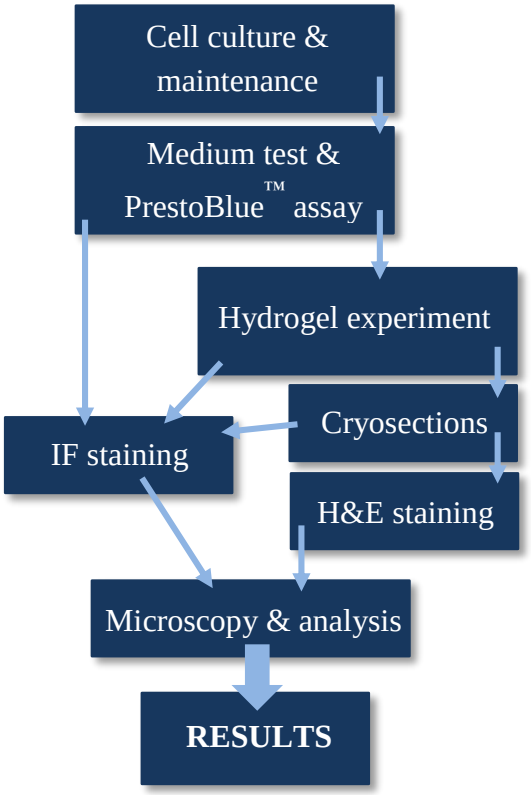

Figure 7. *The contents and order of the experimental part.*

This chapter begins with a description of the cell lines involved in the experiments and how the cell lines were maintained. Then, the first experiment, which is the medium test, is described. In this medium test, different culture media were tested with the cell lines to see their viability in different environments. This was an important preparation for the main experiment of this thesis, which was a hydrogel experiment. In the hydrogel experiment, the cell lines were co-cultured and evaluated in 3D hydrogel cultures. Both experiments were analysed with methods such as IF and H&E.

5.1 Human corneal cells

In this study, the experiments were conducted using two separate immortalised cell lines: HCEs and HCKs. Both of these cell lines were a kind gift from Professor Hannu Uusitalo at UTA.

The cell lines were maintained in Nunc™ T25 cell culture flasks (Thermo Fisher Scientific, Waltham, MA, USA). HCEs were cultured in HCE maintenance medium, modified from Greco et al. (2010), containing Dulbecco's Modified Eagle Medium (DMEM)/F12 as a basal medium with 15 % inactivated foetal bovine serum (FBS), 1x Glutamax, 5 µg/ml insulin (all from Gibco®, Thermo Fisher Scientific) and 10 ng/ml epidermal growth factor (EGF) (PeproTech, Rocky Hill, NJ, USA). HCKs were cultured in commercial Chemically Defined Keratinocyte Growth Medium (KGM-CD™, Lonza Ltd, Basel, Switzerland), supplemented with the supplements provided by the manufacturer (Manzer et al. 2009). Both of the culture media were supplemented also with 1 % penicillin/streptomycin (Lonza Ltd). The media for these cells were changed 3 times a week and they were subcultured when confluent, once or twice a week.

Subculturing of both cell types was performed with the following protocol. The culture flask was first washed twice with phosphate-buffered saline (PBS) (Lonza Ltd) and detached with 2 ml of TrypLE™ Select (Gibco®, Thermo Fisher Scientific), HCEs for 5 minutes and HCKs for 6 minutes at +37 °C. The cells were then collected with pre-warmed medium to a 15 ml Falcon tube. The cells were centrifuged 1000 rpm for 5 minutes to a pellet and supernatant was carefully removed. The pellet was resuspended in 1 ml of medium and 100 000 - 150 000 cells were passaged to new T25 flasks.

5.2 Medium test and PrestoBlue™ proliferation assay

This medium test was conducted before the hydrogel experiment to find a culture medium suitable for both cell lines, HCEs and HCKs. The aim is to use the best medium option to co-culture these cell lines in the hydrogel experiment, described in Chapter 5.4.

There were three commercial options for the medium test: CnT-20, CnT-30 and CnT-Prime-CC (CELLnTEC Advanced Cell Systems AG, Bern, Switzerland). CnT-20 is a proliferation medium formulated for corneal epithelial cells. CnT-30 is a differentiation medium for the induction of stem cells to be differentiated to corneal epithelium. Both of these media have the same basal medium which contains amino acids, minerals, vitamins and organic compounds. CnT-20 and CnT-30 are fully defined, low calcium and serum-free formulations, and both of the media are supplemented with supplements provided by the manufacturer, as well as 1 % penicillin/streptomycin. At the time of this study, CnT-Prime-CC was a new product, only available for testing. The formulation of this medium is proprietary but intended for keratinocyte and fibroblast co-culturing. For comparison of cell viability and behaviour, also both HCE and HCK maintenance media were tested, adding up to 5 different media altogether. This medium test was repeated three times to get comparable results with three different cell passages.

The medium test was carried out on a Nunc™ Delta Surface 48-well plate with culture area of 1.1 cm^2 per well (Thermo Scientific), HCEs and HCKs separately. The cells were seeded with low densities (HCEs 50 000 cells/cm^2 and HCKs 10 000 cells/cm^2) in order

to study their growth and proliferation. The cells were cultured in the 5 media options with medium volume of 500 µl/well. In the first repetition, the medium test was carried out with 4 wells for each medium and in the second and third repetition, with 3 wells per cell line per medium. Medium was changed 3 times a week.

During the medium test, cell proliferation was measured with PrestoBlue™ Cell Viability Reagent (Invitrogen, Carlsbad, CA, USA), which is a live cell assay. This assay is based on resazurin reduction to resorufin which indicates cell viability. This reaction is possible due to cellular respiration by accepting electrons from various macromolecules related to the respiration process such as phosphates, co-enzymes and cytochromes. This reduction converts PrestoBlue™ from non-fluorescent state to strong fluorescent form. This conversion can then be measured quantitatively as the proportion of fluorescence intensity where the results are proportional to the number of metabolically active cells. (Xu et al. 2015)

The PrestoBlue™ assay was performed according to the instructions provided by the manufacturer. For the first repetition only at the end-point on day 7 and for the second and the third repetition, the assay was performed at three time-points, on day 1, day 4 and day 7.

The reagent was added to HCE medium with ratio of 1/10. HCE medium was used in the measurements due to its stronger colour compared to other media options. The colour of the culture medium has an effect on the fluorescence results and to get comparable results, it was preferred to use the same medium for all of the cell-medium combinations in the test. The assay was carried out protected from light due to the photosensitivity of the PrestoBlue™ reagent. As the assay was performed, first old culture media were removed and then the medium with added PrestoBlue™ was pipetted, 200 µl/well and incubated at +37 °C for 30 minutes. This was also done for 3 additional empty wells for background comparison. After the incubation, the medium was transferred to a Nunc™ Delta Surface 96-well plate (Thermo Scientific™). Always one well from the 48-well plate was divided to two wells on the 96-well plate, meaning 100 µl/well. Cell proliferation levels were measured as fluorescence intensity and the values received from the spectrophotometer were relative fluorescence units (RFU). The fluorescence intensity was measured with Wallac Viktor^2 1420 Multilabel Counter spectrophotometer (Perkin Elmer, Waltham, MA, USA).

The results from these multiple 100 µl samples were averaged to get one RFU value per cell-medium combination. The empty wells with PrestoBlue™ -HCE medium were used for determining the background fluorescence. The averaged RFU value from the empty wells was subtracted from the test sample averages. This way the background fluorescence of the well plate and the medium was removed from the actual results.

During the second and third repetition, on days 1 and 4, after the PrestoBlue™ containing medium was removed, the wells were washed once carefully with fresh media to remove PrestoBlue™ residues and then fresh media were added before resuming cell culture. Day 7 was the end-point of all test replicates and cells were fixed with 4 % paraformaldehyde (PFA) and analysed using IF as described in Chapter 5.4.

5.3 Hydrogels

The hydrogel experiment was conducted with five hydrogels. Four of the options, A, B, C and D were provided by Lic. Phil. Jennika Karvinen from the BioMediTech Biomaterials and Tissue Engineering Group, TUT. Another tested hydrogel was HyStem®-C (ESI BIO A Division of BioTime, Inc., Alameda, CA, USA), which consists of three components and deionised DG Water as the mixing solution. According to the datasheet provided by the manufacturer, the first component is a thiol-modified sodium hyaluronate Glycosil®, which is a HA-based component, a constituent of native ECM. The second component is a thiol-modified gelatin Gelin-S®, which is type A gelatin derived from porcine skin. The crosslinker for these two components is a thiol reactive PEGDA Extralink® which reacts to thiol groups of Glycosil® and Gelin-S® to form viscoelastic and transparent hydrogel.

5.3.1 Hydrogel preparation and culture with corneal cells

The hydrogel experiment was conducted three times. The replicates of this experiment varied in relation to which of the hydrogel options and culture media were tested. The variations of the experiment are presented in Table 4.

Table 4. *The three replicates of the hydrogel experiment. The culture time is presented as the amount of days cultured submerged in medium with additional seven days in air-lifting. Either polycarbonate (PC) or polyethylene terephthalate (PET) hanging inserts were used.*

Exp.	Hydrogels	Volume	Media	Culture (t)	Insert
1	Hydrogels A, B, C and D	200 µl	CnT-20 CnT-30 CnT-Prime-CC	7+7 days	PC
2	Hydrogel A	300 µl	CnT-20 CnT-Prime-CC	14+7 days	PET
3	Hydrogel A HyStem®-C	300 µl	CnT-20 CnT-Prime-CC	14+7 days	PET

Hydrogels A, B, C and D were prepared according to the instructions given by Karvinen and preparation of HyStem®-C samples followed the instructions provided by the

manufacturer. The main steps of the preparation protocol of the hydrogels are presented in Figure 8.

Figure 8. *Preparation steps of the hydrogel samples.*

HyStem®-C The components were stored at -20 °C and thawed before the experiment. The deionised DG Water was added with a syringe to the Glycosil® and Gelin-S® component vials, 1 ml to each. The vials were put on a shaker to ensure complete dissolving of the components for 40 minutes.

The hydrogel sample preparation began with preparation of HCKs for the hydrogels. The cells were detached according to the subculturing protocol described in Chapter 5.1 and counted. Amount of HCKs for one sample was 30 000 cells, which was retrieved from literature 200 000 cells/ml (Engelke et al. 2013). The cells were carefully mixed with the hydrogels A, B, C and D by pipetting very carefully, avoiding creating any air bubbles to the resulting hydrogel samples.

As the HyStem®-C samples were prepared, the instructions advised to mix the components with the HCKs, leave for 10 minutes, mix again and only then pipette to the culture inserts. This step was left out and the HyStem-C® hydrogels were prepared by mixing the components and cells carefully with a pipette and then pipetting the hydrogels to the inserts without additional mixing. The samples were prepared by mixing the Glycosil®, Gelin-S® and Extralink® with component volume ratio of 2:2:1

HCEs were detached and counted according to the subculture protocol as well. The suggested amount of HCEs was 50 000 cells/cm^2 and since the culture area of the inserts was 1.13 cm^2, the amount of HCEs was 56 500 cells/insert (Engelke et al. 2013). The HCEs were seeded carefully on top of the hydrogels with chosen culture medium. The hydrogels were cultured with following amounts of the CnT media, 800 µl below and 300 µl on top of samples. The media were changed 3 times a week.

The used inserts in the first hydrogel experiment replicate were standing non-transparent Nunc™ PC Membrane Inserts with 1.13 cm^2 culture area and cultured on 12-well plate without matrix coating (Thermo Scientific). Insert type was changed in the second and third replicate to transparent Millicell Hanging Cell Culture Inserts with PET membranes with 1.1 cm^2 culture area (Merck Millipore, Darmstadt, Germany) on Nunc™ Delta Surface 12-well plate (Thermo Scientific) to enable visualisation and microscopy imaging.

In the first hydrogel experiment replicate, all of the samples contained both cell types, HCEs seeded on top and HCKs mixed into the hydrogels. In the second and third replicates, half of the hydrogel samples were prepared without HCKs for comparison. In the first replicate, 3 samples from each hydrogel option were prepared to have one hydrogel for each CnT medium option. In the second and third replicates, 10 hydrogel A samples were prepared to have 5 samples for the two used media, CnT-20 and CnT-Prime-CC. From these 5 samples per medium, 2 were prepared without HCKs and 3 with HCKs. Six samples with volume of 300 µl were prepared from the HyStem®-C, 3 for each, CnT-20 and CnT-Prime-CC, including one sample without HCKs and two samples with HCKs.

The first replicate of this experiment was performed with hydrogels A, B, C and D. The second replicate was conducted only with hydrogel A and the third replicate was conducted with hydrogel A and HyStem®-C. Hydrogels were cultured submerged in medium for either 7 (replicate 1) or 14 (replicates 2 and 3) days. After this, the culturing continued with air-lifting for 7 days. To promote HCE stratification, the culture media were supplemented with 1 mM calcium chloride ($CaCl_2$, Sigma Aldrich) and the samples were cultured with 1 ml under the inserts. The medium was changed 3 times during the week.

The hydrogels were imaged with light microscope throughout the culturing. The cells were fixed with 4 % PFA for 30 minutes after the 7 days of air-lifting for further analysis on either day 14 (replicate 1) or day 21 (replicates 2 and 3).

5.3.2 Hydrogel preparation for analysis

Cryosections and samples suitable for confocal microscopy were selected as methods to analyse the hydrogel experiment. Cryosections were prepared from hydrogel A of every replicate of the hydrogel experiment and additionally sections were prepared from the hydrogels C and D of the first replicate. Confocal microscopy samples were prepared from hydrogel A of the last experiment replicate.

One hydrogel insert from each cell and medium environment was prepared for confocal microscopy, altogether four hydrogel A inserts. The samples were prepared to uncoated 8-well microscopy chamber µ-Slides (ibidi GmbH, Martinsried, Germany). For this, the hydrogel inserts were cut to 4 pieces and each piece was placed in a separate well of the chamber slider. These hydrogel pieces were then further analysed with IF staining described in Chapter 5.4.

For the preparation of cryoblocks, the film bottom of the hydrogel insert was carefully cut out from the insert frame with a sharp scalpel. The hydrogel insert film was placed on a drop of PBS on a lid of a well plate and cut in half. Both halves of each hydrogel sample were placed with tweezers to a cryomould that was filled with optimal cutting temperature

(O.C.T) cryomould matrix compound Tissue-Tek® (Sakura Finetek Europe B.V., Alphen aan den Rijn, The Netherlands). The prepared cryomoulds were frozen with liquid nitrogen and stored in -80 °C. The preparation protocol was continuously optimised, and this is further discussed in Chapter 7.4.

The prepared cryoblocks were sectioned with Leica CM3050 S Research Cryostat (Leica Biosystems, Nussloch, Germany). The thickness of the cut cryosections was 7 µm and the sections were placed on Superfrost™ Plus microscope slides (Thermo Fisher Scientific), approximately 3 sections per slide and 5 slides per hydrogel sample. Slides were left to dry for 1 hour before storing at -20 °C, and later analysed using IF staining.

5.4 Immunofluorescence staining

IF staining was performed for all medium test and hydrogel experiment replicates to examine the protein expression of both HCEs and HCKs. For the hydrogel test, IF staining was performed for the cryosections and confocal microscopy samples.

IF staining was carried out with following primary antibodies: Ki67, ABCG2, vimentin (VIM), p63, PAX6, CK15, CK3, CK12, keratocan (KTN) and α-SMA. These antibodies are important for evaluating protein expression of the corneal epithelium and the stroma. All used primary antibodies are immunoglobulin G (IgG) and presented in Table 5 with data such as dilution and their specific localisation in a cell.

Table 5. *The primary antibodies (IgG) used in the experiments.*

Antibody	Host	Manufacturer	Dilution	Cell line	Localisation
anti-p63	Rabbit	Cell Signaling Technology Danvers, MA, USA	1:200	HCE	Nucleus
anti-Ki67	Rabbit	Merck Millipore	1:500	HCE, HCK	Nucleus
anti-PAX6	Rabbit	Sigma-Aldrich St. Louis, MO, USA	1:200	HCE	Nucleus
anti-ABCG2	Mouse	Merck Millipore	1:200	HCE	Membrane
anti-CK15	Mouse	Thermo Fisher Scientific	1:200	HCE	Cytoskeleton
anti-CK3	Mouse	Abcam plc Cambrige, USA	1:200	HCE	Cytoskeleton
anti-CK12	Goat	Santa Cruz Biotechnology Inc, Dallas, TX, USA	1:200	HCE	Cytoskeleton
anti-α-SMA	Mouse	R&D Systems Inc., Minneapolis, MN, USA	1:400	HCK	Cytoskeleton
anti-VIM	Goat	Merck Millipore	1:200	HCK	Cytoskeleton
anti-KTN	Rabbit	Santa Cruz Biotech.	1:200	HCK	Cytoskeleton

The important IF markers to observe HCE protein expression are p63, Ki67, PAX6, ABCG2, CK15, CK3 and CK12 and the IF markers for HCK protein expression are Ki67,

α-SMA, VIM and KTN. For the evaluation of the results, the meaning of the IF primary antibody markers need to be understood for further analysis.

ATP-binding cassette sub-family G member 2 (ABCG2) protein belongs to the large family of transmembrane proteins know as ATP binding cassette (ABC) transporters (Ding et al. 2010; de Paiva et al. 2005). ABCG2 is widely expressed in different tissues including epithelial tissues but it is a putative marker for stem and progenitor cells such as LESCs rather than for mature epithelial cells (Ding et al. 2010; Kubota et al. 2010; Kayama et al. 2007). Therefore ABCG2 should not be expressed in the layers of the corneal epithelium but rather in the limbal region. Nuclear protein and transcription factor p63, member of p53 family, is closely related to ABCG2 since it is proposed to be an epithelial stem and progenitor cell marker also found in LESCs in the limbal region (de Paiva et al. 2005; Kayama et al. 2007) and the TACs have shown to express p63 (Kobayashi et al. 2015).

PAX6 is a transcription factor, member of PAX family that is essential for ocular development and due to this reason, expressed in the ocular progenitor cells (Funderburgh et al. 2005). PAX is also expressed in mature cornea, since it is required for epithelial maintenance (Dhouailly et al. 2014).

Cytokeratins are cytoskeletal component proteins of the epithelial cells. These proteins create filament structures which are responsible for the structural integrity of the epithelial cells. Cytokeratins have an important role in epithelial tissue differentiation and various cytokeratins are expressed throughout the differentiation process. Here, important for this study, CK3 and CK12 are known expressed protein markers for mature, terminally-differentiated corneal epithelial cells. (Kayama et al. 2007; Yoshida et al. 2006) CK15 is a marker for the basal layer of stratified epithelium and it is also expressed by TACs (Kobayashi et al. 2015; Yoshida et al. 2006).

Ki67 is large kinase protein present in the nucleus during the cell cycle, which means that it is a nuclear marker for actively cycling and proliferating cells (Francesconi et al. 2000; Joyce et al. 1996). This marker is expressed in both, HCEs and HCKs, if the cells are proliferating.

KTN is a member of the small leucine-rich PG family (Joseph et al. 2011) and it is considered to be a phenotypic marker for healthy stromal keratocytes. The function of KTN is essential for corneal stromal transparency (Espana et al. 2003; Carlson et al. 2005). However, in case of an injury, the keratocytes lose their specific phenotype and acquire fibroblastic morphology and start to express α-SMA protein which is a marker of myofibroblasts. In culture environment this happens easily if keratocytes are cultured in serum containing medium. This transformation happens as well if cell density is too low. (Espana et al. 2003) VIM is a member or intermediate filament protein family that are part of the cytoskeleton structure with microtubules and actin microfilaments. It is

expressed in HCKs when the cells undergo wound healing and stress-related situations. (Joseph et al. 2011)

Primary antibodies were detected using the secondary antibodies (Thermo Fisher Scientific) presented in Table 6. To counterstain cell nuclei, Vectashield® mounting medium (Vector Laboratories Inc., Burlingame, CA, USA) was used which contained 4',6-diamidino-2-phenylidole (DAPI).

Table 6. *Secondary antibodies for detection of primary antibodies.*

Antibody	Host	Manufacturer	Dilution
anti-mouse Alexa Fluor 568	Donkey	Thermo Fisher Scientific	1:800
anti-mouse Alexa Fluor 488	Donkey	Thermo Fisher Scientific	1:800
anti-goat Alexa Fluor 568	Donkey	Thermo Fisher Scientific	1:800
anti-rabbit Alexa Fluor 488	Donkey	Thermo Fisher Scientific	1:800

The IF staining for the medium test was performed for the 48-well plate and the cryosections were stained in planar fashion on a wet surface to keep the samples from drying. The confocal microscopy samples were stained on their 8-well microscopy chamber µ-Slides. The same protocol for the IF staining was used for all samples.

The time periods indicated here are for the medium test and cryosections. The incubations for confocal microscopy samples were longer, if time periods for these samples were different, these are indicated in brackets. The samples were first washed twice with PBS, followed by permeabilisation with 0.1 % Triton X-100 (Sigma Aldrich) in PBS for 15 minutes. As a next step was blocking with 3 % bovine serum albumin (BSA, Sigma Aldrich) in PBS for 1 hour followed by the primary antibodies diluted to 0.5 % BSA in PBS as shown in Table 6. The incubation period for primary antibodies was overnight at +4 °C (2 days). The next day the staining protocol was continued with three PBS washes followed by the secondary antibodies diluted to 0.5 % BSA in PBS and incubated for 1 hour (1 day) and the samples were protected from light on a shaker at room temperature to ensure proper staining. Finally, the IF stained samples were mounted with drops of Vectashield® mounting medium containing DAPI and suitable cover slips. The stained samples were kept at +4 °C and protected from light due to the photosensitivity of the antibodies.

5.5 Haematoxylin and eosin staining

Two hydrogel cryosection slides per hydrogel sample were stained with H&E, a histological staining method to stain tissue samples for microscopy inspection. The stain reagents for the protocol were Harris' haematoxylin and Eosin Y (Merck KGaA, Darmstadt, Germany). Haematoxylin was filtered every time before the staining and Eosin Y was diluted to purified water, MilliQ, with concentration of 0.2 %.

The staining was performed in planar fashion by pipetting the reagents on the microscopy slides to cause minimal loss and damage to the cryosection samples. The staining protocol began with 30 seconds in Harris' haematoxylin, followed by 10 seconds wash with Milli-Q water. This was followed by 30 seconds in 0.2 % Eosin Y and also with 10 seconds wash with Milli-Q water. Ethanol (EtOH) was used to dehydrate the samples as a rising series of 70 % for 10 seconds, 94 % for 10 seconds and <99 % for 30 seconds. After the EtOH series was three Xylene (VWR International LLC, Radnor, PA, USA) treatments, each 3 minutes. This last phase was not performed in planar fashion due to toxicity of the reagent, but in proper containers. The microscopy slides after the last xylene step were mounted with xylene-based EUKITT® (ORSAtec GmbH, Freiburg, Germany) and coverslips. The slides were left in a fume hood for 2 days before imaging to vaporise the toxic residues of xylene.

5.6 Microscopy and image processing

The progress of the medium test and hydrogel experiment was imaged with ZEISS Axio Vert.A1 inverted light microscope (Carl Zeiss AG, Jena, Germany). The IF stained medium test and cryosections were imaged with Olympus IX51 fluorescence microscope (Olympus Corp., Tokyo, Japan). The confocal microscopy samples were imaged with ZEISS LSM 780 LSCM (Carl Zeiss AG). The H&E stained cryosections were imaged with Nikon Eclipse T2000-S phase contrast microscope (Nikon Instruments Europe B.V., Amstelveen, The Netherlands).

ZEISS LSM 780 LSCM confocal microscopy images and ZEISS Axio Vert.A1 microscopy images were processed with ZEN Blue Imaging Software (Carl Zeiss AG). All the Olympus IX51 fluorescence microscope images were processed and all image panels created with Adobe Photoshop CS6 (Adobe Systems Incorporated, San Jose, CA, USA).

6. RESULTS

This chapter presents the relevant and important results from the experimental part. This chapter begins with the results from the 2D cell culture medium test. First there are images from the medium test showing cell morphology in different culture media and the PrestoBlue™ proliferation assay results, followed by the IF staining results from this test.

The results chapter continues then to the hydrogel experiment where the preparation and execution of the experiment are presented with microscopy images from 3D hydrogel cell cultures. Next are the IF staining results from the hydrogel cryosections and confocal microscopy samples. Finally, the H&E stained cryosections are presented at the end of this chapter.

6.1 Cell growth and proliferation in different cell culture media

Several different culture medium alternatives were analysed in order to find the most suitable options for the purpose of this project. In the medium test, both HCEs and HCKs were cultured separately in the following media alternatives: HCE maintenance medium, HCK maintenance medium, CnT-20, CnT-30 and CnT-Prime-CC. Cells were imaged throughout the test on days 1, 4 and 7. To illustrate the HCE and HCK cultures, Figure 9 shows images from day 4 of the first medium test. HCEs seemed to have rounder morphology in the commercial serum-free CnT media compared to the HCE maintenance medium. The HCKs seemed to have similar morphology in CnT-20 and CnT-30 media compared to the HCK culture medium but more round in CnT-Prime-CC with less adhesions to the substrate and more dead cells than in other media.

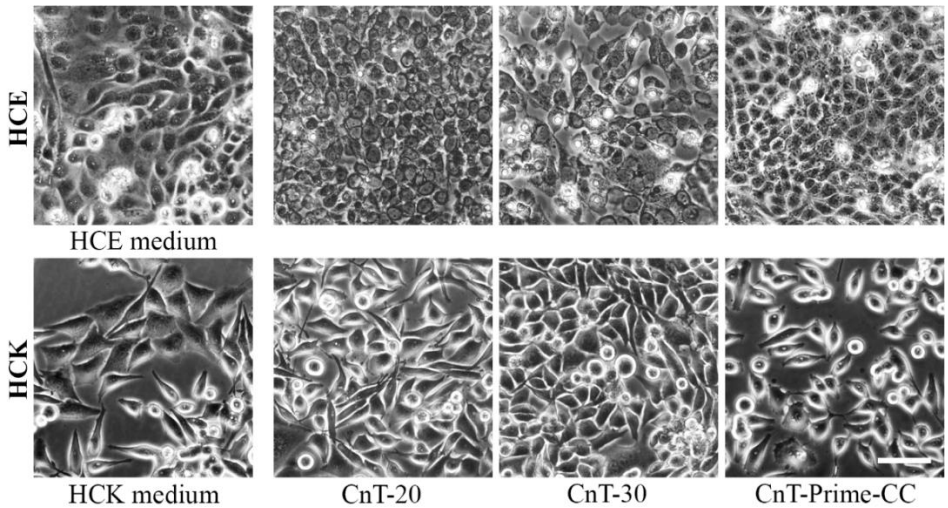

Figure 9. *HCEs (upper row) and HCKs (bottom row) in different CnT culture media compared to their own maintenance media. Scale bar represents 100 µm.*

The duration of this test was 7 days and it was conducted 3 times to get comparable results. The purpose of the PrestoBlue™ analysis was to evaluate metabolic activity and proliferation of the cells in different media and the results were measured as RFUs. Higher relative fluorescence indicates higher metabolic activity and proliferation levels. Two kind of results were obtained from this assay. The first presented results here illustrate metabolic activity of the cells in different medium options at the end-point of the experiment on day 7 (Figure 10). Figure 10A presents the results for HCE cell line in different media compared with the HCE culture medium and Figure 10B presents the results for HCK cell line compared with the HCK culture medium. The vertical axis in these charts represents the measured RFU values.

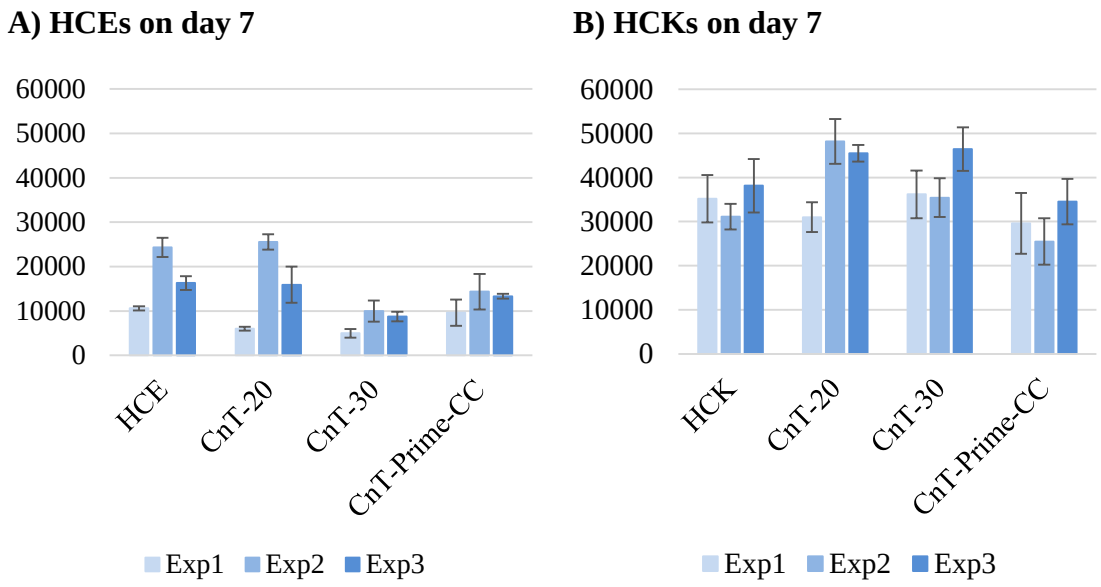

Figure 10. *The PrestoBlue™ results on day 7. A) HCE cell metabolic activity in CnT media compared with the HCE maintenance medium. B) HCK cell metabolic activity in CnT media compared with the HCK maintenance medium. Vertical axis represents the measured relative fluorescence units (RFU). Results are average values from three separate biological replicates of the medium test and error bars represent standard deviations.*

As it can been seen from Figure 10A, HCE cell proliferation was highest in CnT-20 medium as well as in HCE maintenance medium. HCE proliferation was relatively low in CnT-30 and CnT-Prime-CC if compared to HCE maintenance medium. PrestoBlue™ assay results for HCKs show more consistent values for each of the CnT media than for HCEs. HCKs seem to prefer CnT-20 as well, and actually have a slightly higher proliferation rate in CnT-20 and CnT-30 media than in their own HCK maintenance medium. In CnT-Prime-CC HCKs stayed viable and proliferated considerably well, even though the proliferation levels were lower than in their maintenance medium.

Next, cell proliferation was measured at three time-points during the 7-day culture, on days 1, 4 and 7. This gave insight how the chosen media affected cell proliferation

throughout the 7 days, and the results are presented as calculated averages of the results from second and third medium test replicates for HCEs (Figure 11A) and HCKs (Figure 11B).

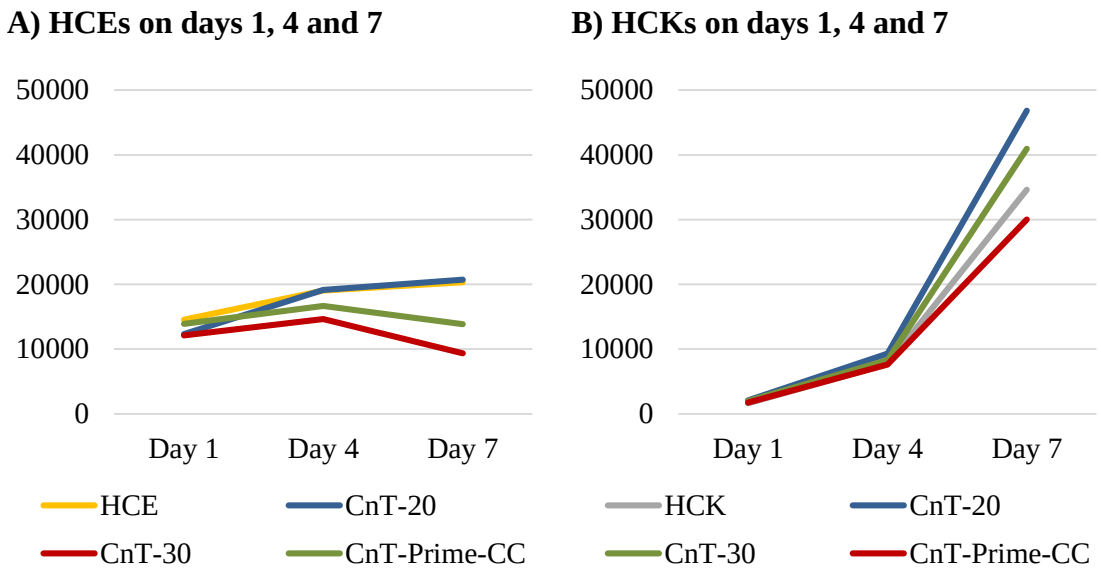

Figure 11. *The progression of metabolic activity and proliferation in different media during the 7-day culture. A) HCE and B) HCK metabolic activity on days 1, 4 and 7. Vertical axis represents relative fluorescence units (RFU).*

Based on these time-point results drawn from the PrestoBlue™ assay, it is visible that HCEs have somewhat consistent metabolic activity throughout the culture period. The proliferation rate gradually increased in CnT-20 and the maintenance medium overtime, but decreased after the day 4 time-point in CnT-30 and CnT-Prime-CC. For HCKs, the proliferation rate increased overtime as the cells seemed metabolically more active towards the end-point in all media. HCKs proliferated considerably well in all of the media, especially in CnT-20 and CnT-30. HCKs cultured in CnT-Prime-CC medium showed only slightly lower proliferation rates compared to HCK maintenance medium.

As a clear outcome, both of these sets of results support each other showing that best cell viabilities with both cell lines are reached with CnT-20 medium according to the fluorescence readings. However, there is no clear difference between CnT-30 and CnT-Prime-CC results for either cell line. HCEs prefer CnT-Prime-CC over CnT-30 and HCKs prefer CnT-30 over CnT-Prime-CC. As a conclusion of this assay to continue to the hydrogel experiment, all three CnT culture media were included in the first replicate of the hydrogel experiment due to the relatively similar cell proliferation rates.

6.2 Cell behaviour in 2D culture

All of the three medium test replicates were IF stained and the complete results for all five medium options can be seen in Appendix A, where HCEs and HCKs are compared

with their own maintenance medium against all three CnT media. Here the presented results show only the main findings. As an overall analysis, CnT-20 and CnT-Prime-CC show very similar results when compared to each other whereas CnT-30 medium brings the differentiation aspect visible in the IF results of the medium test.

HCEs did not show particular corneal epithelial cell behaviour in 2D cell culture in the medium test according to the cytokeratin markers. As seen in Figure 12, HCEs do not express epithelial cell markers CK3 and CK12, and the results are consistent with all of the studied media.

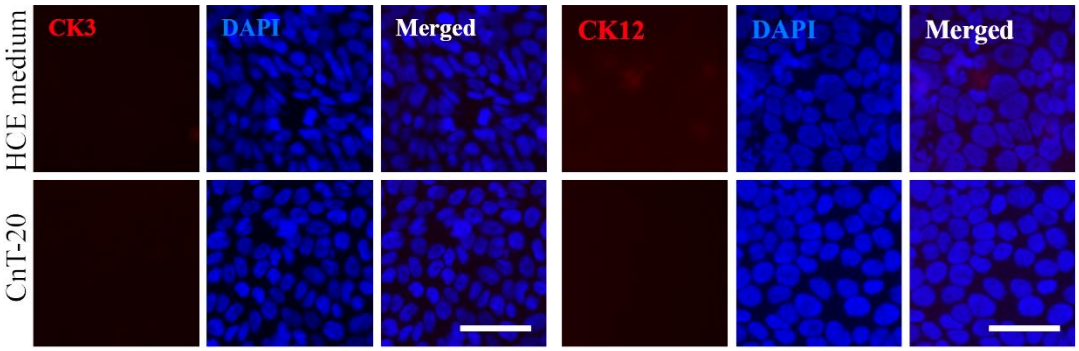

Figure 12. *Markers of mature corneal epithelium, CK3 and CK12, were not expressed in HCEs in any of the media options. (See Figures S2 and S3 for complete results). Scale bars represent 50 µm.*

HCEs weakly expressed CK15, a protein expressed in the basal layer of stratified epithelium, in all CnT media, but not in HCE maintenance medium (Figure 13). PAX6, a marker of corneal development and maintenance was weakly expressed in HCEs cultured in the HCE maintenance medium, CnT-20 and CnT-Prime-CC, and at a slightly more intense in the differentiation medium CnT-30 (Figure 13).

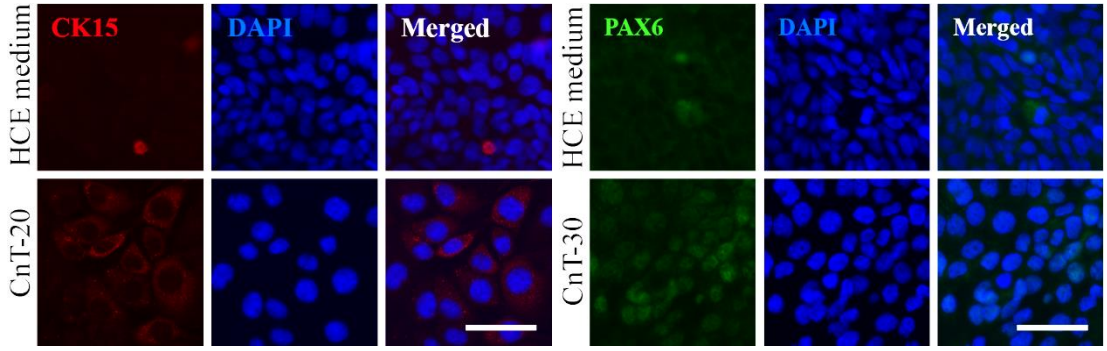

Figure 13. *Progenitor marker CK15 was very slightly expressed, whereas development and maintenance marker PAX6 was slightly more expressed. (See Figures S2 and S4 for complete results). Scale bars represent 50 µm.*

The LESC markers p63 and ABCG2 were very weakly expressed (Figure 14), and the results were consistent for the HCE maintenance medium and all CnT media.

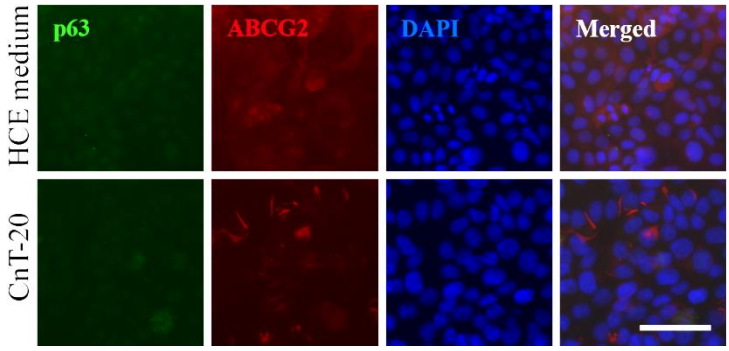

Figure 14. *The progenitor marker p63 was not expressed and stem cell marker ABCG2 was only slightly expressed. (See Figure S1 for complete results). Scale bar represents 50 µm.*

HCEs seemed to proliferate quite well in all of the media options except for CnT-Prime-CC, as evidenced by protein expression of proliferation marker Ki67 (Figure 15). In contrast, HCKs showed strong proliferation in the PrestoBlue™ assay which is also supported by the IF results for Ki67 in all of the culture media (Figure 15).

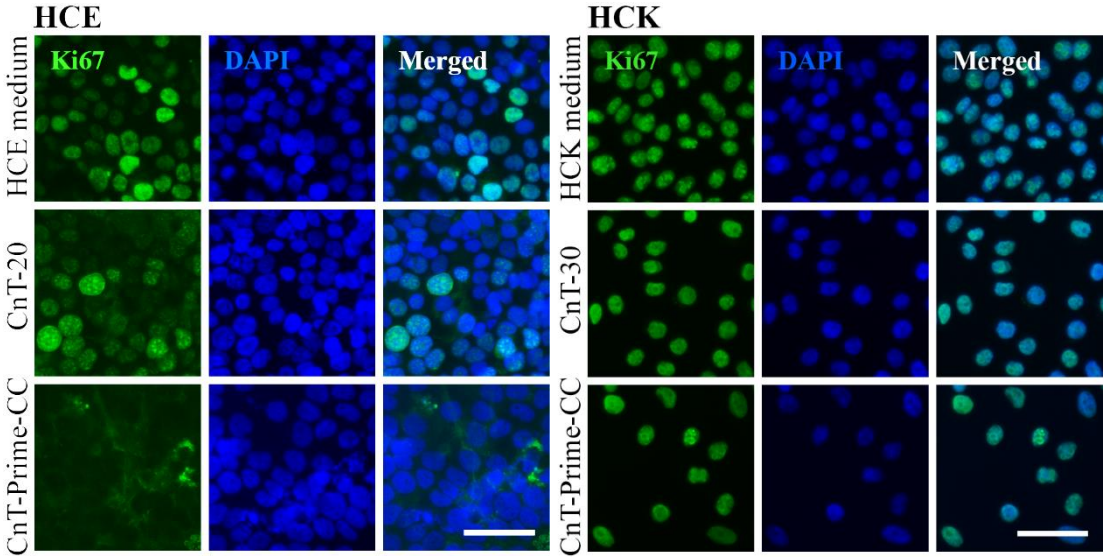

Figure 15. *Protein localisation of proliferation marker Ki67 confirmed the results obtained from the PrestoBlue™ assay in both, HCEs and HCKs. (See Figures S5 and S6 for complete results). Scale bar represents 50 µm.*

The myofibroblast markers α-SMA and VIM for HCKs were positive in all of the media. Protein expression in the CnT media were similar for CnT-20 and CnT-30 (Figure 16), and the IF staining was slightly more intense for CnT-Prime-CC.

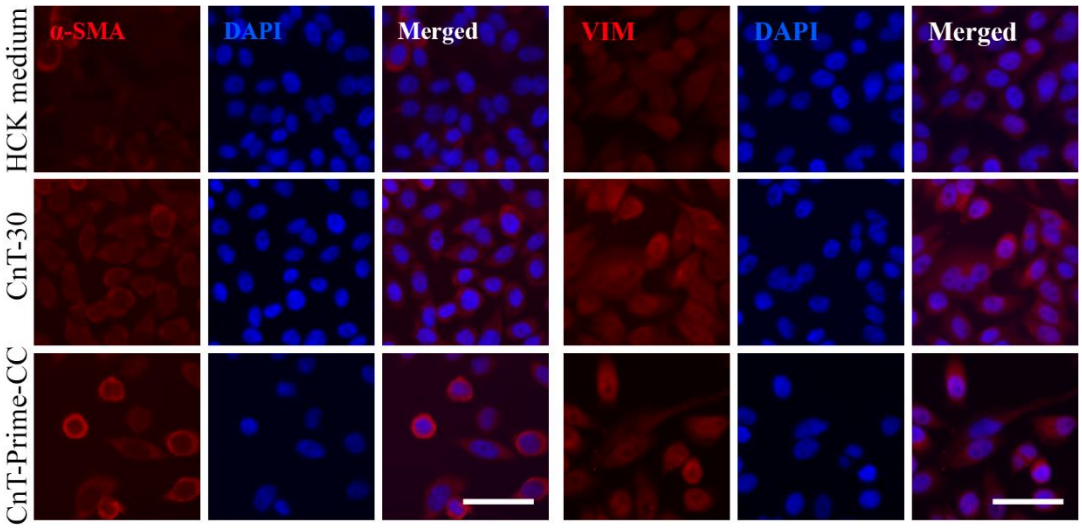

Figure 16. *Myofibroblast markers α-SMA and VIM were expressed in HCK cells in all media. CnT-20 not shown but results were similar to CnT-30 (See Figures S6 and S8 for complete results). Scale bar represents 50 µm.*

The healthy corneal stroma marker KTN was expressed in all media quite well (Figure 17). This showed that although the myofibroblast markers were expressed, also healthy keratocyte specific behaviour was maintained.

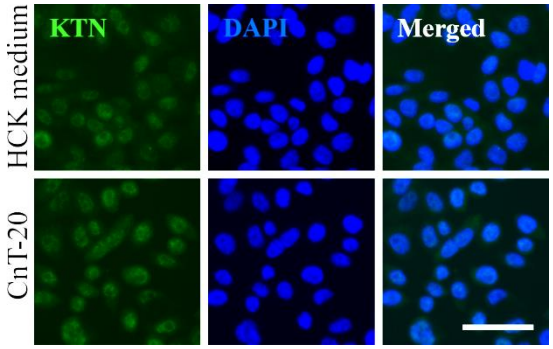

Figure 17. *The healthy keratocyte marker KTN was expressed visibly in all of the CnT medium options. (See Figure S7 for complete results). Scale bar represents 50 µm.*

Expression and localisation of different markers showed that HCKs cultured in different media possessed both non-keratocyte and keratocyte-like properties. Based on the results of IF stainings, there were no clear or substantial differences between the cell culture media, apart from the slightly higher α-SMA expression in CnT-Prime-CC.

6.3 Hydrogel preparation and 3D cell culture

The preparation and culturing of all three hydrogel experiment replicates were documented to observe the progress of this study. As the experiment was conducted for the first time with the four hydrogels shown in Table 4, some minor problems were faced

with hydrogel B and therefore, hydrogel B could not be prepared at all. The first replicate was then conducted with hydrogels A, C and D.

In the first experiment replicate the hydrogels were cultured for a total of 14 days: first submerged in the medium for 7 days, and then 7 days in air-lifting for stratification of HCEs. At the beginning of the culture, it took time for the HCEs to attach to the surface of the hydrogels and first medium change had to be performed very carefully to avoid losing the HCEs along with the medium.

At the end of the experiment, hydrogel A had quite firm structure, whereas hydrogels C and D seemed soft and HCEs were in clump formations on the surface of the hydrogel samples (Figure 18). These material-based results were consistent with all samples and there were no visible differences between CnT media.

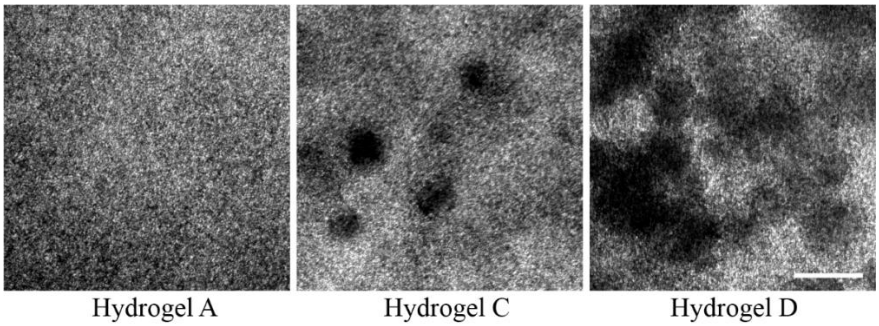

Figure 18. *Light microscopy images of hydrogels A, C and D on day 14. Scale bar represents 500 µm.*

Due to the difficulties met with the hydrogels C and D, the second experiment replicate was conducted only with hydrogel A. In this replicate the culturing time was increased to a total of 21 days: 14 days submerged and 7 days in air-lifting, and also the sample size was increased from 200 µl to 300 µl. The hydrogel A samples behaved similarly to the samples of the first replicate, it took time for the HCEs to attach to the hydrogel surface but after few days, the cells proliferated to confluent and stratified layer (Figure 19).

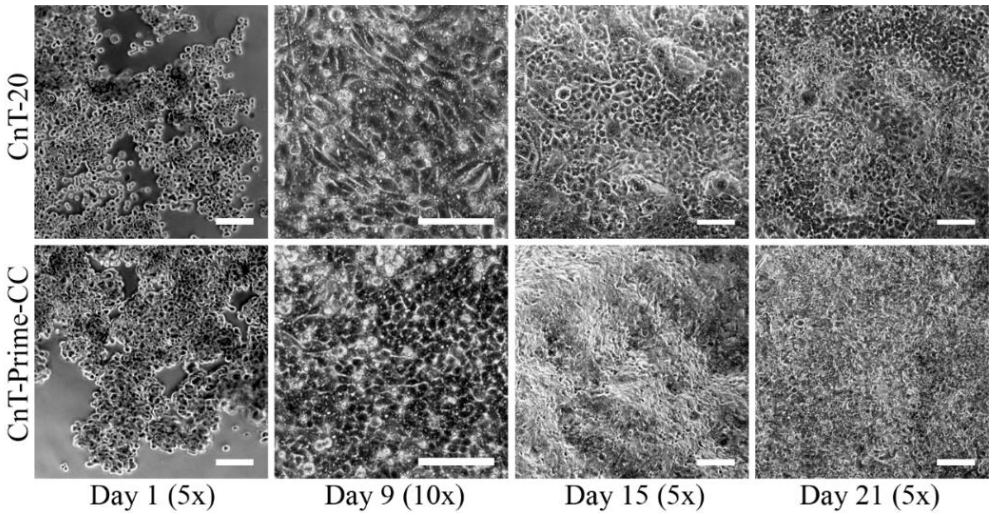

Figure 19. *The progression of HCE proliferation on hydrogel A culture on days 1, 9, 15 and 21. Scale bars represent 200 µm.*

As can be seen from Figure 19, on the first day the cells were round and in clump-like formations which indicate that the cells have not yet attached to the hydrogel surface. However, clear attachment is visible on day 9 and stratification is already visible on the first day of air lifting on day 15. On day 21 the HCEs have proliferated to even and confluent stratified layers in both, CnT-20 and CnT-Prime-CC media, stratification was especially visible in the CnT-Prime-CC samples.

The last experiment replicate was conducted with hydrogel A and HyStem-C® using the same culturing time and hydrogel volume as in the second replicate. HyStem-C® was prepared according to the instructions provided by the manufacturer. While the preparation of HyStem-C® was successful, cell culture using HyStem-C® was unsuccessful for unknown reason (Figure 20).

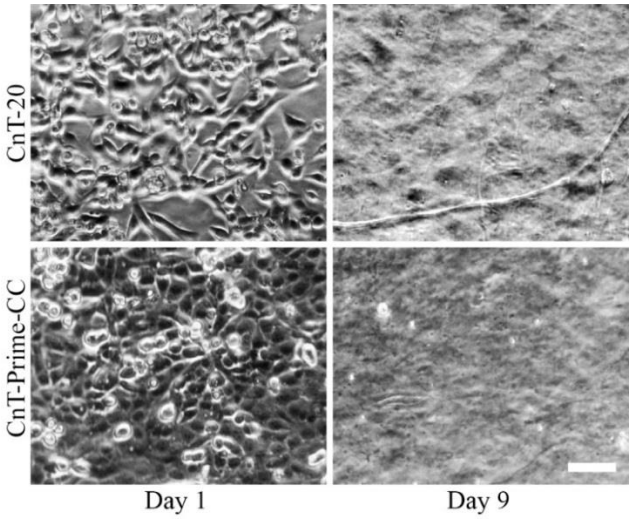

Figure 20. *HyStem-C® culture was unsuccessful for unknown reason since HCEs had detached from the material by day 9. Scale bar represents 100 µm.*

HCEs had attached well to the surface of the material already on day 1 but by day 9, all of the HCEs had detached and moved to the edges of the inserts, forming cell aggregates. The HyStem-C® hydrogel cultures were continued until day 21 but no change was observed after day 9. Therefore, the HyStem-C® hydrogel samples were not analysed further.

6.4 Cell behaviour in 3D culture

The IF staining for hydrogel cryosections was performed using three double IF stainings: ABCG2 and VIM, α-SMA and CK12 and KTN and CK3. These double stainings have one HCE marker and one HCK marker. The results presented in this section show hydrogel samples that included both, HCEs and HCKs. The samples without HCKs showed similar results. All of these images can be found together in the complete collection of IF staining results in Appendix A. The results from hydrogels C and D in this section include only samples cultured in CnT-Prime-CC. The samples cultured in CnT-30 were similar and these can also be seen in Appendix A.

Cells cultured in hydrogel A showed stronger expression of ABCG2 only in the differentiation medium CnT-30 but not in the other CnT options, and quite strong expression of VIM in CnT-20 and CnT-30, but not in CnT-Prime-CC (Figure 21). Cells cultured in hydrogels C and D showed stronger expression of ABCG2 and VIM, but formed large clumps (Figure 22).

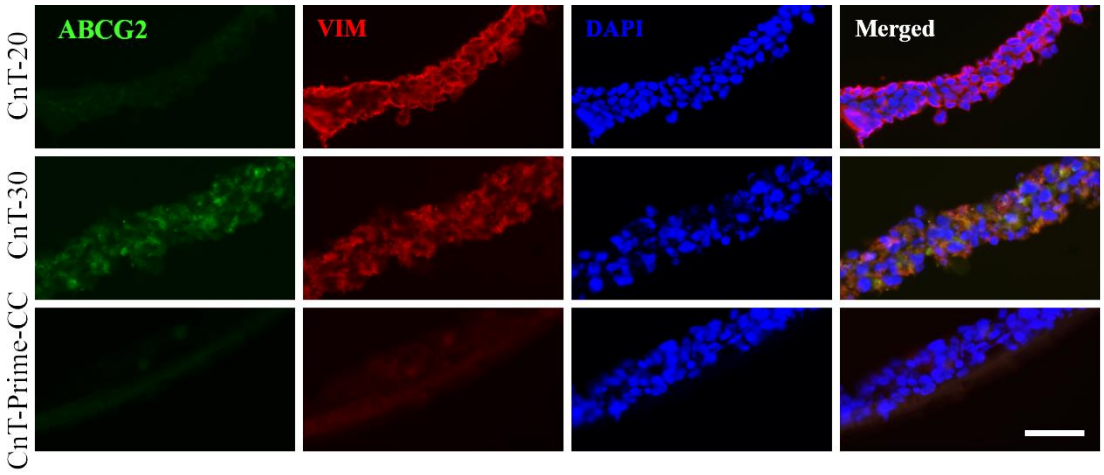

Figure 21. *Hydrogel A samples cultured in CnT-20, CnT-30 and CnT-Prime-CC media stained with ABCG2 and VIM. (See Figure S10 for complete results). Scale bar represents 50 µm.*

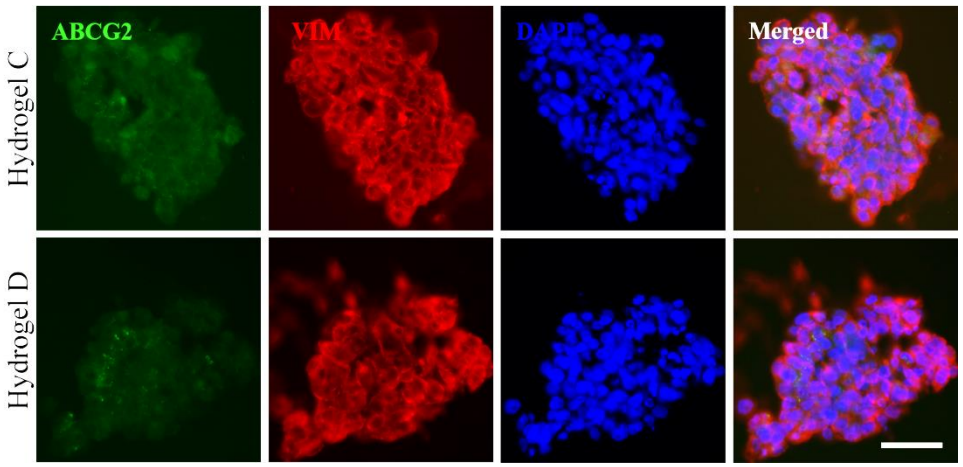

Figure 22. *Hydrogel C and D samples cultured in CnT-Prime-CC, IF stained with ABCG2 and VIM. (See Figures S13 and S15 for complete results). Scale bar represents 50 µm.*

The second double IF stain for the cryosections was α-SMA and CK12. Myofibroblast activity marker α-SMA was quite strongly expressed in all CnT media for hydrogel A (Figure 23) and strongly expressed in hydrogels C and D (Figure 24). The epithelial marker CK12 was very weakly expressed in hydrogel A samples cultured in CnT-30 or CnT-Prime-CC but slightly expressed in CnT-20. CK12 was weakly expressed in hydrogels C and D in all media.

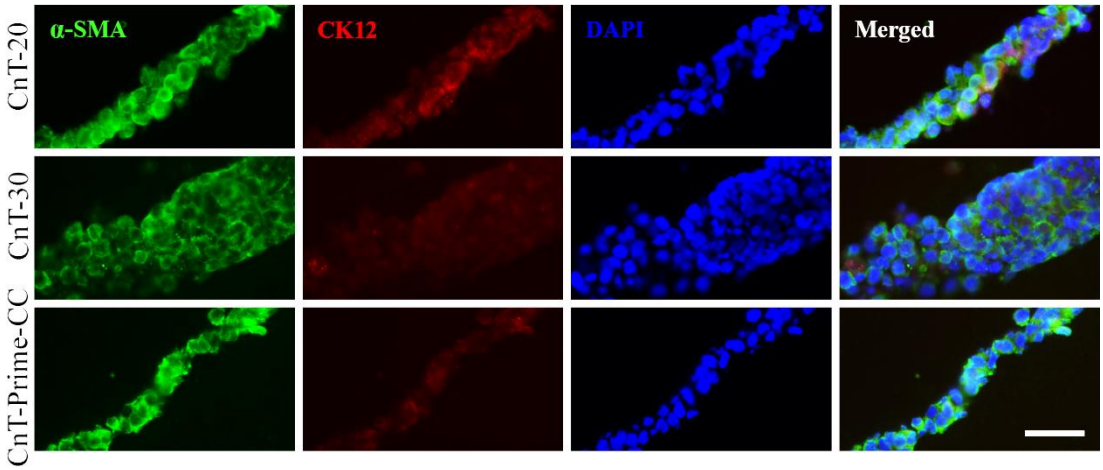

Figure 23. *Hydrogel A samples cultured in CnT-20, CnT-30 and CnT-Prime-CC media stained with α-SMA and CK12. (See Figure S9 for complete results). Scale bar represents 50 µm.*

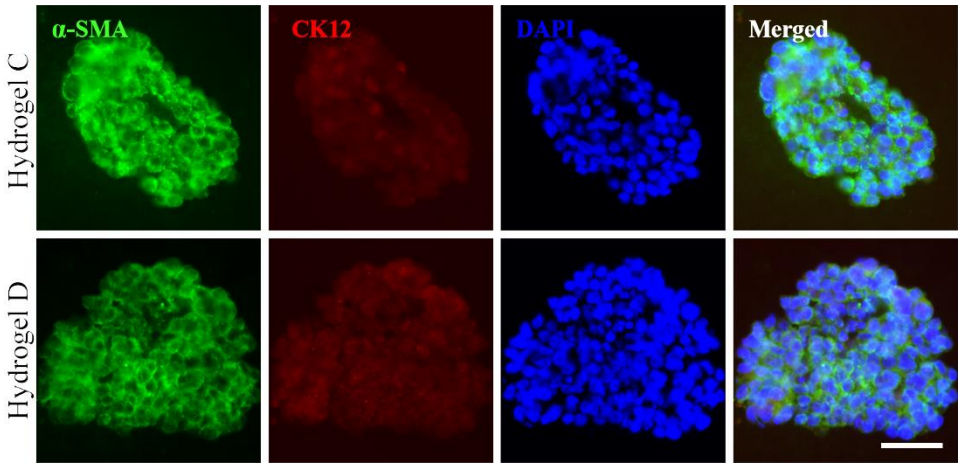

Figure 24. *Hydrogel C and D samples cultured in CnT-Prime-CC IF stained with α-SMA and CK12. (See Figures S12 and S14 for complete results). Scale bar represents 50 µm.*

The last double IF staining was the healthy keratocyte marker KTN and healthy epithelial cell marker CK3 (Figure 25). KTN was expressed in both of the CnT media that were used in the second experiment. CK3 marker was weakly expressed, but only in CnT-20.

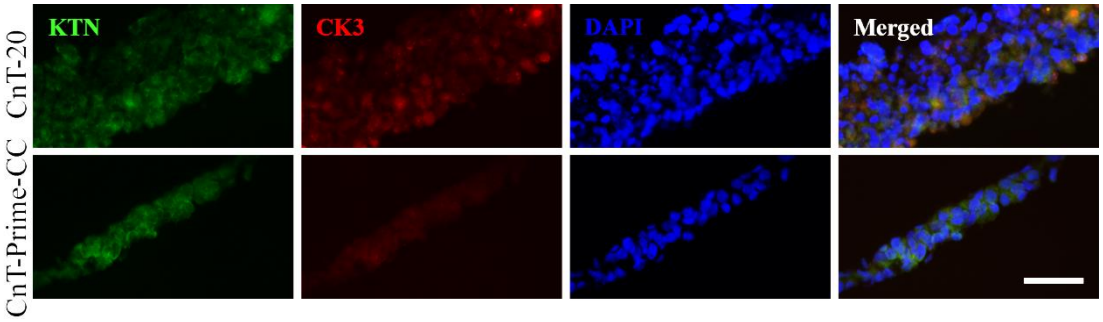

Figure 25. *Hydrogel A samples cultured in CnT-20 and CnT-Prime-CC IF stained with KTN and CK3. (See Figure S11 for complete results). Scale bar represents 50 µm.*

HCE and HCK protein expression of different markers was quite similar in both the 2D and 3D culture conditions. Also the structure of the hydrogel samples is visible in the hydrogel test IF results, how in some samples the cells have stratified to several layers and some of the samples have fewer cell layers.

The confocal microscopy samples were IF stained with three double stainings: α-SMA & CK12, KTN & CK3 and CK15 & VIM. These confocal microscopy images are presented in orthogonal view to show the protein expression in the hydrogel structures from the sides and inside the cell layers. The first presented results in Figure 26 are the hydrogel A samples cultured without HCKs and the second set of results in Figure 27 are the hydrogel A samples cultured with HCKs. The orthogonal projection of the samples shows the stratified nature of the hydrogel samples. The images show that the cell layers are somewhat uneven but confluent. Protein expression of the myofibroblast marker α-SMA

was quite strong in all samples, but especially in the sample with HCKs cultured in CnT-20. The second stain from this pair, epithelial cell marker CK12 is expressed more strongly in CnT-Prime-CC samples than in CnT-20 samples. KTN was expressed mildly throughout all of the samples, especially in the samples cultured in CnT-20. The epithelial marker CK3 was also expressed but more strongly in the samples cultured in CnT-Prime-CC. VIM expression was quite strong in all of the samples, especially in the CnT-20 cultured hydrogels, whereas CK15 showed only minimal expression in CnT-Prime-CC cultured samples.

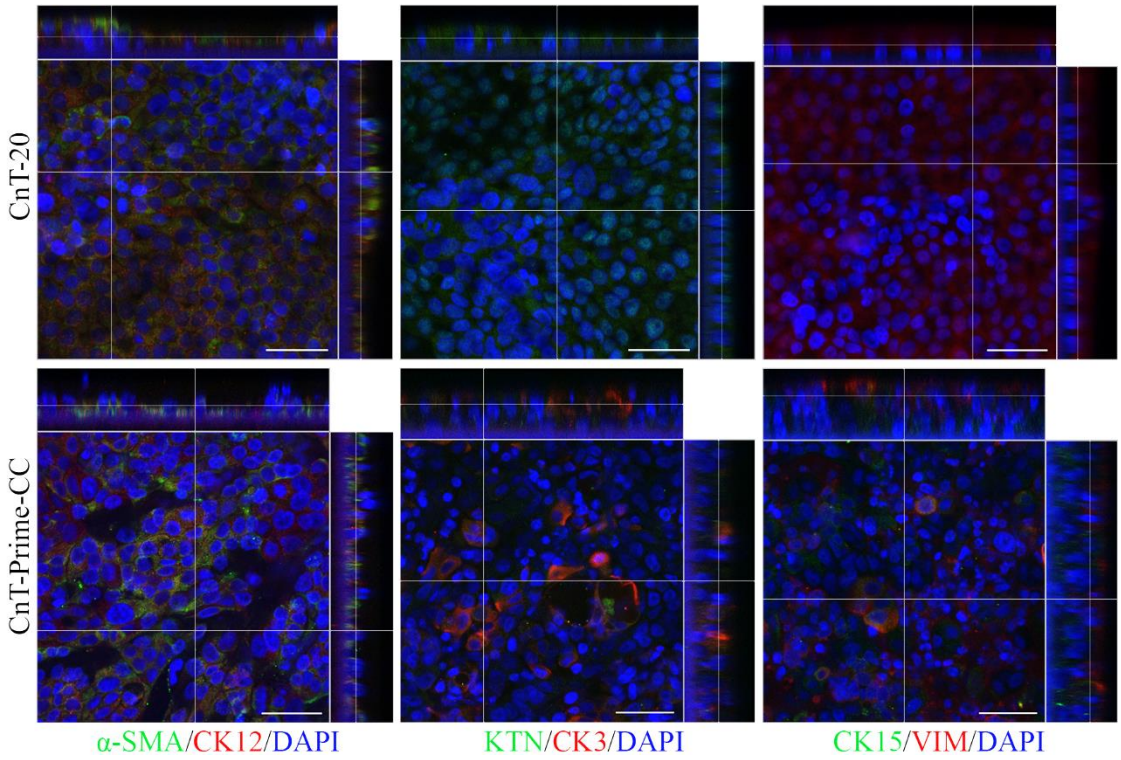

Figure 26. *Hydrogel A confocal microscopy images from samples cultured <u>without</u> HCKs. IF stains are indicated for every column. Scale bars 50 µm.*

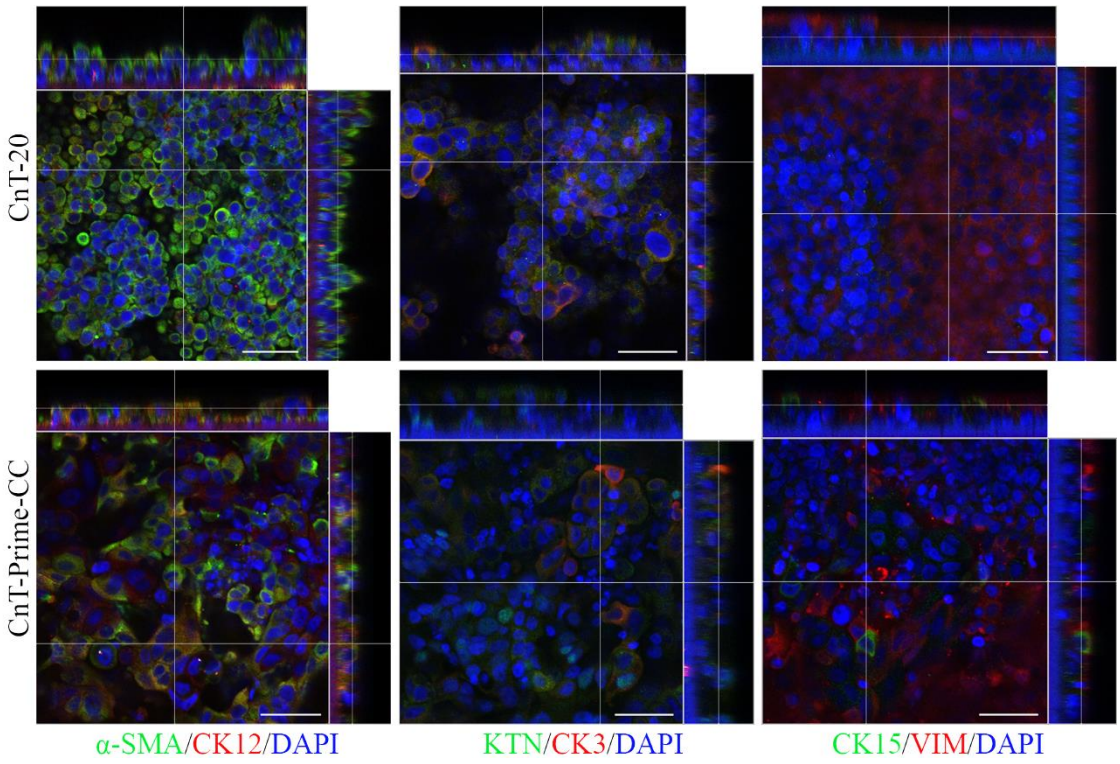

Figure 27. *Hydrogel A confocal microscopy images from samples cultured with HCKs. IF stains are indicated for every column. Scale bars 50 µm.*

Part of the hydrogel A cryosections were stained with H&E histological stain (Figure 28). Haematoxylin stains the nucleus of the cell dark blue or violet and eosin stains the cytoplasm and intercellular substances red. This is done to visualise the structure of the samples.

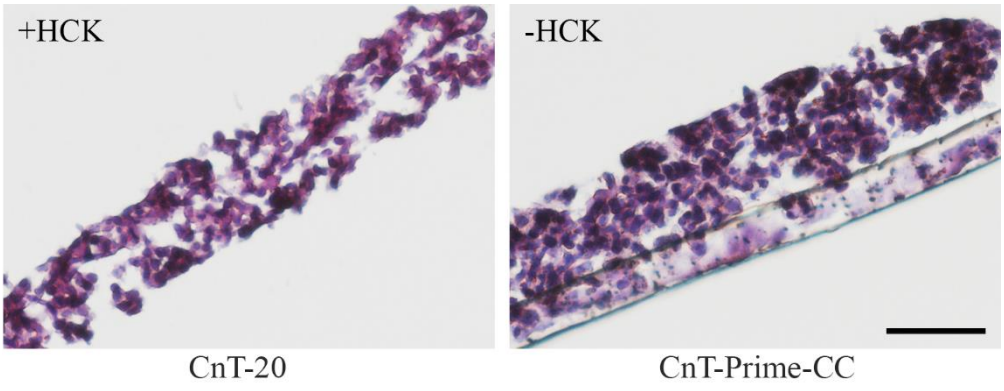

Figure 28. *H&E stained cryosections. Sample on the left was cultured in CnT-20 medium and the sample on the right was cultured in CnT-Prime-CC medium. Scale bar represents 50 µm.*

Due to preparation problems with the staining protocol, the imaged samples have suffered damage in the process. Nevertheless, it can be seen from these images how the HCEs have stratified to multiple layers.

7. DISCUSSION

Millions of people in the world suffer from cornea related injuries and diseases that cause partial or complete blindness (Deng et al. 2010). The field of corneal tissue engineering aims to provide treatment options with artificial biomaterial-based approaches for those who are in need of conventional transplant or even for those who are not eligible to receive donor cornea due to their disease or condition (Deng et al. 2010; Rahman et al. 2009). Tissue engineering is a promising and rapidly developing field of science, and many important discoveries have been made already in the past years. Biomaterials have shown to be powerful and versatile as tissue scaffolds. Especially the use of polymers and hydrogels are an interesting aspect in soft tissue engineering since these materials can be modified in numerous ways to mimic the natural environment of different cell types and to function as their ECM. (Malafaya et al. 2007)

The aim of this thesis was to study different hydrogels and their biocompatibility and suitability with corneal cells in 3D cell culture. The study was conducted with two types of immortalised corneal cells, HCEs and HCKs. First suitable growth media for the hydrogel experiment were tested with a medium test, where the cells were cultured in five different media: HCE and HCK maintenance media and three commercial CnT media. In the experimental part, five different hydrogels were studied in 3D cell culture: A, B, C, D and one commercial hydrogel, HyStem-C®.

7.1 Cell growth and proliferation in different culture media

This medium test was conducted to evaluate different media options which would be optimal for co-culturing HCEs and HCKs in the hydrogel experiment. Cells were cultured at low densities to observe their behaviour in the different commercial serum-free media (CnT-20, CnT-30 and CnT-Prime-CC), as well as the maintenance media of HCE and HCK. CnT-20 and CnT-30 are in use of the Eye Group in the stem cell differentiation protocol since CnT media are produced especially for epithelial cell culturing (Mikhailova et al. 2015). The advantage of CnT media is that they are serum-free, which means less variation between different batches, which provides a more consistent culture environment for the cells.

HCE and HCK cells were cultured 7 days for the assay and during this time cell morphology in the media was observed. It could be observed that HCE cell morphology was quite different between the maintenance medium and the CnT media, especially CnT-20 and CnT-30 cultured cells seemed to have rounder morphology and CnT-Prime-CC more similar to the maintenance medium. Especially the bigger cell size and different

morphology of the cells cultured in CnT-30 could be due to the fact that this medium induces differentiation rather than proliferation.

HCKs, on the other hand, seemed more even in all media, although there were more dead cells visible in CnT-30 and CnT-Prime-CC compared to other environments. In all media, but especially in CnT-Prime-CC, cells seemed to have very round morphology which is not typical for keratocytes, which are known to be highly adherent to their environment (Hassell & Birk 2010). This could be due to the 2D culture environment since in the native stroma keratocytes reside sparsely in highly ordered ECM composed of collagen fibrils and PGs (DelMonte & Kim 2011; Hassell & Birk 2010) and not in 2D monolayer culture as the cells were cultured here.

The purpose of PrestoBlue™ proliferation assay was to give insight about the cell behaviour between different media at the end-point and also how the cell behaviour changes throughout the week. Since the comparison was done between tested media and due to the small sample size, it was not necessary nor possible to perform statistical analysis only with three replicates that would bring more credibility for the results. Only the standard deviations are shown in the day 7 end-point averaged results to show variation between test replicates. It can been observed that the averaged results seem to be comparable since the trend between different media and their proliferation rates are similar.

HCEs showed slightly decreased proliferation rates after day 4, which does not indicate that the tested media would have been unsuitable for the cell line, since the results seem to be quite consistent throughout the 7-day culture. The most probable reason for the decrease is that the epithelial cells are known to be rapidly proliferating cells and the number of seeded cells was quite high at the beginning, giving more volume to proliferate from the start. This means that the cells reach confluence faster and therefore use up the culture surface and nutrients faster. This may cause the decrease in proliferation rates.

HCKs seemed to proliferate very well in all of the tested media since the cells stayed viable and proliferation rates rapidly increased between the day 4 and 7 time-points. HCKs are typically quiescent cells with low proliferation rates, which could explain the peak in their proliferation only at the end of the test. In the beginning, the cells have more space and time to proliferate before the number rises too high and limits further proliferation.

To obtain even more detailed proliferation profiles from these cell lines, the PrestoBlue™ assay should be performed with more biological and technical replicates, and perhaps cells should be seeded at different densities. However, the main objective of this medium test was to see how the cells behave in these media and which support proliferation best. Also the results would have indicated if some of the media would have not been suitable

for either of the cell lines but as it was observed, both cell lines remained viable and proliferated in all of the tested media.

As mentioned earlier, the goal was to find possible media options to co-culture these two cell lines within hydrogels. The best option for both cell lines from the CnT media was the proliferation medium CnT-20, while CnT-30 and CnT-Prime-CC showed very mixed results in preference when HCE and HCK results were compared. For this reason, both of these more uncertain media were included in the first replicate of the hydrogel experiment to actually see how the cells behave in these media in 3D environment. Also since the CnT-Prime-CC was a new medium specifically developed for co-culture of two cell types, and still only available for testing, it was very interesting to include it to the thesis since it gave aspect of novelty to the experiments. It is also possible that this medium is better suited for co-culture than the other CnT media.

7.2 Cell behaviour in 2D culture

As the IF staining results are evaluated, it is important to understand that the used cell lines, HCEs and HCKs are both immortalised cell lines. They may behave differently than primary cells would, for instance losing tissue-specific functions with time and obtaining altered phenotype from the cells *in vivo*, and therefore also altered protein expression (Pan et al. 2009). This means that the protein expression can be different than expected and may not necessarily indicate healthy mature corneal behaviour. Moreover, in this 2D medium test, the cell behaviour was evaluated on day 7, which was the end-point of the test. Behaviour of the cells could change during prolonged culture as the cells would mature further in different media. Also with more time, cells would reach confluence and possibly start to stratify, which would as well alter protein expression.

It is also essential to compare cell behaviour in CnT media with the maintenance media for both cell lines. The HCE and HCK media are preferred maintenance media for the used cell lines and support the cell-specific functions (Greco et al. 2010; Manzer et al. 2009). Overall, it would be ideal for the cells cultured in CnT media to possess appropriate cell morphology, protein expression, and other properties.

HCE cells did not show particular mature cornea protein expression in any of the tested media which was studied with cytokeratin markers specific for mature cornea, CK3 and CK12. Though these markers should be expressed in terminally differentiated epithelial cells, it could indicate that the phenotype of these immortalised HCEs is not as mature to express CK3 and CK12. It could be that maybe the cells would express some other cytokeratin markers that are expressed in different stages of epithelial cell development. (Sidney et al. 2015) The basal epithelial marker CK15 was only weakly positive, indicating corneal behaviour in the CnT media but not in the HCE maintenance medium. The corneal development and maintenance marker PAX6 was only clearly expressed in CnT-30 medium. The LESC marker p63 was not expressed in any of the media and

ABCG2 expression was weak. Protein expression of proliferation marker Ki67 is quite strong which supports the results received from the PrestoBlue™ assay. Protein expression for CnT media were consistent with the HCE maintenance medium which indicates that the cell behaviour is similar in all of the media despite the differences in cell morphology. There were some differences in cells cultured in CnT-30, such as PAX6 protein expression, which could indicate that the cells express more developmental than proliferative proteins. For all media, weak expression of ABCG2 and absence of CK3 and CK12 supports that the HCE phenotype is slightly different from mature corneal epithelial cell phenotype *in vivo*.

HCKs express very strongly Ki67, and similarly as for HCEs, this expression confirms the high proliferation rates measured in the PrestoBlue™ assay. The cells also quite strongly express the myofibroblast marker α-SMA and wound healing marker VIM in the CnT media and slightly less in the HCK maintenance medium. The HCKs may express α-SMA if the cells are cultured with low density which is the case here (Espana et al. 2003). The clear expression of both VIM and α-SMA could also indicate that the cells are under stress (Joseph et al. 2011) or otherwise express fibroblastic and myofibroblastic behaviour (Espana et al. 2003; Joseph et al. 2011). Nevertheless, clear expression of healthy keratocyte marker KTN suggests that HCKs possess also keratocyte *in vivo* phenotype properties. It could be that some of the cells express VIM and α-SMA and others express KTN. To obtain more information about the co-expression of VIM, α-SMA and KTN in HCKs, it could be beneficial to perform IF staining with two double stains: VIM and KTN, and α-SMA and KTN.

The use of this kind of 2D monolayer culture is a very efficient way to study cell behaviour. However, it is rather difficult to evaluate which of the media options are suitable for the 3D hydrogel experiment because cell function is likely affected by the unnatural 2D environment. In monolayer culture the cells have an unusual setting that provides nutrients and growth factors homogeneously to all cells and dead cells are regularly removed from culture with medium change. It has been studied that cells grow flatter and more stretched out in monolayer culture which affects their functions, such as proliferation, differentiation and protein expression. In a natural state, cells interact with the microenvironment of the tissue, such as the ECM and nearby cells. (Edmondson et al. 2014) With this information, the results from this 2D medium test are not definitive, and cell behaviour may be very different in 3D culture with hydrogels.

7.3 Hydrogel preparation and 3D cell culture

The suggested cell density for seeded HCEs (56 500 cells/insert, 50 000 cells/cm^2) was enough for the cells to begin proliferation to confluent layer and the cells also stratified during air-lifting. (Engelke et al. 2013) The amount of HCKs mixed in the hydrogels was problematic, and it could be that the HCK density was too low in the hydrogel environment. After the experimental part was performed, it seems that the number of

HCKs could have been higher in the experiments. The suggested amount was approximately 200 000 cells/ml (Engelke et al. 2013), which would mean approximately 40 000 cells for 200 µl of hydrogel. Now the number was 30 000 cells/sample in all hydrogel experiment replicates, even though hydrogel volume varied between replicates. After seeing all the results from the three hydrogel experiment replicates, number of HCKs could have been raised to 40 000 or even to 60 000 cells/sample, depending on the total volume of the hydrogel samples. It could have been beneficial to monitor the viability of HCKs somehow, but for example imaging of HCKs was difficult with the light microscope after the HCEs had proliferated and attached to the hydrogel surface.

In all three replicates of the hydrogel experiment, CnT-20 and CnT-Prime-CC media were used. Also CnT-30 was included in the first experiment replicate due to the inconclusive results of the medium test. However, after the first replicate, it was evident that CnT-Prime-CC was a better choice, since CnT-30 as a differentiation medium did not serve the purpose of this experiment.

Hydrogels A, C and D, all seemed to be biocompatible since cells seemed to proliferate well according to obtained microscopy images. However, in the first hydrogel experiment replicate, the outcome of the prepared hydrogels C and D was somewhat surprising, since there was drastic difference in appearance between these two and hydrogel A. The samples were softer than hydrogel A and the cells seemed to form clumps, whereas hydrogel A samples were consistently firmer and more even with confluent cell layer. As these hydrogels C and D where studied only in one hydrogel test replicate, it cannot be concluded that these hydrogels are not suitable with corneal cells. On the contrary, the reason why this clumping happened needs to be evaluated if it could be avoided in the future studies with these hydrogels.

As mentioned, hydrogel A samples seemed more consistent in all of the three hydrogel experiment replicates. HCE attachment to the hydrogel surface took approximately three to four days but after that, cells seemed to be viable and proliferating since even and confluent layers of cells were already visible in CnT-Prime-CC cultured samples before air-lifting was initiated. It seemed that there was slightly less cells in CnT-20 cultured samples and the layer was not confluent in the beginning of air-lifting. This was observed, since the CnT-20 culture media penetrated the hydrogel samples and there was always excess medium on top of the samples, even though, in air-lifting, there should not be culture medium on top of the samples. If HCEs would have been present as confluent layer, the medium would not have been able to penetrate the sample, which was the case with hydrogel A samples cultured in CnT-Prime-CC.

As the physical appearance of the hydrogel A was observed, the samples were even, transparent and visible throughout the 3D cell culture but became thinner during the air-lifting phase. It is possible that the hydrogels could have lost water from their structures during the air-lifting and become dehydrated which would affect the thickness of the

samples. Thinning was already noticed in the first experiment replicate, and due to this reason the volume of hydrogel samples was increased from 200 µl to 300 µl to the second and third replicates.

HyStem®-C was chosen for this thesis study as a commercial hydrogel option. As the 3D cell culture was observed, it was evident that HCEs rapidly attached to the surface of the hydrogel, faster than to the other hydrogel surfaces. However, there were no longer any cells visible on day 9. It was discussed in the laboratory that the shelves of the incubator, where these samples were kept, had an unusual slight tremor which could have caused the cells to detach. As a commercially available hydrogel application, it would be highly unlikely that the cells would have detached from the samples due to issues with compatibility since according to the manufacturer, HyStem®-C should be very biocompatible and suit all kinds of cell lines.

7.4 Cryoblock preparation

Cryoblock preparation turned out to be quite challenging, as the samples became easily damaged due to the softness of the hydrogels. The most important step of the preparation process was to keep these somewhat fragile samples, especially hydrogels C and D, intact along with the supporting insert films to minimise damage. The preparation caused the samples to slightly fall apart as the insert halves were moved to the mould with tweezers. This meant that the hydrogel samples were not fully immersed into the viscous O.C.T and also, the broken samples spread around the O.C.T in the moulds. This was visible in the IF stained samples, since the cells are in small clumps and not as layers on top of the insert film. These difficulties with cryoblock preparation led to a need for protocol optimisation.

In the following hydrogel tests with only hydrogel A, cryoblock preparation was modified. First, a small amount of O.C.T was added on top of the insert, fully covering the hydrogel. Before cutting out the insert film, the whole insert with O.C.T was frozen. After the freezing process, the film was carefully cut out and then the entire block frozen in O.C.T was cut in half quickly, before the block began to melt. These halves were placed to the mould with O.C.T the same manner as in the original protocol and then frozen. This modified protocol helped to preserve the hydrogel structure and this is reflected in the higher quality of IF images compared to the first hydrogel test. However, this needed still optimisation since the there was a risk that in the cutting process, O.C.T melt too quickly and caused slipping of the insert film apart from the hydrogel, that could cause damage to the sample.

In the third hydrogel experiment cryoblock preparation, the insert film was cut out with a scalpel similarly as in the original protocol. This time as a change, the whole film with the hydrogel was placed horizontally to lay on top of the O.C.T in the mould. Then a small amount of O.C.T was added to cover the sample, completely submerging the insert

film with hydrogel in O.C.T. The block was then frozen and removed from the mould. The mould was then filled again with O.C.T and the frozen block was cut in half and placed back to the mould as in the original protocol, the halves cut sides down and parallel to each other. Then some O.C.T was added on top to ensure the halves stayed in place, and frozen again.

In this last modified version of the protocol, the insert film stayed intact and in place quite well since O.C.T supported the samples from both sides like a frame. However, the preparation had to be done fast since frozen O.C.T melts very quickly at room temperature as it was mentioned earlier. All in all, the last optimised version of this protocol produced the best and least damaged samples to be sectioned with the cryotome. The IF staining images from the last hydrogel experiment support this, and the cryosections were better preserved than the sections from the previous hydrogel experiments.

7.5 Cell behaviour in 3D culture

Behaviour of HCEs and HCKs in 3D culture was somewhat different compared to the behaviour in 2D culture. The 3D environment altered the cell behaviour slightly more similar to protein expression in native tissue. However, to keep in mind, native corneal tissue is constructed from tightly packed collagen-rich structures that influence greatly on behaviour of different corneal cells (DelMonte & Kim 2011; Hejtmancik & Nickelson 2015; Massoudi et al. 2015), which means that a biomaterial-based approach cannot fully mimic the native ECM and induce specific corneal cell behaviour even in ideal situation but it can be used as a reference as the compatibility of different biomaterials is evaluated.

The IF stained cryosections from the second and third hydrogel experiment replicates showed more similar protein expression profiles. The first replicate was cultured for 14 days and second and third replicates were cultured for 21 days, both time periods including air-lifting of 7 days. As the cryosections of the first replicate were evaluated, it was visible that the cells had not had enough time to stratify, since not too much stratification was visible. For this reason, the culture time of the hydrogel experiment was increased with 7 days. As a result, the prolonging the culture time was beneficial since second and third replicates show better stratification of the cells. For future studies, it could be considered if the culture time could be further prolonged and optimised to see how the cell behaviour changes in this 3D cells culture with hydrogels. Although, it could cause cells to stratify too much which is not the intention since the epithelium contains only 5 to 7 cells layers of HCEs *in vivo*.

As the 3D cell culture hydrogels are evaluated, there was no particular difference between samples that contained only HCEs and samples that contained both, HCEs and HCKs. As for the media, the hydrogel samples cultured in CnT-Prime-CC and CnT-20 exhibit similar results and more mature corneal epithelial protein expression than CnT-30 cell cultured hydrogel samples with expression of CK3 and CK12 but not ABCG2. The CnT-

30 cultured samples stronger expression. The stratified epithelial marker CK15 was only weakly expressed in CnT-Prime-CC cultured samples. Hydrogel A samples cultured in CnT-30 did not express cytokeratin markers but ABCG2 was expressed quite strongly. Finally, hydrogels C and D in CnT-30 and CnT-Prime-CC expressed both ABCG2 and CK12, but only very slightly.

Furthermore, there were no major differences between samples that only contained HCEs and samples that contained HCEs and HCKs when the keratocyte marker expressions were evaluated. Healthy corneal marker KTN was quite strongly expressed in all CnT-20 and CnT-Prime-CC 3D cell cultured hydrogel A samples. The myofibroblast marker α-SMA was expressed only slightly in stratified cell layers of hydrogel A samples that were cultured in CnT-Prime-CC. Otherwise α-SMA was expressed quite strongly in all other hydrogel samples similarly to 2D cultured cells, especially in samples that contained HCKs. The wound healing and stress marker VIM was expressed quite strongly in all other hydrogel samples, except only slightly in the cells of hydrogel A samples that were cultured in CnT-Prime-CC.

Overall, the hydrogel A 3D cell cultured sample protein expression resembled most native healthy corneal cell behaviour in CnT-Prime-CC medium, since most of the epithelial cell markers indicate similarities to epithelial cell behaviour. Similarly, the stromal markers indicate that there is stromal cell behaviour but it seems that even though the healthy keratocyte marker KTN is expressed, HCKs and even HCEs express slightly VIM and α-SMA which could indicate similar behaviour of the cells as in 2D culture environment. It could be beneficial to perform the previously suggested double stainings: VIM and KTN, and α-SMA and KTN to obtain more information about the co-expression of these markers.

As the H&E stained cryosections are evaluated, the stratification of HCEs is visible in hydrogel A samples cultured in both CnT-20 and CnT-Prime-CC media. Overall, CnT-Prime-CC samples seemed to be thicker and more stratified, and cells were ordered to tighter constructs than the CnT-20 samples, since more haematoxylin stained nuclei are visible. CnT-20 samples seems more eosin stained, which stains the ECM and intercellular material. However, as it can be seen from samples cultured in both media, there is not much hydrogel material visible which supports the thinning of hydrogel material discussed in Chapter 7.3. As there were some difficulties with the H&E protocol, not many samples survived the staining protocol, so evaluation of the hydrogels was based on few samples. The cryosectioned hydrogels seemed to detach from the Superfrost™ Plus microscope slides quite easily during the rising alcohol series and the insert films teared off from the hydrogels, damaging the samples further. Due to the problems with the H&E staining, the protocol needs further optimisation and to get more presentable results, larger number of samples should be stained.

All in all, the 3D co-culturing of these cell lines in different hydrogels showed surprising results. The proliferation assay results carried out in 2D culture indicated that the best medium would be CnT-20 for both cell lines separately. Also the 3D cell culture results partly support the use of CnT-20 since the protein expression indicated corneal cell-like behaviour. However, after evaluating the results carefully, it could be concluded that CnT-Prime-CC would be an even better choice since hydrogel A samples cultured in this medium showed the most favourable proliferation during the 3D culture and in the qualitative assessment, the results with these immortalised cell lines indicated closest resemblance to protein expression of healthy corneal cell phenotype *in vivo*.

These results indicate the best suitable hydrogel and culture medium from the ones tested for further research, although it is still unclear how much the HCKs affected the results. There is not much indication that the samples that contained HCKs would be different from those that did not contain HCKs. It could be that the number of HCKs was too low to actually see their influence on the results, as discussed in Chapter 7.3.

As these IF stained 2D and 3D cell culture results are evaluated, there are important factors to be considered that affect protein expression of the corneal cells. The main two factors to be considered are: in 3D cell culture cells behave differently than in 2D, and there is an interaction relationship between epithelial cells and stromal keratocytes. (Edmondson et al. 2014; Kobayashi et al. 2015; Rah 2011)

It was previously explained in Chapter 2 that epithelial and stromal cells interact strongly to maintain the integrity and homeostasis of the cornea. It has been studied that for example keratocytes regulate wound healing and maintenance of the epithelium with growth factors and cytokines. Meanwhile, pathological conditions of the epithelium activate the keratocytes and transform them to fibroblasts and myofibroblasts. It means that this stromal-epithelial interaction plays a crucial role in the cellular responses of these cell types if something happens in their environment by altering their protein expression profiles. (Kobayashi et al. 2015)

In Chapter 7.1. it was mentioned how cell behave differently in 2D environment, since in 3D environments it is increasingly evident, that cells can create more accurate microenvironments compared to native tissue. This leads to more reflective results when compared to *in vivo* cellular responses. It has been studied that cells actually have different morphological and physiological properties depending on the cell culture type, 2D or 3D. Allowing the cells to interact with their 3D environment that contains other cells and ECM, the stimuli received affect cellular functions such as proliferation, differentiation, morphology, and protein expression. (Edmondson et al. 2014) In this study, hydrogels functioned as ECM for the corneal cells and this interaction between the cells and materials were studied if studied hydrogels and their chemical composition and physical properties support corneal cell behaviour and functions.

8. CONCLUSIONS

This thesis studies hydrogels and their suitability for the purpose of biomaterial-based artificial corneal substitute. The experimental part was conducted with two immortalised human corneal cell lines, HCEs and HCKs. 2D cell culture test was performed for both cell lines with three different potential CnT media (CnT-20, CnT-30 and CnT-Prime-CC) compared to HCE and HCK maintenance media to find suitable culture media options for the 3D co-culture of the cell lines with hydrogels. Cellular behaviour was evaluated with a proliferation assay and qualitative IF staining to examine the protein expression the corneal cells. According to the results, although all media supported cell growth and proliferation, CnT-20 was the best option out of the tested media.

The hydrogel 3D cell culture experiment was conducted with five hydrogels: A, B, C and D and commercial HyStem®-C. The first replicate of the hydrogel experiment was conducted with hydrogels A, B, C and D. Hydrogel A proved to be superior, and the other three hydrogels were omitted from the following replicates. CnT-30 medium was also discarded at this point, leaving only CnT-20 and CnT-Prime-CC for the second and third replicates. In the third replicate was conducted with hydrogel A and HyStem®-C.

During the 3D cell culture, HCEs proliferated and stratified best in samples cultured in CnT-Prime-CC. According to qualitative IF staining results, also the corneal markers indicated that CnT-Prime-CC was the best option since the cell behaviour in these samples was the closest to phenotypic healthy epithelial and stromal cells *in vivo.* Hydrogel A, was tested in all of the hydrogel experiment replicates, and it proved to be the best option from the beginning. The structure of hydrogel A samples supported cell proliferation and stratification, and the samples were even, clear and transparent but somewhat thin and soft.

REFERENCES

Ahn, J-I., Kuffova, L., Merrett, K., Mitra, D., Forrester, J.V., Li, F. & Griffith, M. (2013). Crosslinked collagen hydrogels as corneal implants: Effects of sterically bulky vs. non-bulky carbodiimides as crosslinkers, Acta Biomaterialia, Vol. 9(8), pp. 7796-7805.

Ambekar, R., Toussaint, K.C. & Wagoner Johnson, A. (2011). The effect of keratoconus on the structural, mechanical, and optical properties of the cornea, Journal of the Mechanical Behavior of Biomedical Materials, Vol. 4(3), pp. 223-236.

Annabi, N., Tamayol, A., Uquillas, J.A., Akbari, M., Bertassoni, L.E., Cha, C., Camci-Unal, G., Dokmeci, M.R., Peppas, N.A. & Khademhosseini, A. (2014). 25th Anniversary Article: Rational Design and Applications of Hydrogels in Regenerative Medicine, Advanced Materials, Vol. 26(1), pp. 85-124.

Avadhanam, V.S., Smith, H.E. & Liu, C. (2015). Keratoprostheses for corneal blindness: a review of contemporary devices, Clinical Ophthalmology, Vol. 9, pp. 697-720.

Bartakova, A., Kunzevitzky, N.J. & Goldberg, J.L. (2014). Regenerative Cell Therapy for Corneal Endothelium, Current Ophthalmology Reports, Vol. 2(3), pp. 81-90.

Boeriu, C.G., Springer, J., Kooy, F.K., van den Broek, L.A.M. & Eggink, G. (2013). Production Methods for Hyaluronan, International Journal of Carbohydrate Chemistry, Vol. 2013, pp. 1-14.

Bray, L.J., George, K.A., Ainscough, S.L., Hutmacher, D.W., Chirila, T.V. & Harkin, D.G. (2011). Human corneal epithelial equivalents constructed on *Bombyx mori* silk fibroin membranes, Biomaterials, Vol. 32(22), pp. 5086-5091.

Carlson, E.C., Liu, C-Y., Chikama, T-I., Hayashi, Y., Kao, C.W.C., Birk, D.E., Funderburgh, J.L., Jester, J.V. & Kao, W.W-Y. (2005). Keratocan, a Cornea-specific Keratan Sulfate Proteoglycan, Is Regulated by Lumican, The Journal of Biological Chemistry, Vol. 280(27), pp. 25541-25547.

Chen, Q., Liang, S. & Thouas, G.A. (2013). Elastomeric biomaterials for tissue engineering, Progress in Polymer Science, Vol. 38, pp. 584-671.

Chen, F-M. & Liu, X. (2016). Advancing biomaterials of human origin for tissue engineering, Progress in Polymer Science, Vol. 53, pp. 86-168.

Chen, S., Mienaltowski, M.J. & Birk, D.E. (2015). Regulation of corneal stroma extracellular matrix assembly, Experimental Eye Research, Vol. 133, pp. 69-80.

Cholkar, K., Dasari, S.R., Pal, D. & Mitra, A.K. (2013). 1 - Eye: anatomy, physiology and barriers to drug delivery, in: Mitra, A.K. (ed.), Ocular Transporters and Receptors, Woodhead Publishing, pp. 1-36.

Chow, S. & Di Girolamo, N. (2014). Vitronectin: A Migration and Wound Healing Factor for Human Corneal Epithelial Cells, Investigative Ophthalmology & Visual Science, Vol. 55(10), pp. 6590-6600.

DelMonte, D.W. & Kim, T. (2011). Anatomy and physiology of the cornea, Journal of Cataract & Refractive Surgery, Vol. 37(3), pp. 588-598.

Deng, C., Li, F., Hackett, J.M., Chaudhry, S.H., Toll, F.N., Toye, B., Hodge, W. & Griffith, M. (2010). Collagen and glycopolymer based hydrogel for potential corneal application, Acta Biomaterialia, Vol. 6(1), pp. 187-194.

de Paiva, C.S., Chen, Z., Corrales, R.M., Pflugfelder, S.C. & Li, D-Q. (2005). ABCG2 Transporter Identifies a Population of Clonogenic Human Limbal Epithelial Cells, Stem Cells, Vol. 23(1), pp. 63-73.

de Roth, A.D. (1940). Plastic repair of conjunctival defects with fetal membranes, Archives of Ophthalmology, Vol. 23, pp. 522-525.

Dhouailly, D., Pearton, D.J. & Michon, F. (2014). The Vertebrate Corneal Epithelium: From Early Specification to Constant Renewal, Developmental Dynamics, Vol. 243(10), pp. 1226-1241.

Diao, J-M., Pang, X., Qiu, Y., Miao, Y., Yo, M-M. & Fan, T-J. (2015). Construction of a human corneal stromal equivalent with non-transfected human corneal stromal cells and acellular porcine corneal stromata, Experimental Eye Research, Vol. 132, pp. 216-224.

Dicker, K.T., Gurski, L.A., Pradhan-Bhatt, S., Witt, R.L., Farach-Carson, M.C. & Jia, X. (2014). Hyaluronan: A Simple Polysaccharide with Diverse Biological Functions, Acta Biomaterialia, Vol. 10(4), pp. 1558-1570.

Ding, X-W., Wu, J-H. & Jiang, C-P. (2010). ABCG2: A potential marker for stem cells and novel target stem cell and cancer therapy, Life Sciences, Vol. 86(17-18), pp. 631-637.

Drupps, W.J. & Wilson, S.E. (2006). Biomechanics and wound healing in the cornea, Experimental Eye Research, Vol. 83(4), pp. 709-720.

Drury, J.L. & Mooney, D.J. (2003). Hydrogels for tissue engineering: scaffold design variables and applications, Biomaterials, Vol. 24(24), pp. 4337-4351.

Duan, X., McLaughlin, C., Griffith, M. & Sheardown, H. (2007). Biofunctionalization of collagen for improved biological response: Scaffolds for corneal tissue engineering, Biomaterials, Vol. 28(1), pp. 78-88.

Edmondson, R., Broglie, J.J., Adcock, A.F. & Yang, L. (2014). Three-Dimensional Cell Culture Systems and Their Applications in Drug Discovery and Cell-Based Biosensors, Assay and Drug Development Technologies, Vol. 12(4), pp. 207-218.

Engelke, M., Zorn-Kruppa, M., Gabel, D., Reisinger, K., Rusche, B. & Mewes, K.R. (2013). A human hemi-cornea model for eye irritation testing: Quality control of production, reliability and predictive capacity, Toxicology in Vitro, Vol. 27(1), pp. 458-468.

Espana, E.M., He, H., Kawakita, T., Di Pascuale, M.A., Raju, V.K., Liu, C-Y. & Tseng, S.C.G. (2003). Human Keratocytes Cultured on Amniotic Membrane Stroma Preserve Morphology and Express Keratocan, Investigative Ophthalmology & Visual Science, Vol. 44(12), pp. 5136-5141.

Espana, E.M., Sun, M. & Birk, D.E. (2015). Existence of Corneal Endothelial Slow-Cycling Cells, Investigative Ophthalmology & Visual Science, Vol. 56(6), pp. 3827-3837.

Fagerholm, P., Lagali, N.S., Ong, J.A., Merrett, K., Jackson, W.B., Polarek, J.W., Suuronen, E.J., Liu, Y., Brunette, I. & Griffith, M. (2014). Stable corneal regeneration four years after implantation of a cell-free recombinant human collagen scaffold, Biomaterials, Vol. 35(8), p. 2420-2427.

Francesconi, C.M., Hutcheon, A.E.K., Chung, E-H., Dalbone, A.C., Joyce, N.C. & Zieske, J.D. (2000). Expression Patterns of Retinoblastoma and E2F Family Proteins during Corneal Development, Investigative Ophthalmology & Visual Science, Vol. 41(5), pp. 1054-1062.

Funderburgh, M.L., Du, Y., Mann, M.M., SundarRaj, N. & Funderburgh, J.L. (2005). PAX6 expression identifies progenitor cells for corneal keratocytes, The FASEB Journal, Vol. 19(10), pp. 1371-1373.

Gefen, A., Shalom, R., Elad, D. & Mandel, Y. (2009). Biomechanical analysis of the kerotoconic cornea, Journal of the Mechanical Behavior of Biomedical Materials, Vol. 2(3), pp. 224-236.

Gelse, K., Pöschl, E. & Aigner, T. (2003). Collagen – structure, function and biosynthesis, Advanced Drug Delivery Reviews, Vol. 55(12), pp. 1531-1546.

Germain, L., Carrier, P., Auger, F.A., Salesse, C. & Guérin, S.L. (2000). Can We Produce a Human Corneal Equivalent by Tissue Engineering?, Progress in Retinal and Eye Research, Vol. 19(5), pp. 497-527.

Ghezzi, C.E., Rnjak-Kovacina, J. & Kaplan, D.L. (2015). Corneal Tissue Engineering: Recent Advances and Future Perspectives, Tissue Engineering Part B: Reviews, Vol. 21(3), pp. 278-287.

Gil, E.S., Mandal, B.B., Park, S-H., Marchant, J.K., Omenetto, F.G. & Kaplan, D.L. (2010). Helicoidal multi-lamellar features of RGD-functionalized silk biomaterials for corneal tissue engineering, Biomaterials, Vol. 31(34), pp. 8953-8963.

Gong, Y., Wang, C., Lai, R.C., Su, K., Zhang, F. & Wang, D-A. (2009). An improved injectable polysaccharide hydrogel: modified gellan gum for long-term cartilage regeneration *in vitro*, Journal of Materials Chemistry, Vol. 19(14), pp. 1968-1977.

Greco, D., Vellonen, K-S., Turner, H.C., Häkli, M., Tervo, T., Auvinen, P., Wolosin J.M. & Urtti, A. (2010). Gene erpression analysis in SV-40 immortalized human corneal epithelial cells cultured with an air-liquid interface, Molecular Vision, Vol. 16, pp. 2109-2120.

Grinstaff, M.W. (2007). Designing Hydrogel Adhesives for Corneal Wound Healing, Biomaterials, Vol. 28(35), pp. 5205-5214.

Grolik, M., Szczubiałka, K., Wowra, B., Dobrowolski, D., Orzechowska-Wylęgała, B., Wylęgała, E. & Nowakowska, M. (2012). Hydrogel membranes based on genipin-cross-linked chitosan blends for corneal epithelium tissue engineering, Journal of Materials Science: Materials in Medicine, Vol. 23(8), pp. 1991-2000.

Haagdorens, M., Van Acker, S.I., Van Gerwen, V., Ni Dhubhghail, S., Koppen, C., Tassignon, M-J. & Zakaria, N. (2016). Limbal Stem Cell Defiency: Cureent Treatment Options and emerging Threapies, Stem Cells International, Vol. 2016, pp. 1-22.

Hassell, J.R. & Birk, D.E. (2010). The molecular basis of corneal transparency, Experimental eye research, Vol. 91(3), pp. 326-335.

Hatami-Marbini, H. (2015). Viscoelastic shear properties of the corneal stroma, Journal of Biomechanics, Vol. 47(21), pp. 723-728.

Hatami-Marbini, H. & Etebu, E. (2013). Hydration dependent biomechanical properties of the corneal stroma, Experimental Eye Research, Vol. 116, pp. 47-54.

Hayes, S., Lewis, P., Islam, M.M., Doutch, J., Sorensen, T., White, T., Griffith, M. & Meek, K.M. (2015). The structural and optical properties of type III human collagen biosynthetic corneal substitutes, Acta Biomaterialia, Vol. 25, pp. 121-130.

Hejtmancik, J.F. & Nickerson, J.M. (2015). Chapter One - Overview of the Visual System, Progress in Molecular Biology and Translational Science, Vol. 134 pp. 1-4.

Hingorani, M., Hanson, I. & van Heyningen, V. (2012). Aniridia, European Journal of Human Genetics, Vol. 20(10), pp. 1011-1017.

Hoffman, A.S. (2002). Hydrogels for biomedical applications, Advanced Drug Delivery Reviews, Vol. 54(1), pp. 3-12.

Islam, M.M., Cėpla, V., He, C., Edin, J., Rakickas, T., Kobuch, K., Ruželė, Ž., Jakson, W.B., Rafat, M., Lohmann, C.P., Valiokas, R. & Griffith, M. (2015). Functional fabrication of recombinant human collagen-phosphorylcholine hydrogels for regenerative medicine applications, Acta Biomaterialia, Vol. 12, pp. 70-80.

Islam, M.M., Griffith, M. & Merrett, K. (2013). Fabrication of a Human Recombinant Collagen-Based Corneal Substitute Using Carbodiimide Chemistry, Methods in Molecular Biology, Vol. 1014, pp. 157-164.

Jia, X., Yeo, Y., Clifton, R.J., Jiao, T., Kohane, D.S., Kobler, J.B., Zeitels, S.M. & Langer, R. (2006). Hyaluronic Acid-Based Microgels and Microgel Networks for Vocal Fold Regeneration, Biomacromolecules, Vol. 7(12), pp. 3336-3344.

Jiang, Y., Chen, J., Deng, C., Suuronen, E.J. & Zhong, Z. (2014). Click hydrogels, microgels and nanogels: Emerging platforms for drug delivery and tissue engineering, Biomaterials, Vol. 35(18), pp. 4969-4985.

Joseph, R., Srivastava, O.P. & Pfister, R.R. (2011). Differential epithelial and stromal protein profiles in keratoconus and normal human corneas, Experimental Eye Research, Vol. 92(4), pp. 282-298.

Joyce, N.C., Meklir, B., Joyce, S.J. & Zieske, J.D. (1996). Cell cycle protein expression and proliferative status in human corneal cells, Investigative Ophthalmology & Visual Science, Vol. 37(4), pp. 645-655.

Kayama, M., Kurokawa, M.S., Ueno, H. & Suzuki, N. (2007). Recent advances in corneal regeneration and possible application of embryonic stem cell-derived corneal epithelial cells, Clinical Ophthalmology, Vol. 1(4), pp. 373-382.

Klintworth, G.K. (2009). Corneal dystrophies, Orphanet Journal of Rare Diseases, Vol. 4(7), 38 pages.

Kobayashi, T., Shiraisi, A., Hara, Y., Kadota, Y., Yang, L., Inoue, T. Shirakata, Y. & Ohashi, Y. (2015). Stromal-epithelial interaction study: The effect of corneal epithelial cells on growth factor expression in stromal cells using organotypic culture model, Experimental Eye Research, Vol. 135, pp 109-117.

Koo, S., Ahn, S.J., Zhang, H., Wang, J.C. & Yim, E.K.F. (2011). Human Corneal Keratocyte Response to Micro- and Nano-Gratings on Chitosan and PDMS, Cellular and Molecular Bioengineering, Vol. 4(3), pp. 399-410.

Kopěcek, J. (2007). Hydrogel Biomaterials: A Smart Future?, Biomaterials, Vol. 28(34), pp. 5185-5192.

Koulikovska, M., Rafat, M., Petrovski, G., Veréb, Z., Akhtar, S., Fagerholm, P. & Lagali, N. (2015). Enhanced Regeneration of Corneal Tissue Via a Bioengineered Collagen Construct Implanted by a Nondisruptive Surgical Technique, Tissue Engineering Part A, Vol. 21(5-6), pp. 1116-1130.

Kubota, M., Shimmura, S., Miyashita, H., Kawashima, M., Kawakita, T. & Tsubota, K. (2010). The Anti-oxidative Role of ABCG2 in Corneal Epithelial Cells, Investigative Ophthalmology & Visual Science, Vol. 51(11), pp. 5617-5622.

Lakshman, N., Kim, A. & Petroll, W.M. (2010). Characterization of corneal keratocyte morphology and mechanical activity within 3-D collagen matrices, Experimental Eye Research, Vol. 90(2), pp. 350-359.

Laurent, T.C. & Fraser J.R.E. (1992). Hyaluronan, The FASEB Journal, Vol. 6(7), pp. 2397-2404.

Lawrence, B.D., Marchant, J.K., Pindrus, M.A., Omenetto, F.G. & Kaplan, D.L. (2009). Silk film biomaterials for cornea tissue engineering, Biomaterials, Vol. 30(7), pp. 1299-1308.

Levis, H.J., Brown, R.A. & Daniels, J.T. (2010). Plastic compressed collagen as a biomimetic substrate for human limbal epithelial cell culture, Biomaterials, Vol. 30(31), pp. 7726-7737.

Levis, H.J., Kureshi, A.K., Massie, I., Morgan, L., Vernon A.J. & Daniels, J.T. (2015). Tissue Engineering the Cornea: Evolution of RAFT, The Journal of Functional Biomaterials, Vol. 6(1), pp. 50-65.

Levis, H.J., Massie, I., Dziasko, M.A., Kaasi, A. & Daniels, J.T. (2013). Rapid tissue engineering of biomimetic human corneal limbal crypts with 3D niche architecture, Biomaterials, Vol. 34(35), pp. 8860-8868.

Lewis, P.N., White, T.L., Young, R.D., Bell, J.S., Winlove, C.P. & Meek, K.M. (2016). Three-dimensional arrangement of elastic fibers in the human corneal stroma, Experimental Eye Research, Vol. 146, pp. 43-53.

Li, Y-H., Cheng, C-Y., Wang, N-K., Tan, H-Y., Tsai, Y-J., Hsiao, C-H., Ma, D.H-K. & Yeh, L-K. (2015). Characterization of the modified chitosan membranes cross-linked with genipin for the cultured corneal epithelial cells, Colloids and Surfaces B: Biointerfaces, Vol. 126, pp. 237-244.

Lim, M., Goldstein, M.H., Tuli, S. & Schultz, G.S. (2003). Growth Factor, Cytokine and Protease Interactions During Corneal Wound Healing, The Ocular Surface, Vol. 1(2), pp. 53-65.

Liu, W., Merrett, K., Griffith, M., Fagerholm, P., Dravida, S., Heyne, B., Scaiano, J.C., Wastky, M.A., Shinozaki, N., Lagali, N., Munger, R. & Li, F. (2008). Recombinant human collagen for tissue engineered corneal substitutes, Biomaterials, Vol. 29(9), pp. 1147-1158.

Liu, Y., Ren, L. & Wang, Y. (2013). Crosslinked collagen–gelatin–hyaluronic acid biomimetic film for cornea tissue engineering applications, Materials Science and Engineering C, Vol. 33(1), pp. 196-201.

Liu, Y., Ren, L., Long, K., Wang, L. & Wang, Y. (2014b). Preparation and characterization of a novel tobramycin-containing antibacterial collagen film for corneal tissue engineering, Acta Biomaterialia, Vol. 10(1), pp. 289-299.

Liu, Y., Ren, L. & Wang, Y. (2014a). A novel collagen film with micro-rough surface structure for corneal epithelial repair fabricated by freeze drying technique, Applied Surface Science, Vol. 301, pp. 396-400.

Ljubimov, A.V. & Saghizadeh, M. (2015). Progress in corneal wound healing, Progress in Retinal and Eye Research, Vol. 49, pp. 17-45.

Long, K., Liu, Y., Li, W., Wang, L., Liu, S., Wang, Y., Wang, Z. & Ren, L. (2014). Improving the mechanical properties of collagen-based membranes using silk fibroin for corneal tissue engineering, Journal of Biomedical Materials Research Part A, Vol. 103(3), pp. 1159-1168.

Malafaya, P.B., Silva, G.A. & Reis, R.L. (2007). Natural-origin polymers as carriers and scaffolds for biomolecules and cell delivery in tissue engineering applications, Advanced Drug Delivery Reviews, Vol. 59, pp. 207-233.

Manzer, A.K., Lombardi-Borgia, S., Schäfer-Korting, M., Seeber, J., Zorn-Kruppa, M. & Engelke, M. (2009). SV40-Transformed Human Corneal Keratocytes: Optimisation of Serum-free Culture Conditions, ALTEX, Vol. 26(1), pp. 33-39.

Massie, I., Kureshi, A.K., Schrader, S., Shortt, A.J. & Daniels, J.T. (2015). Optimization of optical and mechanical properties of real architecture for 3-dimensional tissue equivalents: Towards treatment of limbal epithelial stem cell deficiency, Acta Biomaterialia, Vol. 24, pp. 241-250.

Massoudi, D., Malecaze, F. & Galiacy, S.D. (2015). Collagens and proteoglycans of the cornea: importance in transparency and visual disorders, Cell and tissue research, Vol. 363(2), pp. 1-13.

Meek, K.M. & Boote, C. (2004). The organization of collagen in the corneal stroma, Experimental Eye Research, Vol. 78(3), pp. 503-512.

Meek, K.M. & Knupp, C. (2015). Corneal structure and transparency, Progress in Retinal and Eye Research, Vol. 49, pp. 1-16.

Merrett, K., Fagerholm, P., McLaughlin C.R., Dravida, S., Lagali, N., Shinozaki, N., Watsky, M.A., Munger, R., Kato, S., Li, F., Marmo, C.J. & Griffith, M. (2008). Tissue-Engineered Recombinant Human Collagen-Based Corneal Substitutes for Implantation: Performance of Type I versus Type III Collagen, Investigative Ophthalmology & Visual Science, Vol. 49(9), pp. 3887-3894.

Mikhailova, A., Jylhä, A., Rieck, J., Nättinen, J., Ilmarinen, T., Veréb, Z., Aapola, U., Beuerman, R., Petrovski, G., Uusitalo, H. & Skottman, H. (2015). Comparative proteomics reveals human pluripotent stem cell-derived limbal epithelial stem cells are similar to native ocular surface epithelial cells, Scientific Reports, Vol. 5, 14684, pp. 1-14.

Nakamura, T., Inatomi, T., Sotozono, C., Koizumi, N. & Kinoshita, S. (2016). Ocular surface reconstruction using stem cell and tissue engineering, Progress in Retinal and Eye Research, Vol. 51, pp. 187-207.

Necas, J., Bartasikova, L., Brauner, P. & Kolar, J. (2008). Hyaluronic acid (hyaluronan: a review, Veterinarni Medicina, Vol. 53(8), pp. 397-411.

Notara, M., Alatza, A., Gilfillan, J., Harris, A.R., Levis, H.J., Schrader, S., Vernon, A. & Daniels, J.T. (2010). In sickness and in health: Corneal epithelial stem cell biology, pathology and therapy, Experimental Eye Research, Vol. 90(2), pp. 188-195.

Osmałek, T., Froelich, A. & Tasarek S. (2014). Application of gellan gum in pharmacy and medicine, International Journal of Pharmaceutics, Vol. 466(1-2), pp. 328-340.

Ozcelik, B., Brown, K.D., Blencowe, A., Daniell, M., Stevens, G.W. & Qiao, G.G. (2013). Ultrathin chitosan-poly(ethylene glycol) hydrogel films for corneal tissue engineering, Acta Biomaterialia, Vol. 9(5), pp. 6594-6605.

Pan, C., Kumar, C., Bohl, S., Klingmueller, U. & Mann, M. (2009). Comparative Proteomic Phenotyping of Cell Lines and Primary Cell to Assess Preservation of Cell Type-specific Functions, Molecular & Cellular Proteomics, Vol. 8(3), pp. 443-450.

Perry, H., Gopinath, A., Kaplan, D.L., Dal Negro, L. & Omenetto, F.G. (2008). Nano- and Micropatterning of Optically Transparent, Mechanically Robust, Biocompatible Silk Fibroin Films, Advanced Materials, Vol. 20(16), pp. 3070-3072.

Petroll, W.M. & Miron-Mendoza, M. (2015). Mechanical interactions and crosstalk between corneal keratocytes and the extracellular matrix, Experimental Eye Research, Vol. 133, pp. 49-57.

Petsch, C., Schlötzer-Schrehardt, U., Meyer-Blazejewska, E., Frey, M., Kruse, F.E. & Bachmann B.O. (2014). Novel Collagen Membranes for the Reconstruction of the Corneal Surface, Tissue Engineering Part A, Vol. 20(17-18), pp. 2378-2389.

Qazi, Y., Wong, G., Monson, B., Stringham, J. & Ambati B.K. (2010). Corneal transparency: Genesis, maintenance and dysfunction, Brain Research Bulletin, Vol. 81(2-3), pp. 198-210.

Rafat, M., Li, F., Fagerholm, P., Lagali, N.S., Watsky, M.A., Munger, R., Matsuura, T. & Griffith, M. (2008). PEG-stabilized carbodiimide crosslinked collagen–chitosan hydrogels for corneal tissue engineering, Biomaterials, Vol. 29(29), pp. 3960-3972.

Rafat, M., Xeroudaki, M., Koulikovska, M., Sherrell, P., Groth, F., Fagerholm, P. & Lagali, N. (2016). Composite core-and-skirt collagen hydrogels with differential degradation for corneal therapeutic applications, Biomaterials, Vol. 83, pp. 142-155.

Rah, M.J. (2011). A review of hyaluronan and its ophthalmic applications, Journal of the American Optometric Association, Vol. 82(1), pp. 38-43.

Rahman, I., Said, D.G., Maharajan, V.S. & Dua, H.S. (2009). Amniotic membrane in ophthalmology: indications and limitations, Eye, Vol. 23, pp. 1954-1961.

Rio-Cristobal, A. & Martin, R. (2014). Corneal assessment technologies: Current status, Survey of Ophthalmology, Vol. 59(6), pp. 599-614.

Ruberti, J.W. & Zieske, J.D. (2008). Prelude to corneal tissue engineering – Gaining control of collagen organization, Progress in Retinal and Eye research, Vol. 27(5), pp. 549-577.

Sidney, L.E., McIntosh, O.D. & Hopkinson, A. (2015). Phenotypic Change and Induction of Cytokeratin Expression During In Vitro Culture of Corneal Stromal Cells, Investigative Ophthalmology & Visual Science, Vol. 56(12), pp. 7225-7235.

Stoppel, W.L., Ghezzi, C.E., McNamara, S.L., Black III, L.D. & Kaplan, D.L. (2014). Clinical Applications of Naturally Derived Biopolymer-Based Scaffolds for Regenerative Medicine, Annals of Biomedical Engineering, Vol. 43(3), pp. 657-680.

Tidu, A., Ghoubay-Benallaoua, D., Lynch, B., Haye, B., Illoul, C., Allain, J-M., Borderie, V.M. & Mosser, G. (2015). Development of human corneal epithelium on organized fibrillated transparent collagen matrices synthesized at high concentration, Acta Biomaterialia, Vol. 22, pp. 50-58.

Tocce, E.J., Smirnov, V.K., Kibalov, D.S., Liliensiek, S.J., Murphy, C.J. & Nealey, P.F. (2010). The ability of corneal epithelial cells to recognize high aspect ratio nanostructures, Biomaterials, Vol. 31(14), pp. 4064-4072.

Torricelli, A.A.M., Singh, V., Santhiago, M.R. & Wilson, S.E. (2013). The Corneal Epithelial Basement Membrane: Structure, Function and Disease, Investigative Ophthalmology & Visual Science, Vol. 54(9), pp. 6390-6400.

Tsai, I-L., Hsu, C-C., Hung, K-H., Chang, C-W. & Cheng, Y-H. (2015). Applications of biomaterials in corneal wound healing, Journal of the Chinese Medical Association, Vol. 78(4), pp. 212-217.

Ueta, M., Sotozono, C., Inatomi, T., Kojima, K., Hamuro, J. & Kinoshita, S. (2008). Association of Combined IL-13/IL-4R Signaling Pathway Gene Polymorphism with Stevens-Johnson Syndrome Accompanied by Ocular Surface Complications, Investigative Ophthalmology & Visual Science, Vol. 49(5), pp. 1809-1813.

Uzunalli, G., Soran, Z., Erkal, T.S., Dagdas, Y.S., Dinc, E., Hondur, A.M., Bilgihan, K., Aydin, B., Guler, M.O. & Tekinay, A.B. (2014). Bioactive self-assembled peptide nanofibers for corneal stroma regeneration, Acta Biomaterialia, Vol. 10(3), pp. 1156-1166.

West-Mays, J.A. & Dwivedi, D.J. (2006). The keratocytes: Corneal stromal cell with variable repair phenotypes, International Journal of Biochemistry & Cell Biology, Vol. 38(10), pp. 1625-1631.

Whitford, C., Studer, H., Boote, C., Meek, K.M. & Elsheikh, A. (2015). Biomechanical model of the human cornea: Considering shear stiffness and regional variation of collagen anisotropy and density, Journal of the Mechanical Behavior of Biomedical Materials, Vol. 42, pp. 76-87.

Williams, G.P., Tomlins, P.J., Denniston, A.K., Southworth, H.S., Sreekantham, S., Curnow, S.J. & Rauz, S. (2013). Elevation of Conjunctival Epithelial $CD45^{INT}$ $CD11b^{+}$ $CD16^{+}$ $CD14^{-}$ Neutrophils in Ocular Stevens - Johnson Syndrome and Toxic Epidermal Necrolysis, Investigative Ophthalmology & Visual Science, Vol. 54(7), pp. 4578-4584.

World Health Organization 2016: Prevention of Blindness and Visual Impairment, Priority eye diseases, web page. Available (accessed 13.5.2016): http://www.who.int/blindness/causes/priority/en/

Wilson, S.E. & Hong, J-W. (2000). Bowman's Layer Structure and Function: Critical or Dispensable to Corneal Function? A Hypothesis, Cornea, Vol. 19(4), pp. 417-420.

Wright, B., Mi, S. & Connon, C.J. (2013). Towards the use of hydrogels in the treatment of limbal stem cell defiency, Drug Discovery Today, Vol. 18(1-2), pp. 79-86.

Wu, J., Du, Y., Mann, M.M., Funderburgh, J.L. & Wagner, W.R. (2014a). Corneal stromal stem cells versus corneal fibroblasts in generating structurally appropriate corneal stromal tissue, Experimental Eye Research, Vol. 120, pp. 71-81.

Wu, J., Rnjak-Kovacina, J., Du, Y., Funderburgh, M.L., Kaplan, D.L. & Funderburgh, J.L. (2014b). Corneal stromal bioequivalents secreted on patterned silk substrates, Biomaterials, Vol. 35(12), pp. 3744-3755.

Xiao, X., Pan, S., Liu, X., Zhu, X., Connon, C.J., Wu, J. & Mi, S. (2014). In vivo study of the biocompatibility of a novel compressed collagen hydrogel scaffold for artificial corneas, Journal of Biomedical Materials Science Research Part A, Vol. 102(6), pp. 1782-1787.

Xu, M., McCanna, D.J. & Sivak, J.G. (2015). Use of the viability reagent PrestoBlue in comparison with alamarBlue and MTT to assess the viability of human corneal epithelial cells, Journal of Pharmacological and Toxicological Methods, Vol. 71, pp. 1-7.

Yoon, J.J., Ismail, S. & Sherwin, T. (2014). Limbal stem cells: Central concepts of corneal epithelial homeostasis, World Journal of Stem Cells, Vol. 26(4), pp. 391-403.

Yoshida, S., Shimmura, S., Kawakita, T., Miyashita, H., Den, S., Shimazaki, J. & Tsubota, K. (2006). Cytokeratin 15 Can Be Used to Identify the Limbal Phenotype in Normal and Diseased Ocular Surfaces, Investigative Ophthalmology & Visual Science, Vol. 47(11), pp. 4780-4786.

Zeng, Y., Yang, J., Huang, K., Lee, Z. & Lee, X. (2001). A comparison of biomechanical properties between human and porcine cornea, Journal of Biomechanics, Vol. 34(4), pp. 533-537.

Zhao, X., Liu, Y., Li, W., Long, K., Wang, L., Liu, S., Wang, Y. & Ren, L. (2015). Collagen based film with well epithelial and stromal regeneration as corneal repair materials: Improving mechanical property by crosslinking with citric acid, Materials Science and Engineering C, Vol. 55, pp. 201-208.

Zhu, J. & Marchant, R.E. (2011). Design properties of hydrogel tissue-engineering scaffolds, Expert Review of Medical Devices, Vol. 8(5), pp. 607-626.

APPENDIX A: A COMPLETE COLLECTION OF THE IMMUNOFLUORESCENCE STAINED SAMPLES FROM THE 2D AND 3D CELL CULTURE STUDIES

In this section, all of the IF stained results are presented from the medium test (Figures S1-S8) and hydrogel experiment (Figures S9-S15). First the medium test with all of the three medium options compared with HCE or HCK culture medium depending on the cell line. The most important results are presented in Chapter 6. After the medium test results are the hydrogel experiment results.

Representative medium test IF images of HCEs and HCKs are presented in Figures S1-S5 and Figures S6-S8, respectively.

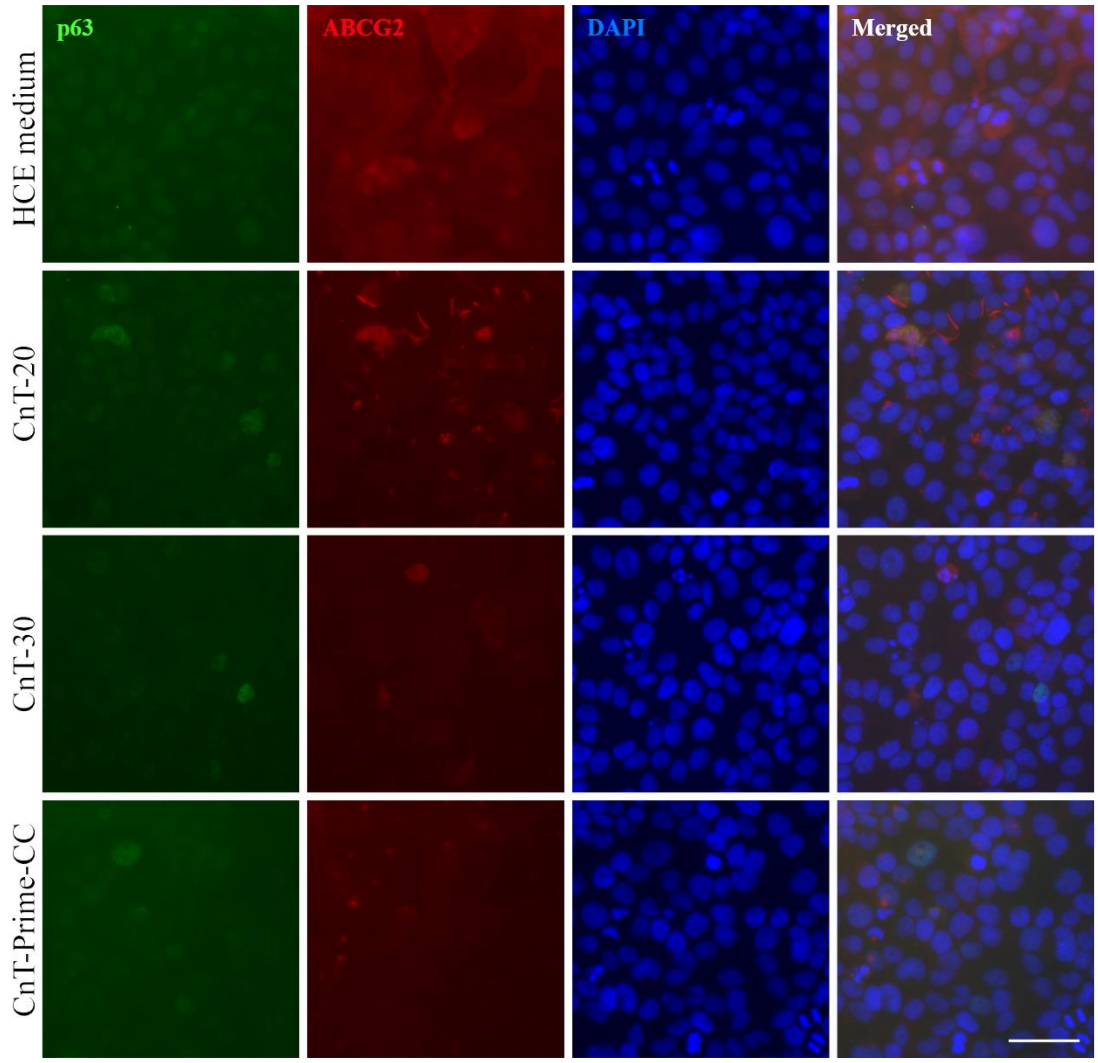

Figure S1. *HCEs stained with anti-p63 (green), anti-ABCG2 (red) and DAPI (blue). Scale bar 50 µm.*

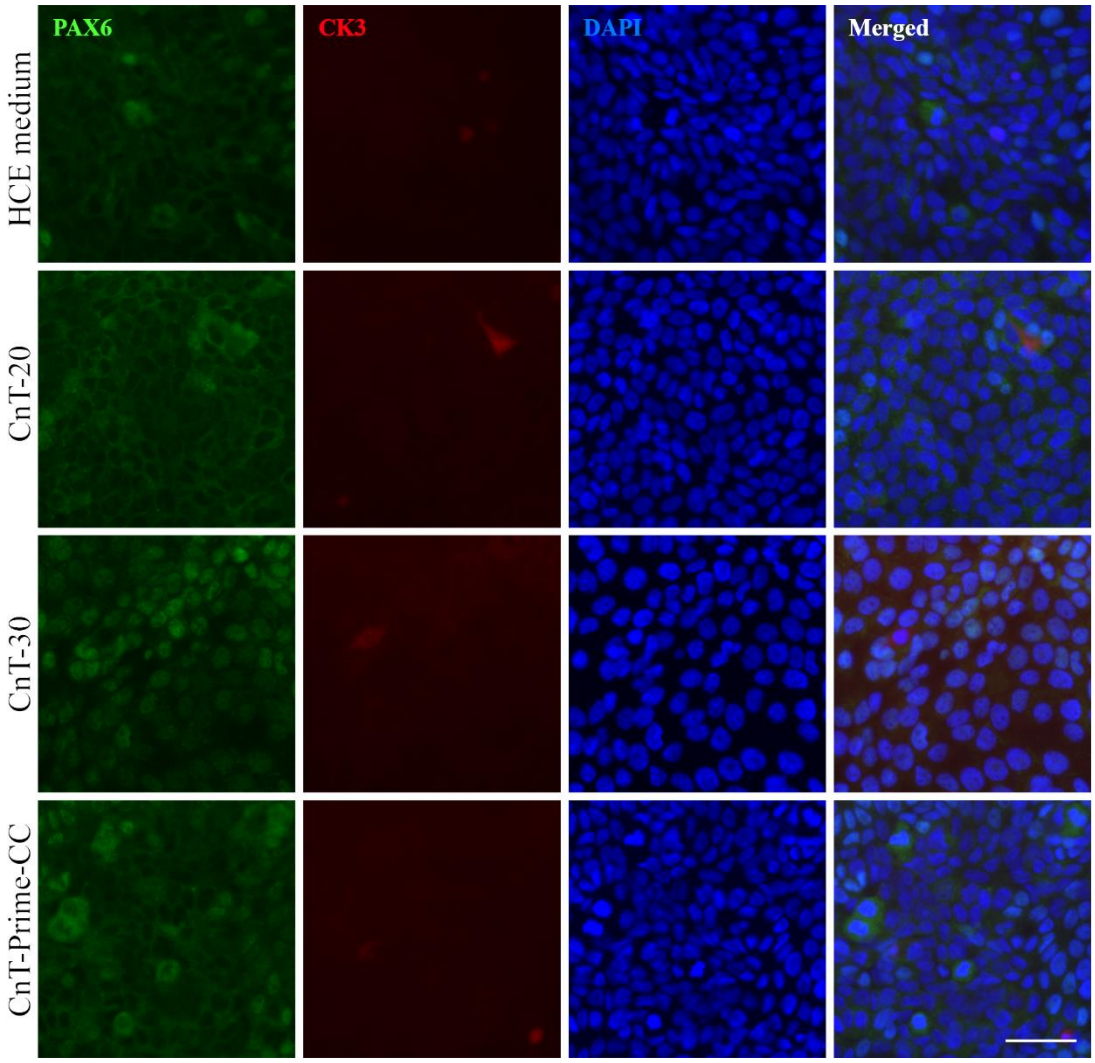

Figure S2. *HCEs stained with anti-PAX6 (green), anti-CK3 (red) and DAPI (blue). Scale bar 50 µm.*

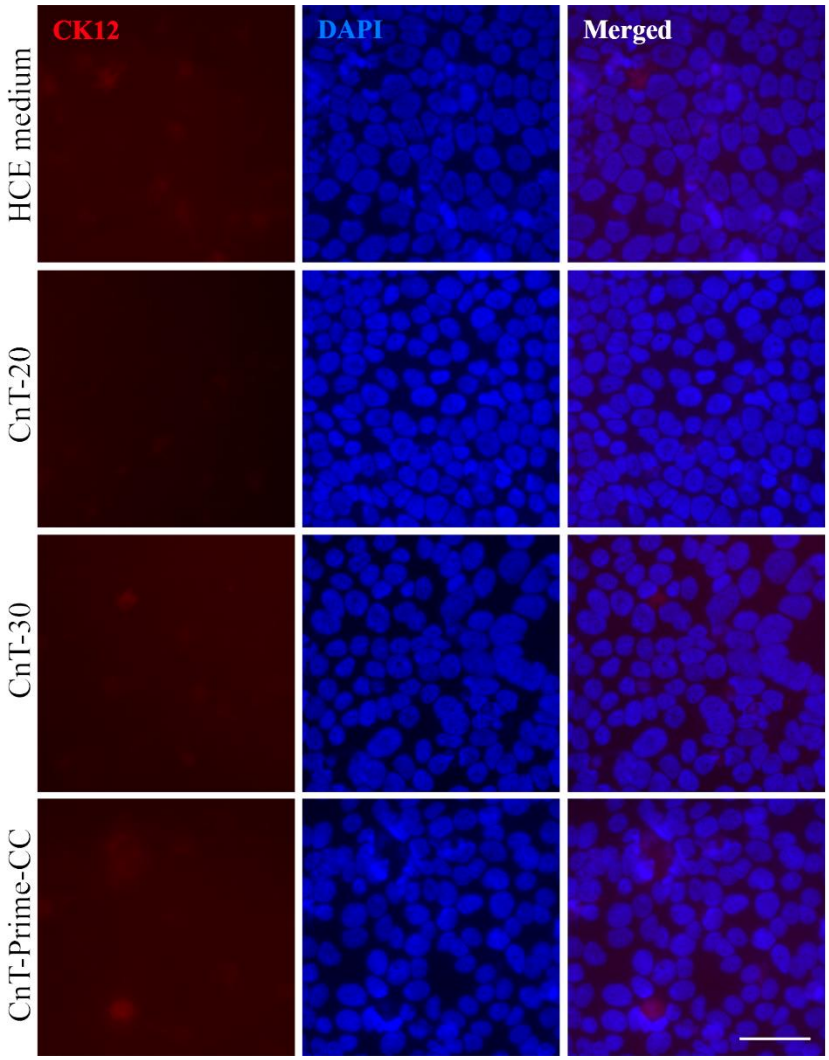

Figure S3. *HCEs stained with anti-CK12 (red) and DAPI (blue). Scale bar 50 µm.*

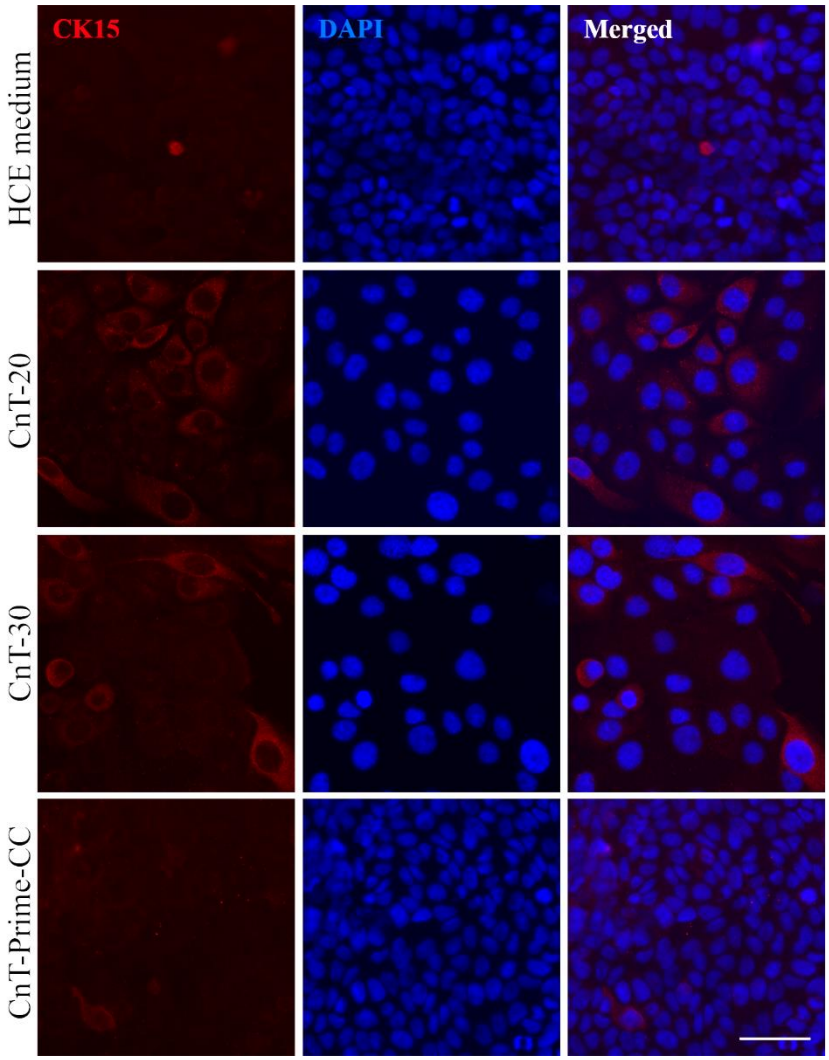

Figure S4. *HCEs stained with anti-CK15 (red) and DAPI (blue). Scale bar 50 µm.*

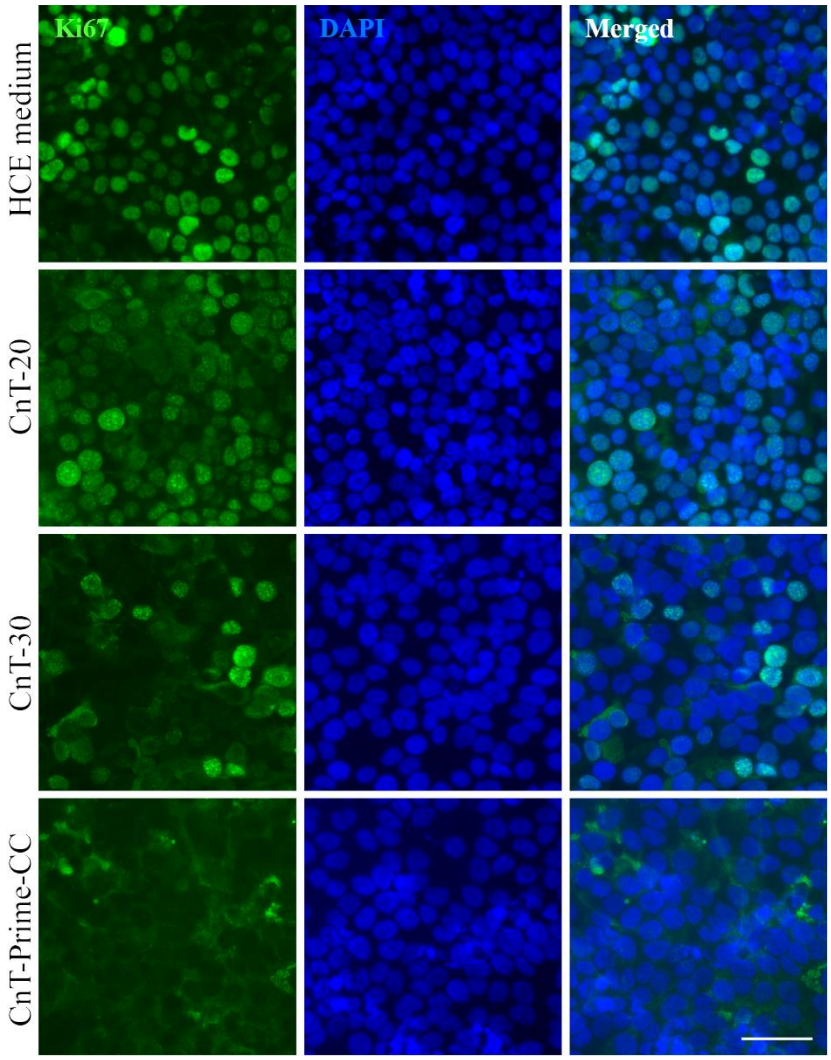

Figure S5. *HCEs stained with anti-Ki67 (green) and DAPI (blue). Scale bar 50 µm.*

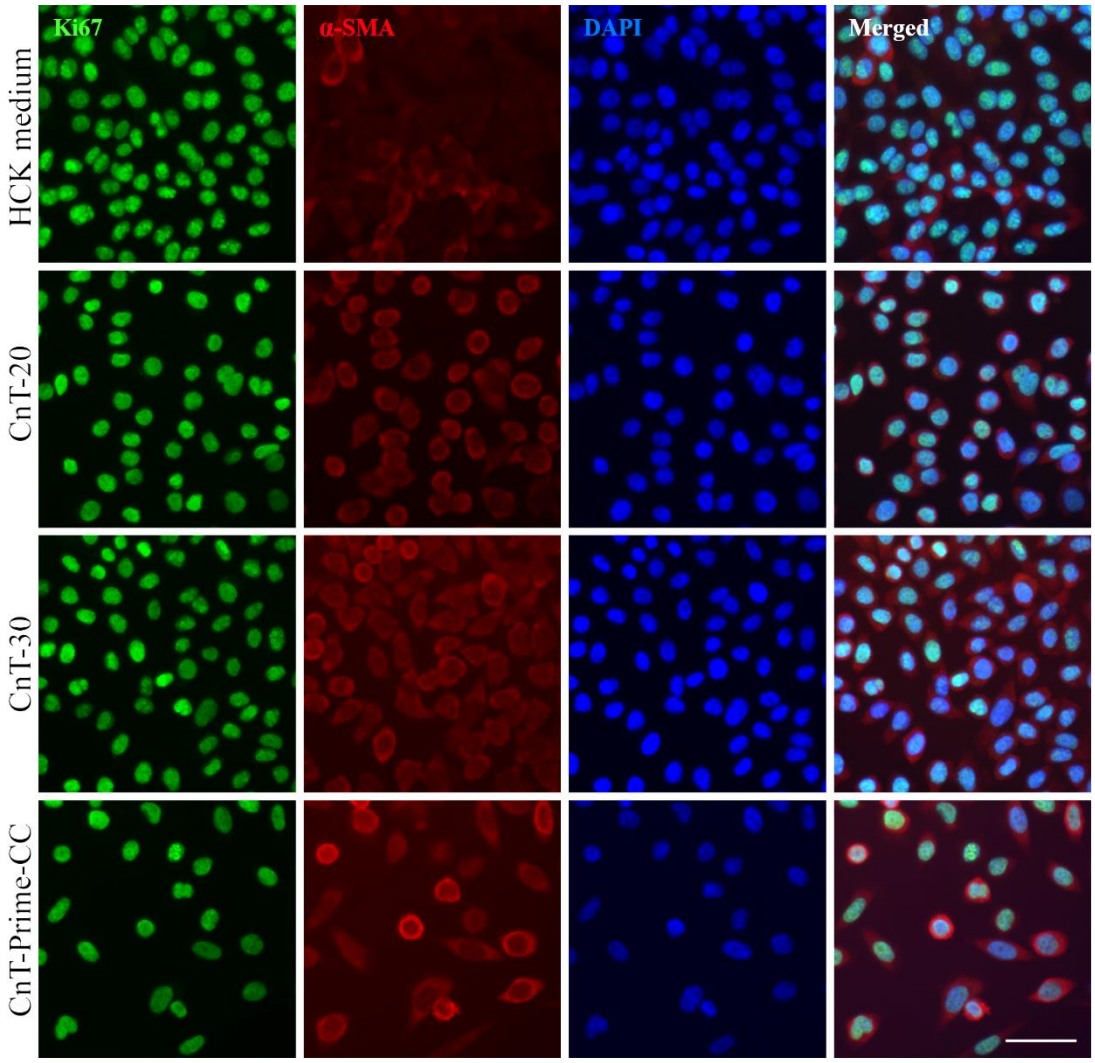

Figure S6. *HCKs stained with anti-Ki67 (green), α-SMA (red) and DAPI (blue). Scale bar 50 µm.*

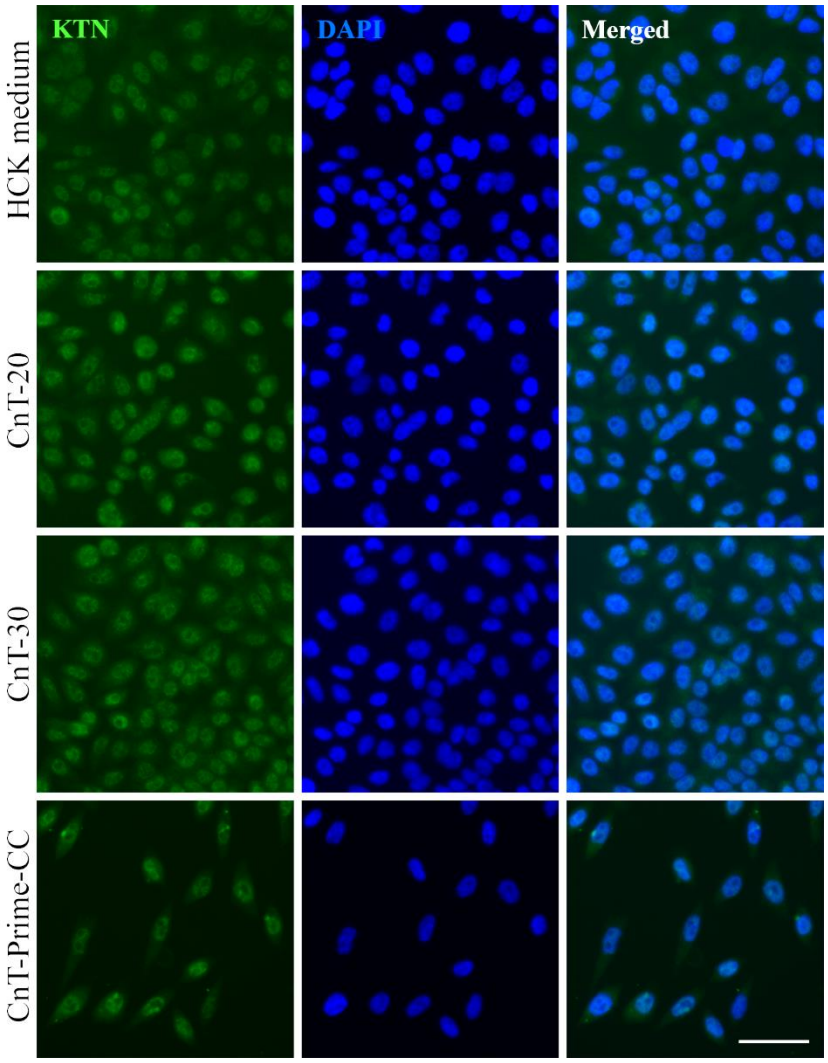

Figure S7. *HCKs stained with anti-KTN (green) and DAPI (blue). Scale bar 50 µm.*

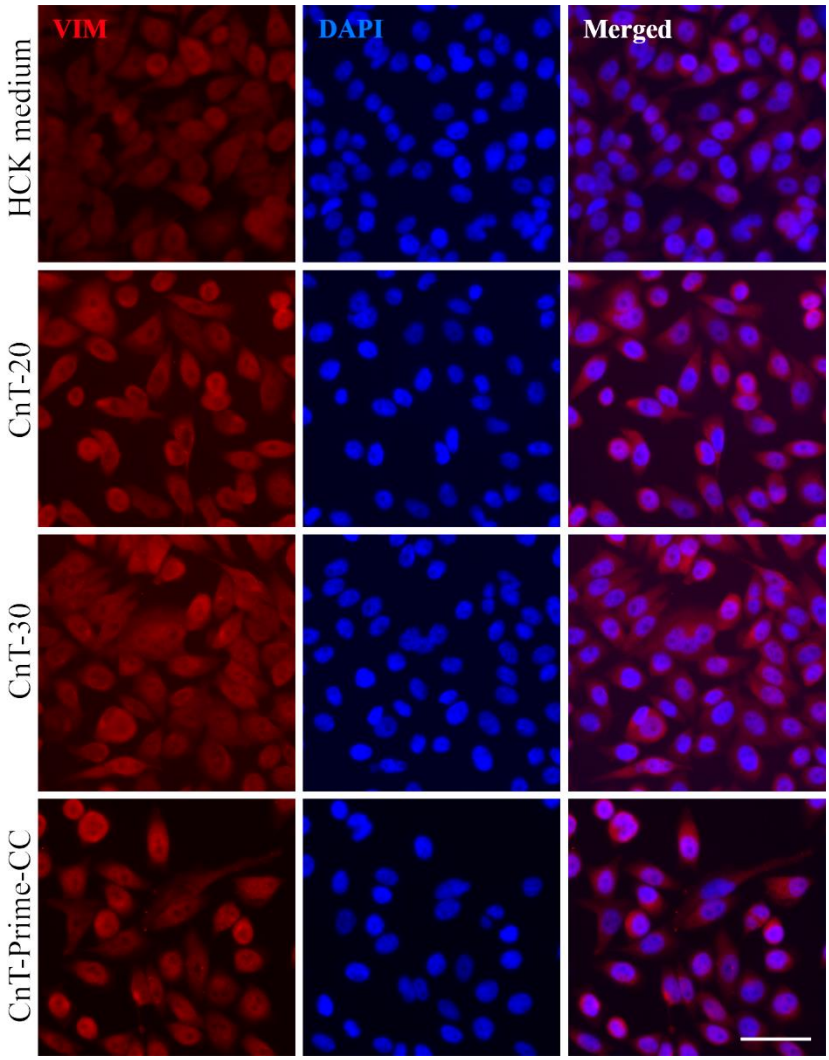

Figure S8. *HCKs stained with anti-VIM (red) and DAPI (blue). Scale bar 50 µm.*

Representative IF images of hydrogel cryosections are presented in Figures S9-S15.

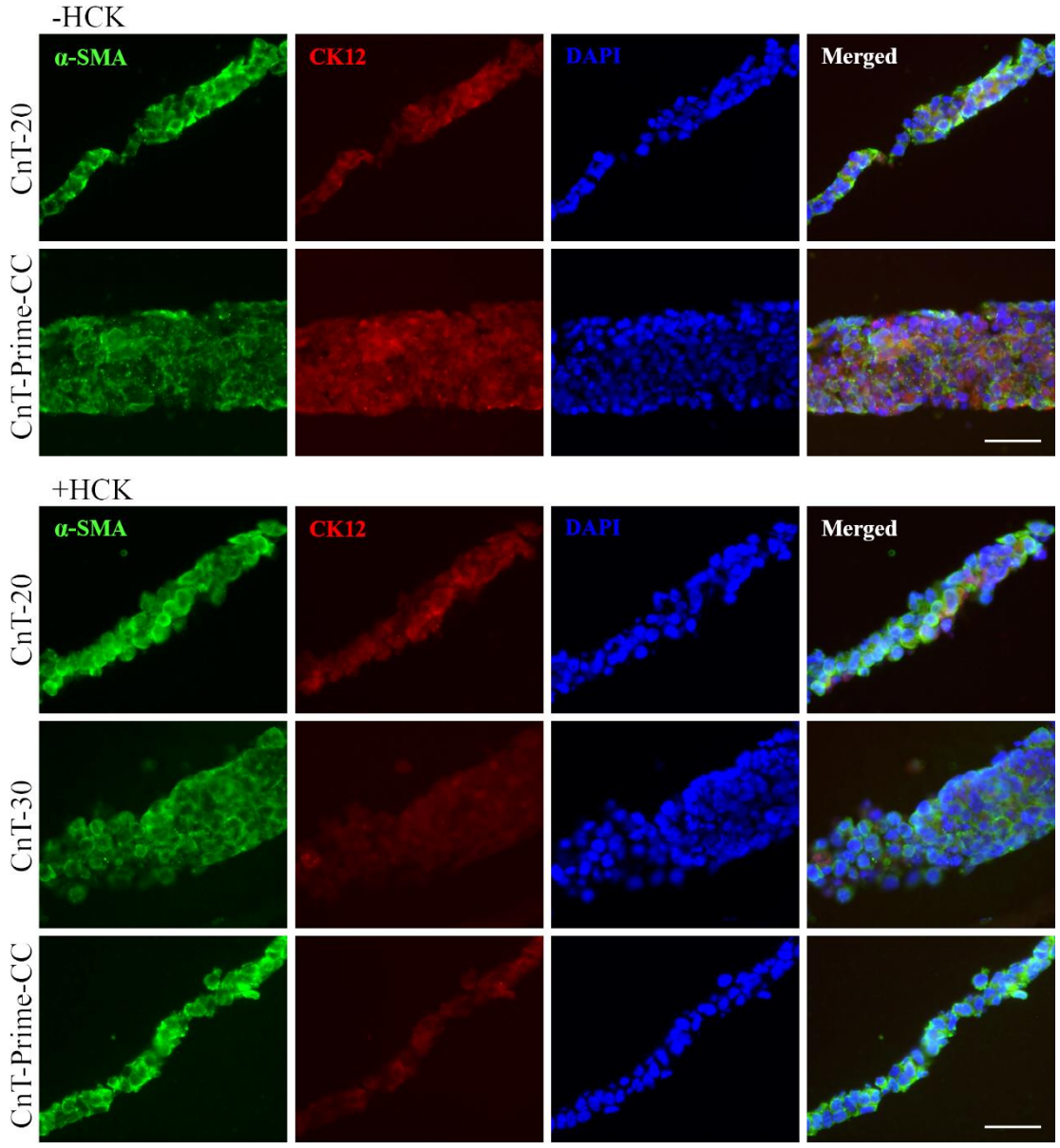

Figure S9. *Hydrogel A cryosection samples are stained with anti-α-SMA (green), anti-CK12 (red) and DAPI (blue). The upper section (2 x 4) presents the results from samples cultured without HCKs and the lower section (3 x 4) presents the results from samples cultured with HCKs. Scale bars 50 µm.*

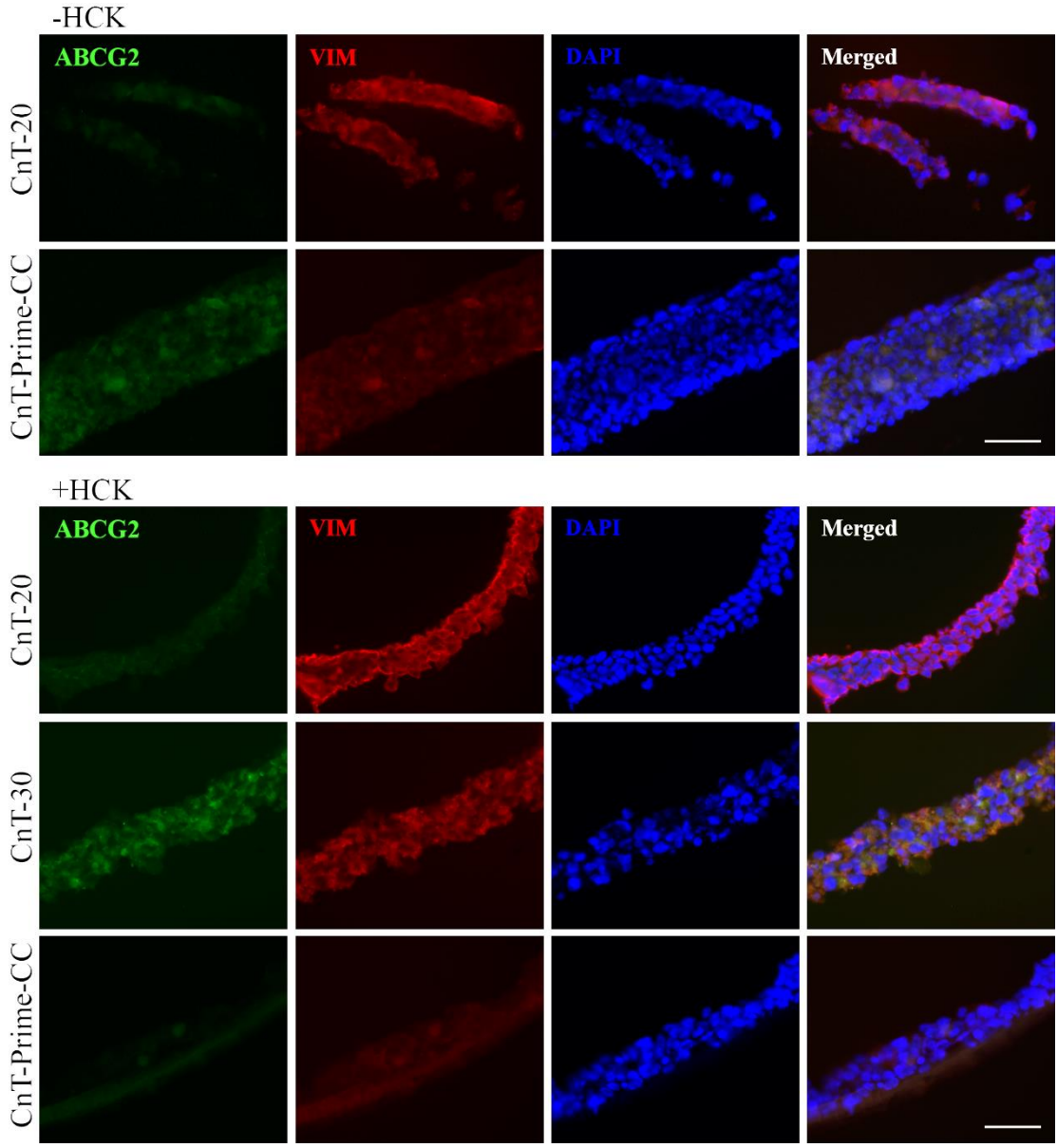

Figure S10. *Hydrogel A cryosection samples are stained with anti-ABCG2 (green), anti-VIM (red) and DAPI (blue). The upper section (2 x 4) presents the results from samples cultured without HCKs and the lower section (3 x 4) presents the results from samples cultured with HCKs. Scale bars 50 µm.*

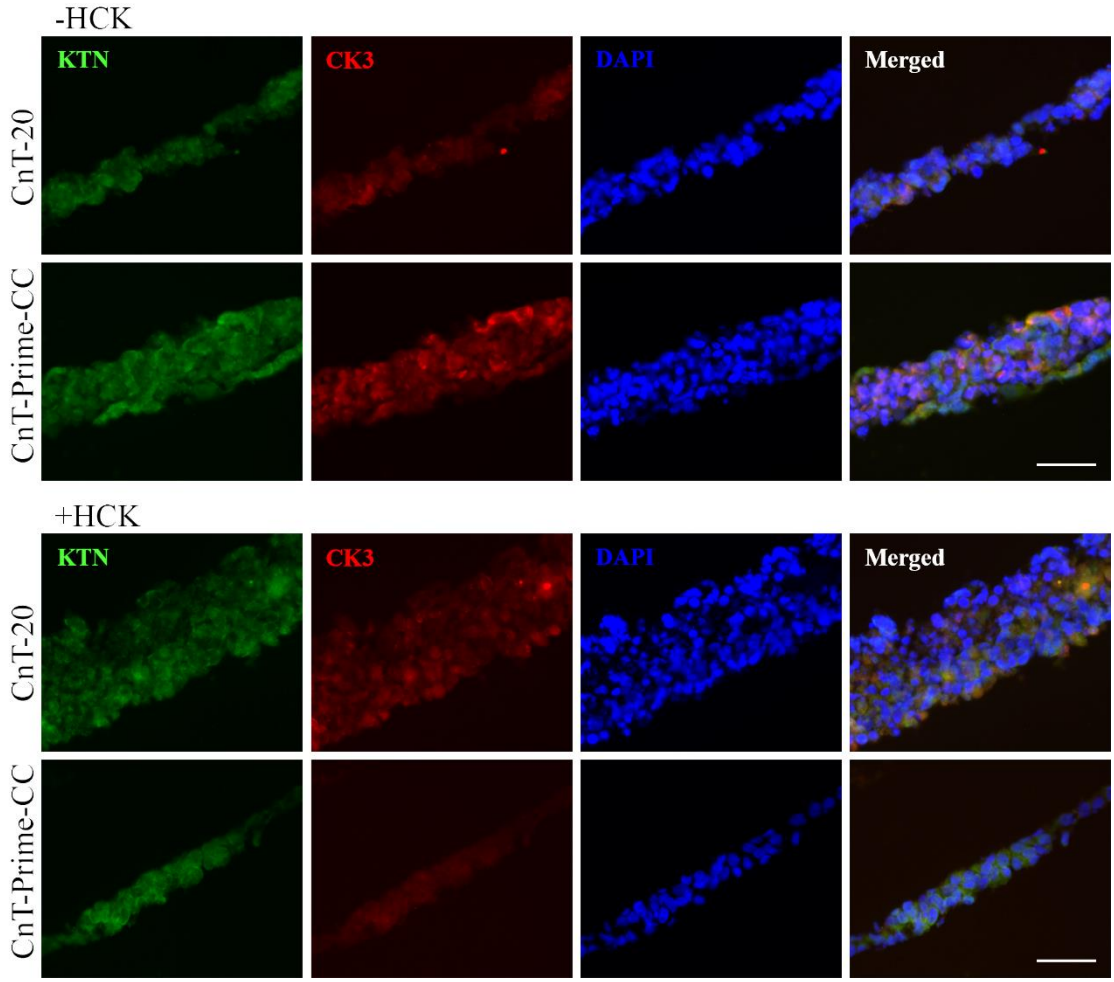

Figure S11. *Hydrogel A cryosection samples are stained with anti-KTN (green), anti-CK3 (red) and DAPI (blue). The upper section (2 x 4) presents the results from samples cultured without HCKs and the lower section (2 x 4) presents the results from samples cultured with HCKs. Scale bars 50 µm.*

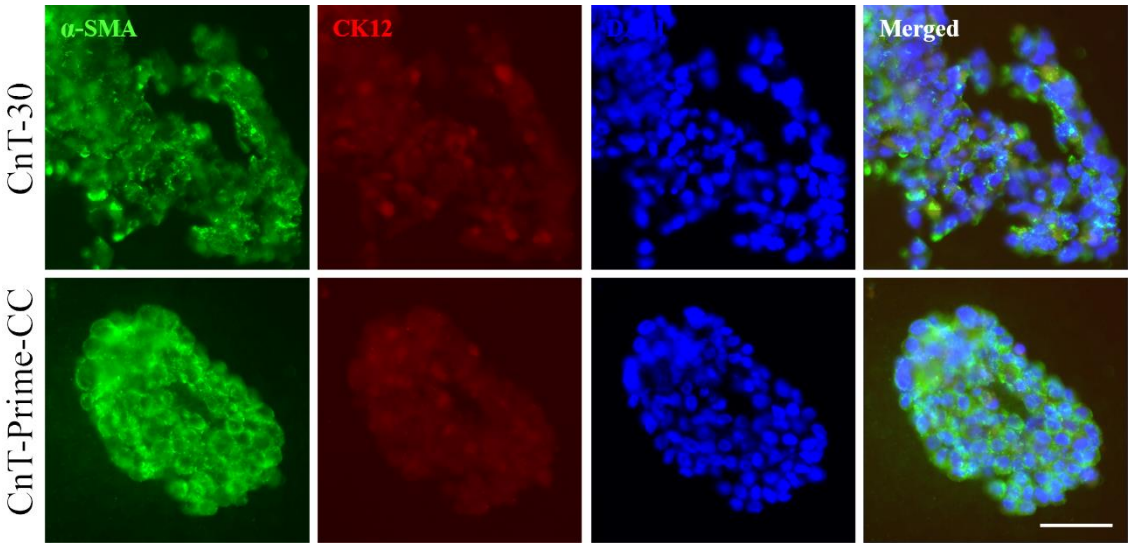

Figure S12. *Hydrogel C cryosection samples are stained with anti-α-SMA (green), anti-CK12 (red) and DAPI (blue). Scale bar 50 µm.*

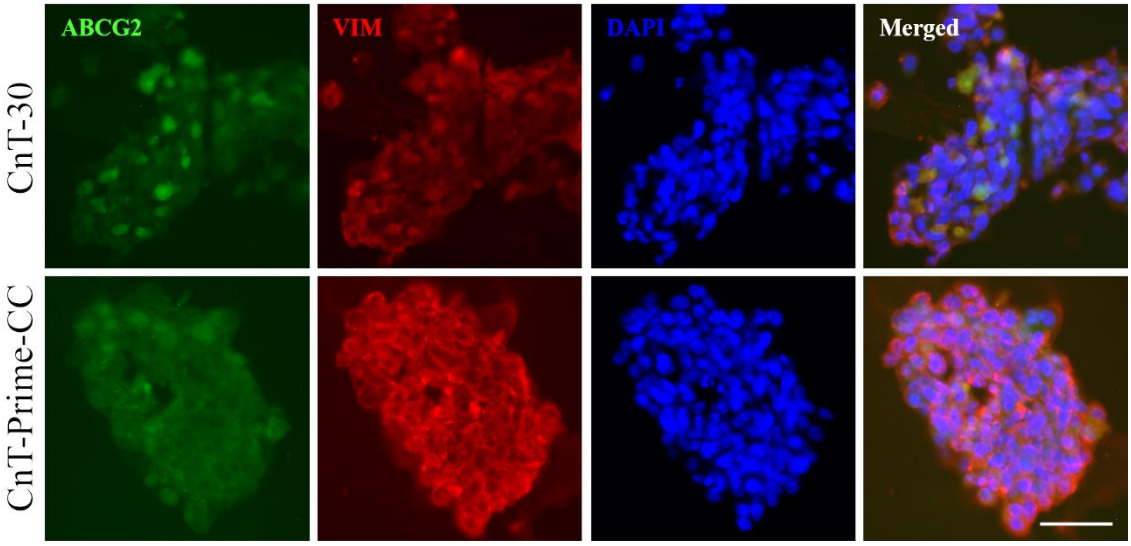

Figure S13. *Hydrogel C cryosection samples are stained with anti-ABCG2 (green), anti-VIM (red) and DAPI (blue). Scale bar 50 µm.*

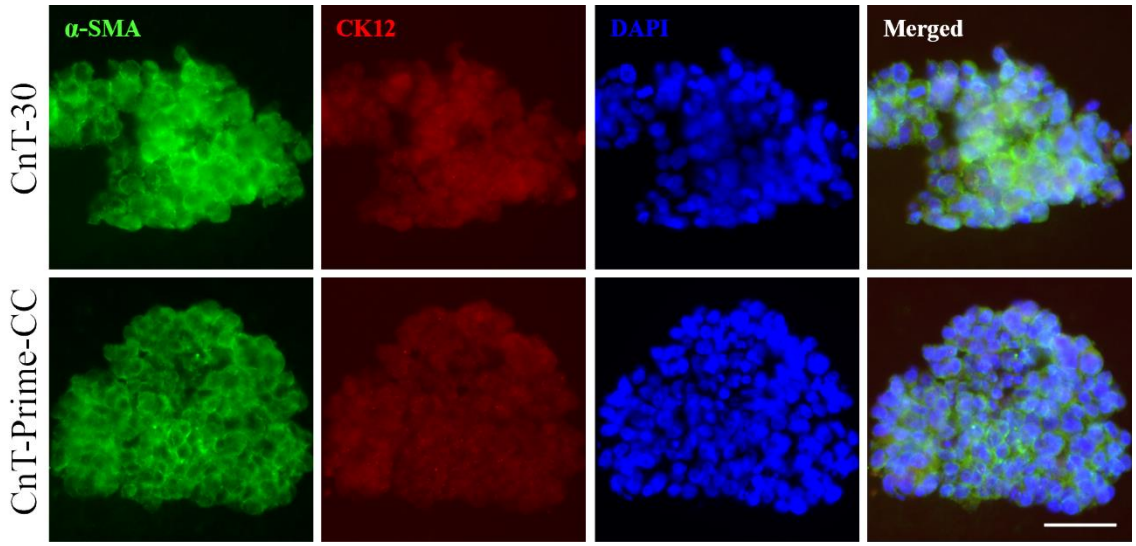

Figure S14. *Hydrogel D cryosection samples are stained with anti-α-SMA (green), anti-CK12 (red) and DAPI (blue). Scale bar 50 µm.*

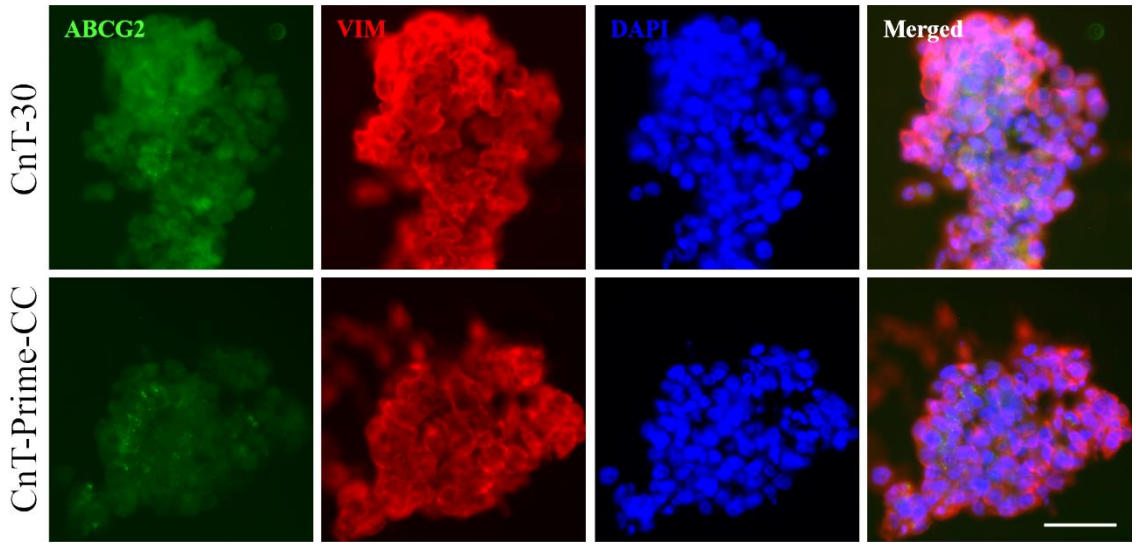

Figure S15. *Hydrogel D cryosection samples are stained with anti-ABCG2 (green), anti-VIM (red) and DAPI (blue). Scale bar 50 µm.*